UNIVERSITÀ
DEGLI STUDI
FIRENZE

DOTTORATO DI RICERCA IN

SCIENZE CHIMICHE

CICLO XXVII

COORDINATORE Prof. Andrea Goti

Synthesis of new macrocyclic and macropolycyclic systems for metal ion recognition

Settore Scientifico Disciplinare CHIM/03

Dottoranda

Dott.ssa. Rania Khaled Zartit

Tutore

Prof. Andrea Bencini

Coordinatore

Prof. Andrea Goti

Anni 2012/2015

To Syria … To My Family … To My Love … To My Friends

Reference

1- INTRODUCTION

1.1- Supramolecular chemistry

Supramolecular chemistry [1] is the chemistry of the molecular aggregates[2] of two or more of the molecules associated with each other by the non-covalent forces [3 , 4] , such as electrostatic interactions, hydrogen bonding, van der Waals forces[5,6], stacking interactions and hydrophobic effect. In other words, it is chemistry of intermolecular forces.

[1] Donald Cram (D.J. Cram, Preorganisation - from solvents to spherands, Angew. Chem. Int. Ed. Engl., 1986, 25, 1039).

[2] J.M.Lehn Molecular To Supramolecular Chemistry, Vch, Weinheim 1995.

[3] Jean-Marie Lehn, premio Nobel 1987.

[4] G.A. Jeffrey, (An Introduction to Hydrogen Bonding, Oxford University Press: Oxford, 1997); D. Braga, F. Grepioni, J.J. Novoa (Inter-anion O-H-O hydrogen bond like interactions: the breakdown of the strength-length analogy, Chem. Commun., 1998, 1959).

[5] J.M.Lehn, Angew. Chem. Int., Ed Engl., 27 (1988), 89.

[6] B. Diederic, Angew. Chem. Int., Ed Engl., 27 (1988), 362.

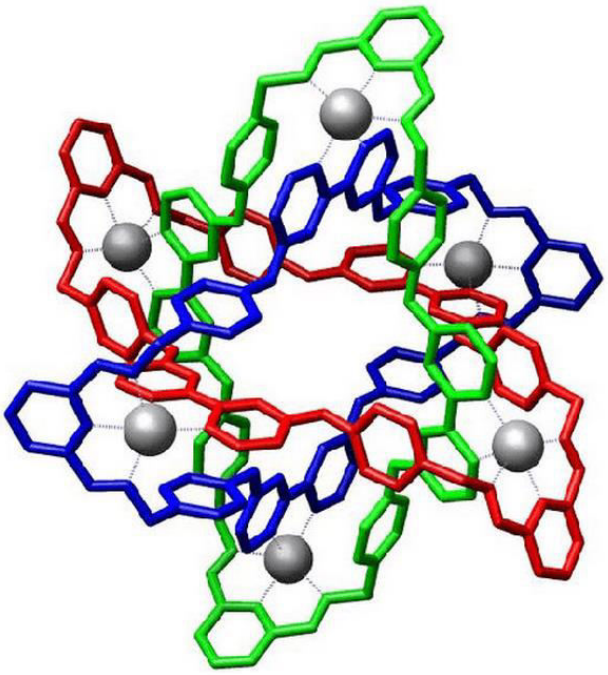

Figure 1. Supramolecular system of molecular Borromean rings reported by Stoddart and co-workers Science 2004, 304, 1308-1312. The receptor is constituted by a hexa-nuclear zinc complex, where the metal ions are linked by three interpenetrated macrocycles (molecular borromean rings) formed from the reaction between 2,6-diformylpyridine and diamine compounds.

The supramolecular adducts are generally composed of two molecular species, where the species with smaller dimension is called "substrate" or "guest", while the species with greater dimension is called "receptor" or "host". To form the supramolecular adduct, the two species must be structurally complementary as much as possible in order to achieve selective complexation of the guest by the host through the formation of a number of weak interactions. Supramolecular adducts are usually linked together by non-covalent interactions and possess physico-chemical characteristics different from those possessed by the isolated molecules. Intermolecular forces are generally weaker than the covalent bonds, and therefore they should be numerous

intermolecular interactions to ensure stability to the adducts and reversibility in the process of complex formation. Therefore, supramolecular species are kinetically more labile, thermodynamically more unstable and dynamically more flexible than the molecules. The energy associated to the host-guest interactions is much lower than that related to covalent bonds in molecules and the absence of covalent bonds allows an easier modification of the structure of the host-guest adducrt, because the energy barrier that must be overcome to break off weak interactions is lower. This can explain the capacity of supramolecular adducts to perform different functions and their basic role in biological systems.

Selective complexation of the guest by the host is often called molecular recognition[7,8]. The molecular recognition event can be followed by other processes involving the substrate, the receptor or both of them. Examples can be chemical modification of the substrate operated by the receptor, as occurring in nature in enzymes or its transport through membranes.

1.1.1- Intermolecular forces

Intermolecular forces play a fundamental role in the stabilization of supramolecular adducts. They are non-covalent bonds and the stability of an adduct is guaranteed by a high number of weak bonds, in order to achieve a stabilization of the supramolecular adducts similar to the occurring in systems held together by covalent bonda.

Intermolecular forces generally occurring in host-guest adducts can be summarized as follows:

[7] D.J.Cram, J.M.Cram, Science, Washington, 183 (1974), 803.

[8] J.M.Lehn, Pure Appl. Chem., 50 (1978), 871.

1.1.1.1- Electrostatic interactions

They are generally coulombic or dipole forces and they are often at the basis of selective interactions between host and guest when these specie feature high polarizability. In some cases these forces are the most relevant in the formation and stabilization of supramolecular adducts, in particular when the interactions occur between electrically charged species. They are inversely proportional to the square of the distance and depend on the dielectric constant. These interactions are reduced in polar media with low dielectric constants (for example, in aqueous environment), while are enhanced in media featuring low dielectric constants, such as apolar or scarcely apolar solvents or some protein matrices.

1.1.1.2- Hydrogen bonding

Hydrogen bonding is an electrostatic interaction involving dipolar groups. Normally, this interaction occurs when a hydrogen atom (H) is covalently bound to a highly electronegative atom (X) of a molecule, schematized as $^{\delta-}X\text{-}H^{\delta+}$. This group interacts with a highly electronegative atom (Y), possessing a free electron pair, schematized as $Y^{\delta-}$. The interaction, normally schematized as $^{-\delta}X\text{-}H^{\delta+\cdots}Y^{\delta-}$, may imply a partial or total transfer of the proton from X-H to Y (see Figure 2). In this case the hydrogen bond is not purely electrostatic, but it has a covalent component. This occurs, in particular, in the case of groups X-H and Y-H with similar pK_a and it originates strong hydrogen bonding contacts. Hydrogen bonding is generally weaker than covalent or ionic bonds but stronger than a van der Waals interaction.

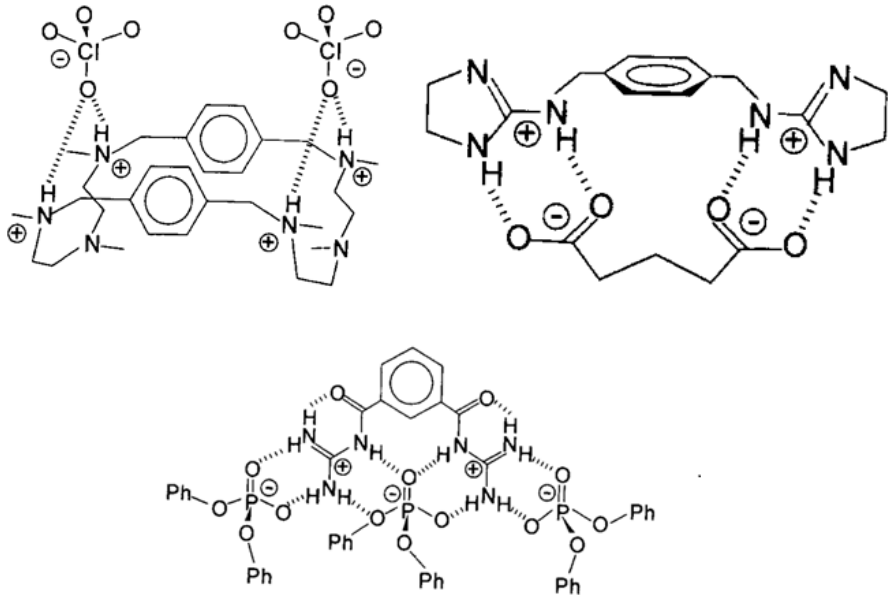

Figure 2. Examples of anionic coordination by synthetic receptors through electrostatic interactions and hydrogen bonds.

Hydrogen bonding interactions are directiona. This type of interaction are often responsible of the high selectivity toward one or more substrates displayed by receptors and actually it is the most exploited interaction in the achievement of synthetic receptors able to selectively recognize targeted substrates. In fact, the host species is often designed to contain several X-H or Y groups in complementary geometrical disposition with respect to the Y or X-H groups of the guest, in order to generate a stabilizing network of hydrogen bonding interactions. An example of hydrogen bonding complementarity between host and guest in molecular recognition is reported in Figure 3, which shows four hydrogen bonds formed by the receptor L, featuring two amide moieties and two benzimidazolium units, opportunely disposed to strongly bind dihydrogen phosphate via hydrogen bonding.

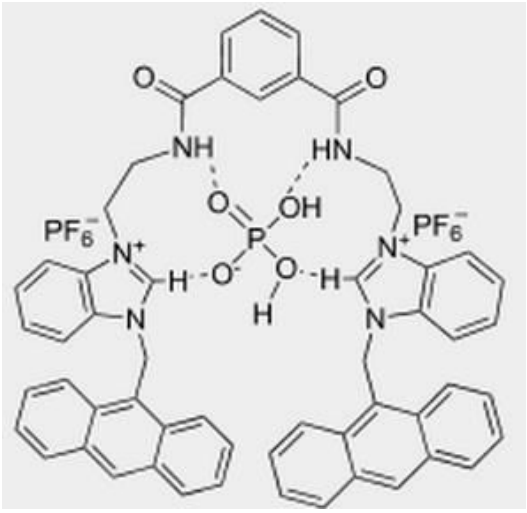

Figure 3. Molecular recognition of the dihydrogen phosphate ion by the receptor containing two amide and two benzimidazolium units.

From the biological point of view, this type of interaction is the principal responsible of the global structure of many proteins, of the recognition of substrates by many enzymes and of structure of the double helix of DNA, where nucleobases are coupled by strong hydrogen bonding interactions.

1.1.1.3- Van der Waals forces

Van der Waals forces include dipole-dipole interactions between permanent dipoles, instantaneous dipoles and induced dipoles. The energy of these interactions markedly depends on the dipole moments of polar molecules and on their polarizability. The latter contribution becomes the most relevant in the case of apolar host and guest. Compared to the interactions between charged species, the energy of these interactions decreases much more quickly as the distance between the interacting species increases. The interactions between non polar species, such as induced dipoles, derive from the balance of attractive forces, also known as London

dispersion forces and repulsive forces, that can be described with the potential of Lennard-Johnes:

$$U = \frac{A}{r^{12}} - \frac{B}{r^{6}}$$

The repulsive contribution increases with r^{-12}, while the attractiveone increases with r^{-6}.

1.1.1.4- Hydrophobic effect

The hydrophobic effect is observed in the association of two or more non polar or scarcely polar units in polar solvents (for example, in aqueous solvent) and it is often based on a dimensional complementarity between host and guest. The formation of the adduct can be driven by an enthalpic contribution or by an entropic contribution. Considering the enthalpic contribution, the attractive interactions between polar solvent and apolar solute are weaker than the interactions—between the molecules of the solvent and of Van Der Waals interactions between the hydrophobic surfaces of host and guest. The entropic stabilization is due to the interaction between the surfaces of the molecular species, which implies desolvation and thus release of a large number of solvent molecules.

1.1.1.5- Stacking interactions

Stacking interactions are electrostatic contacts between two aromatic systems featuring a delocalized π cloud and they generally occurs between an electron-rich and electron poor system, such as, for instance, two aromatic group containing an electron-donor and an electron-withdrwing group. The two aromatic moiety can be faced one another ("face to face" interaction) or they can assume a perpendicular disposition ("edge-to-face" interaction). The formed adducts are known as π complexes. In

some cases, a charge transfer process can occur from the electron-rich to the electron-poor system, to give a 'charge-transfer' complex. This kind of interaction is common in Nature, in particular in biological macromolecules (proteins, nucleic acids). The face-to-face disposition of nucleobases in doble-stranded DNA represents the most cited example.

Figure 4. illustrates the electrostatic and π-stacking interactions between the cationic [(μ-{(3,4-pyridyl)porphyrazine}-tetrakis{bis-bipiridine(chloro)ruthenium(II)]$^{4+}$ complex (TRPz^{4+}) and the anionic [tetrasolfunatephthalocyaninatecopper(II)]$^{4-}$ complex ([CuTSPc]$^{4-}$), yielding a TRPz/CuTSPc double layered films[9,10].

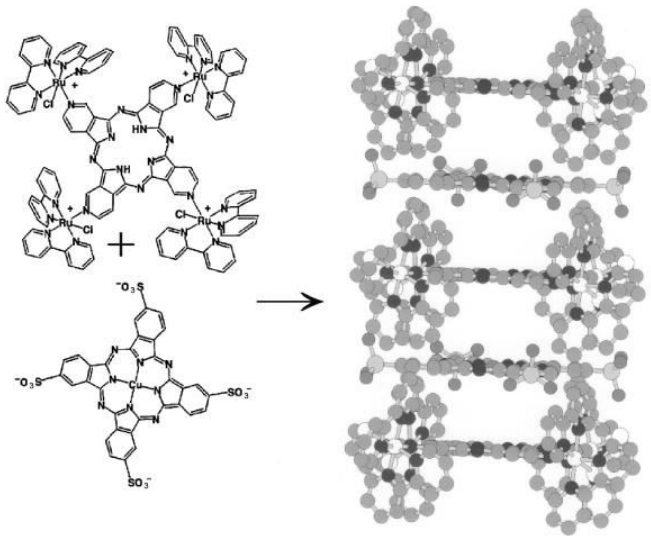

Figure 4. Clarification of electrostatic / π-stacking assembly of cationic TRPz and tetrasolfunatephthalocyaninatecopper (II) complex.

[9] Araki, K.; Toma, H. E.; J. Photochem. Photobiol. A 1994, 83, 245.

[10] Araki, K.; Wagner, M.J.; Wrighton, M.S.; Langmuir 1996, 12, 5393.

1.1.2- Molecular recognition

Molecular recognition can be defined as selective binding by a receptorof a targeted substrate in presence of other chemical species. Normally, the recognized substrate is the species that shows the structural and electronic complementarity with the receptor, thus achieving the largest possible number of contacts of bonds.

To achive selective interaction between the receptor and the substrate, two main preliminary conditions should be accomplished.

1.1.2.1- Stereochemical complementarity of the coordination sites

The binding sites on the receptor must have a geometrical disposition corresponding to the binding sites of the substrate, in order to form the larger as possible number of non-covalent interactions, ensuring a high the stability to the supramolecular adduct.

1.1.2.2- Preorganisation of the ligand

Before the process of coordination, if the receptor should already possess a conformation similar to that assumed in adduct. In fact, the energy required to bring the receptor to its final conformation would be lower and thus the formed complex will be more stable. Furthermore, an optimal receptor should possess a great surface of contact with the substrate and, in most case, is capable to wrap it, giving several non-covalent interactions.

Typical substrates considered in supramolecular chemistry can be eithr neutral molecules or charged species, including cationic

substrates (metal ions, organic systems containing ammonium groups) or anionic species, both organic and inorganic.

1.1.3- Macrocyclic ligands

Macrocyclic ligands are among the most largely used classes o receptors used in supramolecular chemistry. They are defined as cyclic molecules which possess at least three donor atoms available for the formation of coordination bonds[11,12].

Macrocyclic molecules have been shown to be optimal receptors for both anionic and cationic species and therefore, they have been the subject several studies of molecular design.

The formed complexes of these species are generally more stable than the corresponding complexes that are obtained from open-chain ligands, because of the macrocyclic effect that combine the chelate effect with the structural preorganization of macrocyclic ligands. Macrocycles are rigid due to their cyclic nature and, at the same time, the coordination sites are in optimal position for substrate binding[13]. Macrocyclic ligands are widely present in Nature. Macrocycles and their complexes with metal cations occur in many biological systems and they are involved in many biological and vital functions, such as the cell breathing and photosynthesis. Their participation to biological processes improved the interest of chemists for their ability in substrate binding. The presence of similar coordination compounds in

[11] C.Bazzicalupi, A.Bencini, A.Bianchi, A.Danesi, E.Faggi, C,Giorgi, S.Santarelli, B.Valtancoli; coordination chemestry reviews 252 (2008) 1052- 1068.

[12] R.M.A.E Martell; Nist Critacal Stability Contants of Metal Complexes Database, V4.0,eot. Of Commerce: Gaithersburg (1997).

[13] H. J. Schneider, D. Guttes, U. Schneider, J. Am. Chem. Soc. 110 (1988) 6449.

nature is strongly motivated by their high kinetic and thermodynamic stability, due to the coordination of metal ions within the macrocyclic cavity. These complexes ensure the maintenance of biological functions. This is the case, for instance, of the heme prosthetic group (Figure 5), which contains iron(II) in its active site or of magnesium in chlorophyll, where magnesium is coordinated within a phorphyrin moiety. Other examples of natural macrocyclic compounds are valinomycin, a known natural antibiotic, and cyclodextrins, which are known since 1891 and are currently used in alimentary[14] and pharmaceutical[15] industry.

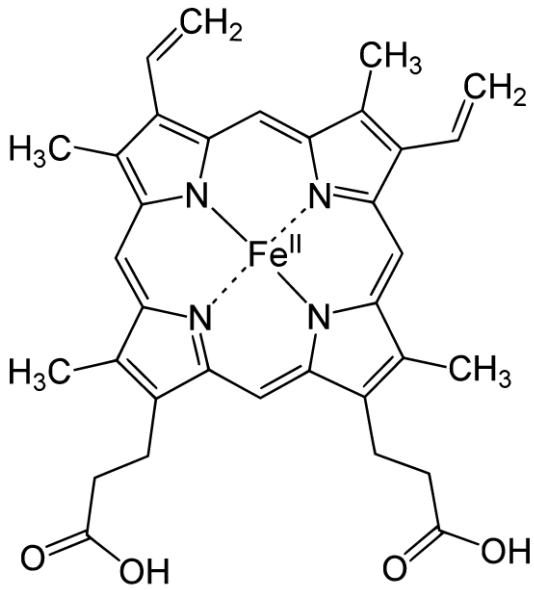

Figure 5. A Natural macrocycle, heme prosthetic group of hemoglobin.

Many macrocyclic ligands were synthesized in the past 50 years, taking into account two principles in their design: the similarity with

[14] V. A. Marcolino, G. M. Zanin, L. R. Durrant, M. D. T. Benassi, G. Matioli, J. Agr. Food Chem. 59 (7), (2011), 3348–57.

[15] T. R. Thatiparti, A. J. Shoffstall, H. A. Von Recum, Biomaterials 31 (8), (2010), 233547.

natural macrocycles, containing oxygen and nitrogen atoms as donors, and the research of structural pre-organization, which ensures a high level of selectivity.

Crown ether, i.e. macrocyclic compounds containing oxygen donors, were the first artificial macrocycles synthesized and studies.

It was found that some of them were capable of selective binding and transport of alkaline and alkaline-earth metal cations across cell membranes (see Figure 6 for some examples). Recently, these molecules have been used as receptors for organic cations containing ammonium groups, where the crown ethers[16] interact through the formation of hydrogen bonding with the substrate.

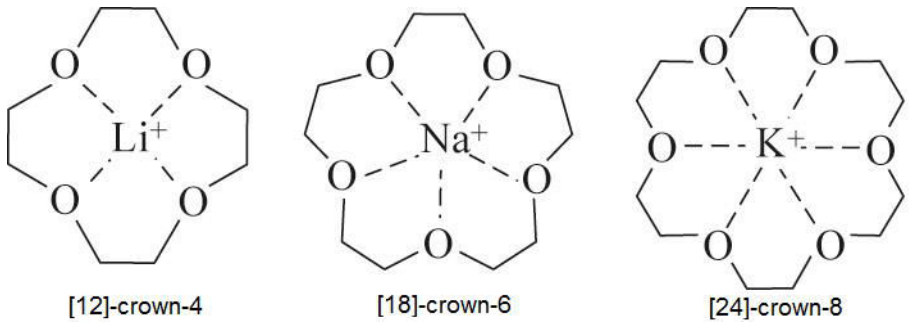

Figure 6. "Host-guest" complexes composed by crown ethers and ions of alkaline metals.

The replacement of oxygen atoms with nitrogen donors lead to cyclic molecules with structure similar to that of crown ethers, but with much different binding ability. The nitrogen atoms are softer than the oxygen atoms, and the resulting polyazamacrocycles systems are more suited for the coordination of transition metals. Furthermore, they can give protonation equilibria in aqueous

[16] C. J. Pedersen, Angew. Chem. Int. 27, (1988), 1021-1027.

solution. Species with a high degree of protonation can also interact with anions through hydrogen bonds and electrostatic interactions, giving rise to the branch of supramoleculr chemistry called ‘anion coordination[17].

Both crown ethrs and polyaazamacrocyles can be further functionalized, introducing different functional groups on the ring in order to increase the interactions between the receptor and the substrate, thus increasing selectivity in the coordination process.Several synthetic strategies has been and still are used to synthesize macrocyclic ligands[18,19], as described below.

1.1.3.1- Direct syntheses [20]

Direct syntheses are reactions of double condensation between two functionalized segments[21,22]. The first step is always an intermolecular condensation (head-tail), leading to formation of an intermediate open-chain product. The desired ligand is generally formed by this intermediate product through an intramolecular reaction resulting from the ring closure. However, this second step of the condensation can lead to undesirable species formed by reaction of oligomerization and polymerization, as shown in Figure 7. The reaction is often performed in conditions of high

[17] E. Graf, J.-M. Lehn, J. Am. Chem. Soc. 98, (1976), 6403–6405.

[18] R. M. Izatt, J. J. Christensen, Academic Press, New York (1978).

[19] S. Karbach, W. Löhr, F. Vögtle, J.Chem. Res.(s), (1981) 314.

[20] G. Illuminati, L. Mandolini, Acc. Chem. Res., 14, (1981), 95–102.

[21] J. E. Richman, T. J. Atkins, J. Am. Chem. Soc. 96, (1974), 2268.

[22] A. Bianchi, M. Ciampolini, M. Micheloni. N. Nardi, B. Valtancoli, S. Mangani, E. Garcia-España, J. A. Ramirez, J. Chem. Soc., Perkin Trans., (1989), 1131.

dilution[23,24], i. e, by slow and simultaneous small additions of of the reagents to the reaction mixxture, in order to maintain very low concentrations of reagents, thus avoiding the possible reactions of oligomerization.

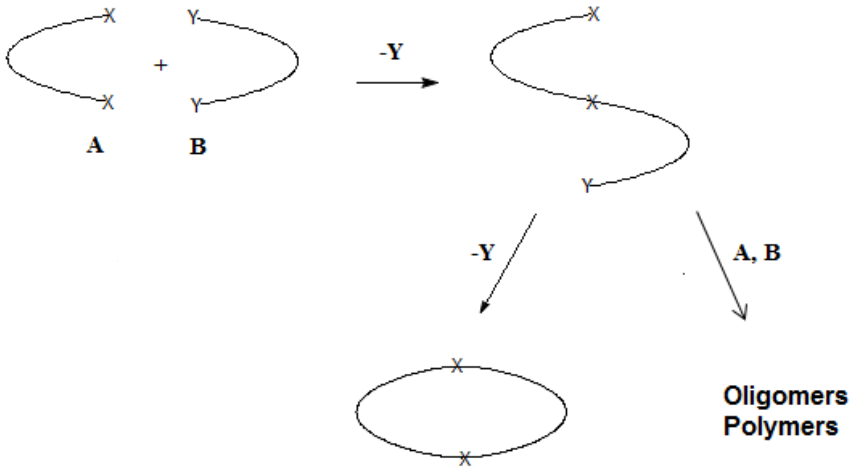

Figure 7. Direct synthesis of a macrocycle.

This synthesis can be successful only when the the condensation reactions would be kinetically are fast and therefore reagents and intermediates have short life time in solution, thus reducing the possible formation of oligomeric or polymeric species.

[23] M. S. Nasir, C. J. Fahrni, D.A. Suhy, K. J. Kolodsick, C. P. Singer, T. V. O'Halloran, J. Bigol. Inorg. Chem., 4 (6), (1999), 775-83.

[24] J. E. Baldwin, P. Permutter, Top. Curr. Chem., 121, (1984), 181.

1.1.3.2- Template synthesis[25]

(metal-assisted synthesis). Template synthesis are synthetic processes where cyclization is driven by the the presence of a metal ion according to two different possible mechanisms. In both cases, the metal ion is first complexed by a polyfunctional open-chain ligand. Then, reaction of the resulting complex with a secobd bifunctionalized fragment leads to the ring closure and to the achievement of a macrocyclic complex, as shown in Figure 8 for the synthesis of the macrocycle 1,4,7,10-tetraazacyclodecane, often called cyclen.

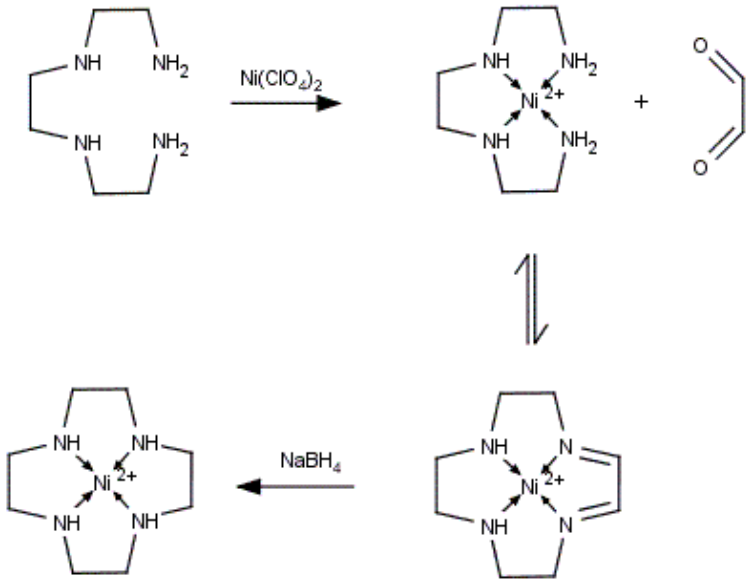

Figure 8. Template synthesis of cyclen.

There are two effects that enhance the efficiency of this synthesis:

a- The thermodynamic template effect: metal complexes with macrocyclic ligands are more termodyamically stable than complexes with open-chain ligands and therefore the equilibrium

[25] N. V. Gerbeleu, V. B.Arion, J. Burgess, Template Synthesis in Macrocyclic Chemistry, John Wiley & Sons, Ltd: Chichester, (1999).

that leads to the formation of the cyclic structure is shifted towards the products

b- The kinetic template effect: the metal ion influence the steric progress of the reaction, favoring the formation of cyclic compound. Basically, the metal ion kept the two reactive sites of the coordinated open-chain ligand in the right disposition and at a suitable distance to favor their simultaneous (or almost simultaneous) reaction with the two reactive groups of the second fragment involved in the cyclization.

1.1.4- Bisaminal derivatives

Recently, synthetic techniques have been developed to achieve macrocyclic systems containing one or more of the functional groups, which are linked with the cyclic structure through a suitable spacer. The synthetic procedures that use the bis-aminals[26,27,28] are numerous, fast and reversible for obtaining of a various molecular structures of "building block" that are composed of polyamine units, especially cyclic or acyclic tetramine. The main advantage of this process is the ability to separate insoluble mono or bis quaternary ammonium salts from the solution during the alkylation process.

Lately, new methods using an aminal intermediate have been developed for cyclen[29] and cyclam[30] mono-N functionalization.

---

[26] J. C. Timmons, T. J. Hubin, Coord. Chem. Rev., 2010, 254, 1661.

[27] S. Develay, R. Triper, M. Le Baccon, V. Patinec, G. Sterratrice, H. Handel, Dalton Trans., 2005, 3016.

[28] S. Develay, R. Triper, M. Le Baccon, V. Patinec, G. Sterratrice, H. Handel, Dalton Trans., 2006, 3418.

[29] W. C. Baker, M. J. Choi, D. C. Hill, J. L. Thompson and P. A. Petillo, J. Org. Chem., 1999, 64, 2683.

Macrocyclic bis-aminals are synthesized by condensation between tetraazamacrocycles of various types: the cyclic type (cyclen and cyclam (Figure 9) are the most common, then this manner was developed to include all the cyclic tetra-ammine systems) or acyclic type (open-chain) with glyoxal.

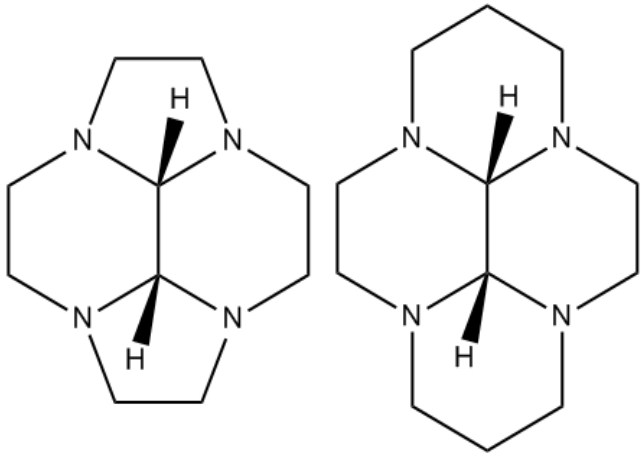

Figure 9. Bisaminal-cyclen and cyclam, are protected with glyoxal.

The bis-aminals has a folded geometry that governs nitrogen reactivity. In this type of compounds only two of the four amine groups present in the macrocycle (those in trans position, i.e. in position 1,7 in the case of cyclen) are very reactive against the electrophilic reagents (Figure 10). The N_2 and N_4 lone pairs are directed towards the concave fold are involved in aminal bridge bonds and are scarcely reactive; on the other hand, the lone pairs that pointed out from the convex side remained localized on N_1 and N_3, which results more reactive toward electrophile reagents.

[30] J. Kotek, P. Herman, P. Vojt s ek, J. Rohovec and I. Lukes— ,Collect. Czech. Chem. Commun., 2000, 65, 243.

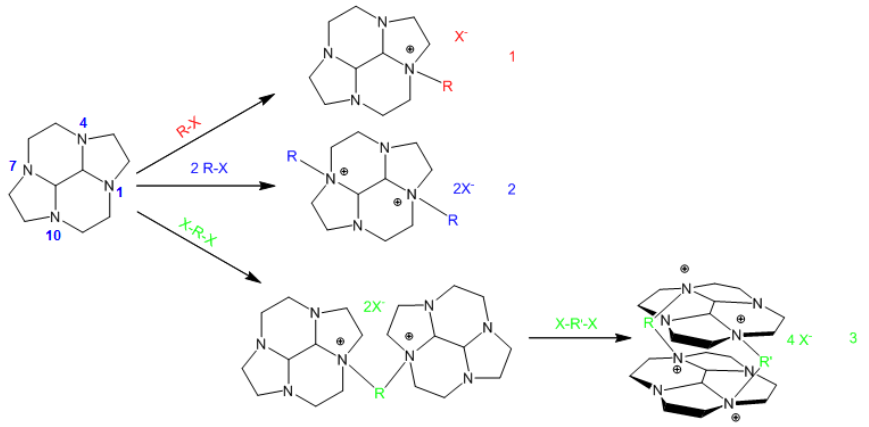

Figure 10. Synthesis of mono-N_1 and di-N_1, N_3 alkylated cyclen glyoxals.

The methylenic spacer that joins the four nitrogen atoms, making the structure orients the lone pairs of the other two amine groups (in the case of cyclen: in position 4,10) towards the center of the cavity (towards to the concave fold) and this leads to inhibit the reactivity. Therefore, the action of an electrophile on bis-aminals leads to N_1 functionalization and these adducts can further be alkylated on the opposing N_3 atom to obtain a diquat salt[31]. This condition makes the nucleophilic substitution reactions stereoselective for the isomer that is replaced in position 1,7.

It is worth mentioning that the attack on the two positions does not happen in the same efficacy, the functionalization of the first nitrogen atom being generally very fast compared with the nucleophilic replacement of the second amine group. This can allow to isolate the mono-functionalized product before the formation of di-functionalized product, as shown in Figure 11.

[31] J. Rohovec, R. Gyepes,I. C sar ova, J.Rudovsky and I. Lukes, T etrahedron L ett., 2000, 41, 1249.

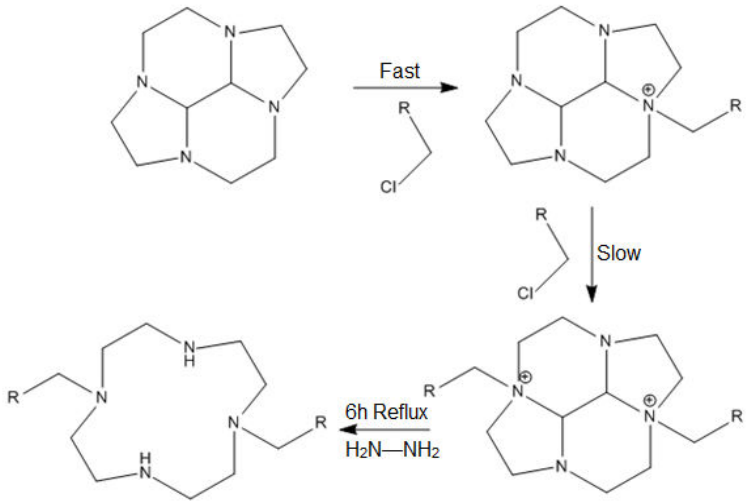

Figure 11. Process of deprotection of cyclen.

This methodology was used for the synthesis of fluorescent systems with the introduction of fluorogenic units that are linked with a single macrocyclic structure or by a bridge between two macrocyclic units.

1.2- Photochemistry

In general, when a molecule interacts with a photon of appropriate energy, the photon is absorbed:

$$A + h\nu \rightarrow A^*$$

A: the molecule in its ground state.

A*: - the molecule in its excited state.

hν – energy of the photon that causese the transition.

After a short time in the excited state, the molecule A* can return in several ways to a more stable energy level, either returning to the ground state or giving different products through intra-or intermolecular processes. Commonly, we can distinguish radiative and non-radiative processes. In the first, the excited species relaxes by emitting of photon, while in the second, the relaxation

occurs by transfer of heat to the environment as vibrational energy or through chemical transformations, such as bonds break and ionization.

1.2.1- Fluorescence

Fluorescence is the emission of a photon due to the electronic radiative transition from the vibrational state of S_1 to the vibrational state of S_0. Relaxation times are of the order of 10^{-8} seconds from the moment of the absorption of radiation. The electronic transition between S_0 and S_1 involves fundamental vibrational levels of the two electronic states and vibrational levels to greater energy, and the electron relaxes after the absorption of radiation in a not radiative manner decaying to the fundamental vibrational level, both before and after the emission of fluorescence. These non-radiative transitions determine the "Stokes shift". The Stokes shift is the difference in energy between the maximum of the absorption band and the maximum of fluorescence band. It can provide information on the excited states, and the detection of a fluorescent species is easier when it is larger. The absorption and emission spectra are generally specular ('mirror image' rule), because of the analogies between the vibrational states of S_0 and S_1.

Most of the molecules that show phenomenon of fluorescence are aromatic molecules or molecules that show conjugated double bonds, because of their ability to easily populate the antibonding orbital π* of these species through photoexcitation. The transitions of $\pi \rightarrow \pi^*$ and/or $\pi^* \rightarrow n$ are observed in the emissions (they mostly are features of heteroaromatic compounds) and are characterized by a high quantum yield.

1.2.2- Quantum yield and quenching of fluorescence

We can define the quantum yield of fluorescence is the fraction of excited molecules that come back to the ground state S_0 through photon emission of fluorescence.

The process that causes a decrease of the fluorescence intensity is ofeten defined as ‘quenching’ while the ‘quencher’ is a molecule that causes the decrease in intensity when it interacts with the fluorophore.

Although many factors can cause a decrease in intensity, the most famous is the interaction of the fluorophore with the quencher.

There are three principal mechanisms of the quencher (see Figure 12):

1- energy transfer between the excited state of the fluorophore and the quencher.
2- chemical reaction between the excited state and the quencher (especially, electron transfer reactions).
3- formation of a complex between the fluorophore and the quencher, with the formation of a not emitting adduct.

The quenching phenomenon are studied by:

a)- measuring the efficiency of the excited state under continuous illumination.

b)-measuring values of emission (or of absorption) of the excited state following discontinuous excitation.

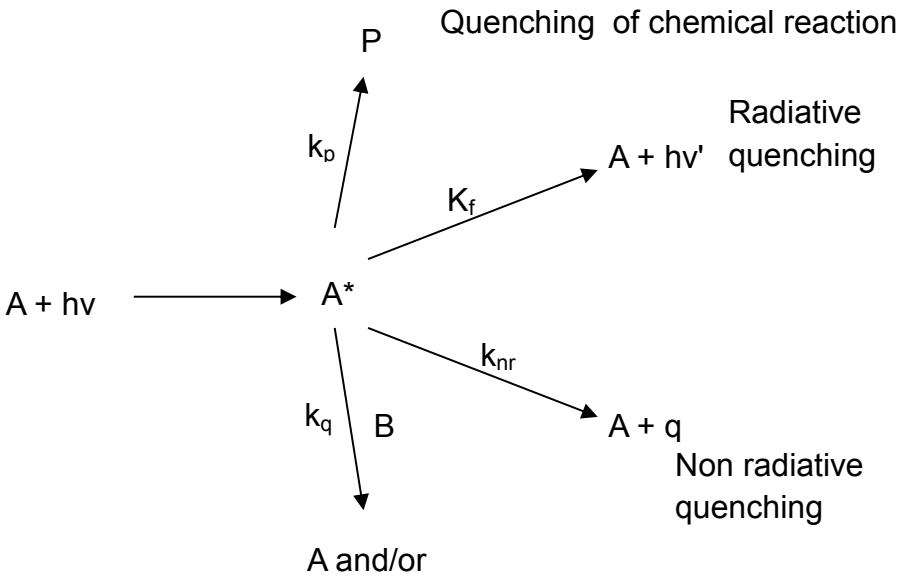

Figure 12. Mechanisms of the quencher.

Considering the scheme that shows in Figure 11, the lifetime of the excited state in the absence of the quencher B, is given by:

$$\tau^0 = 1/(k_p + k_f + k_{nr})$$

where k_f is the first-order rate constant relative to luminescence, k_p the first-order rate constant relative to intramolecular reactions, k_{nr} the first-order rate constant relative to the non-radiative deactivation processes of the excited state.

The lifetime is lower by repeating the experiment in the presence of a real quantity of quencher and it is given by:

$$\tau = 1/(k_p + k_f + k_{nr} + k_q[B])$$

where k_q is the second-order rate constant relative to the reaction quenching with the quencher B.

Finally, we obtain the equation of Stern-Volmer:

$$\tau^0/\tau = 1 + k_q\tau^0[B]$$

$k_q\tau^0$ is the constant of the quenching of Stern-Volmer $K_{sv.}$ This equation allows one to easily determine k_q.

1.2.3- Modulation of the fluorescence

After the coordination of the analyte with the receptor, the intensity of the fluorescence of the complex decreases or increases (e.g., it causes detectable variations of fluorescence emission), depending on the type of interaction that occurs between receptor and substrate as well as on some structural and/or electronic characteristics of the target substrate.
There are different types of effects that due to the interaction:

1- Photoinduced Electron Transfer PET[32].
2- Internal Charge Transfer ICT[33].
3- Electron Energy Transfer EET[34].
4- Photoinduced Proton Transfer PPT.
5- Formation of Excimer or Exciplexes[35].

1.2.3.1- Photoinduced electron transfer PET

The PET [36] effect is often responsible for quenching of the fluorescence emission, and it is the basical principle for many fluorescence chemosensors. This interaction can take place when receptor and fluorophore in the excited state are at medium to long distances.

---

[32] S. Karbach, W. Löhr, F. Vögtle, J.Chem. Res.(s), (1981) 314.

[33] B. Valeur; Molecular Fluorescence, Wiley-VCH Wenheim, (2002).

[34] J.E. Richmann, T.J. Atkins; J. Am. Chem. Soc 1974, 96, 2268.

[35] A. Bianchi, M. ciampolini, M. Micheloni, N. Nardi, B. Valtancoli, S. Mangani, E. Garcia Espana, J. A. Ramirez; J. Chem. Soc., Perkin Trans (1989), 113.

[36] B. Valeur, I. Leray, Coord. Chem. Rev., 205, (2000), 3-40.

The oxidative and reductive properties of a molecule can be shown even when it is in the electronic excited state, and this can lead to electron transfer processes, as shown in Figure 13.

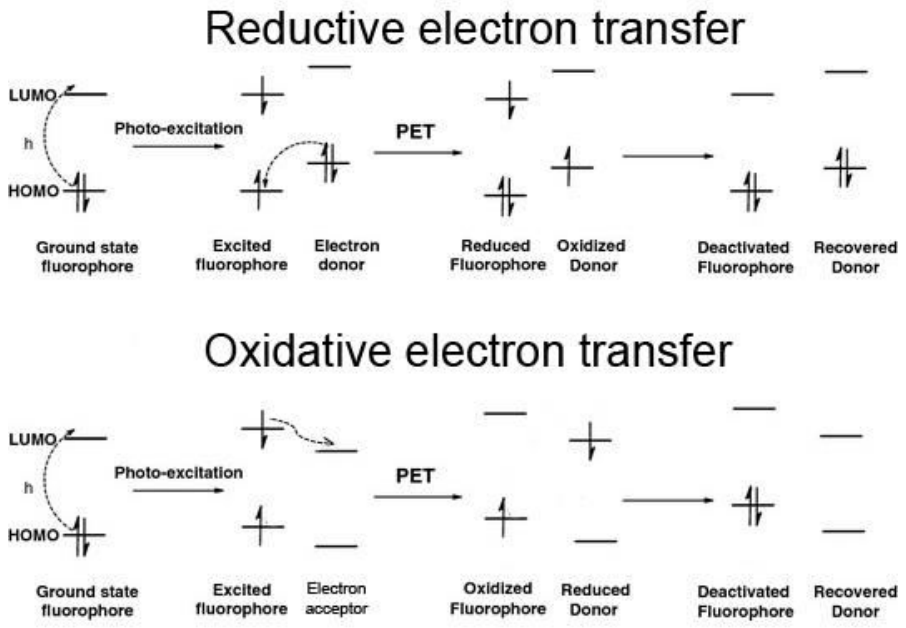

Figure 13. Reductive and oxidative electron transfers.

The PET process can be either of the oxidative type or reductive type, and the mechanism can be described as follows:

1.2.3.1.1- Reductive type of PET

A fluorophore A is excited by light to the species A*. This leads an electron to move from the highest occupied molecular orbital HOMO of the fluorophore to the lowest unoccupied molecular orbital LUMO of the same molecule. When the receptor unit is electron rich, an electron moves from the orbital HOMO of the receptor to the orbital HOMO of the fluorophore to fill the gap that is formed. In this way, it realizes the quenching of the fluorescence. In other words, the fluorescence emission is obviously inhibited,

because the electron in the orbital SOMO of the fluorophore can only decay towards the orbital HOMO of the receptor in a non-radiative manner, as shown in Figure 14.

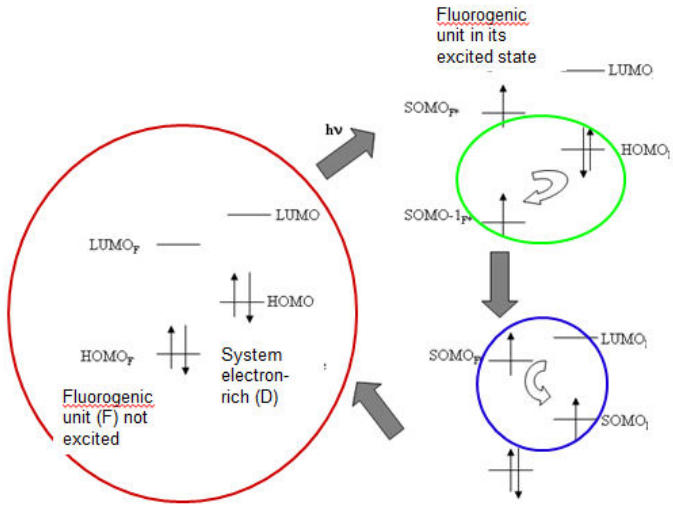

Figure 14. Reductive Electronic Transfer.

This process occurs when the HOMO of the receptor is located at intermediate energy between the two frontier orbitals of the fluorophore, as shown in Figure 15.

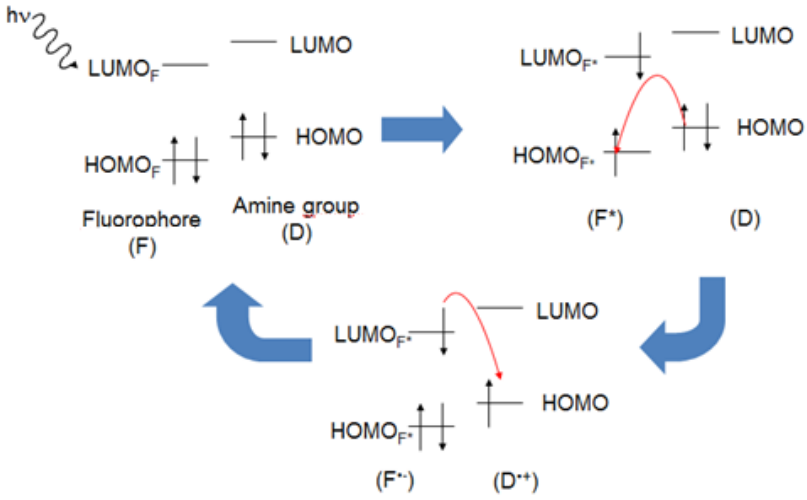

Figure 15. Photoinduced Electron Transfer PET.

1.2.3.1.2- Oxidative type of PET

In this case, an electron-free orbital of the receptor is located at intermediate energy between HOMO and LUMO of the fluorophore. After the excitation of the fluorophore, the electron in the LUMO of the fluorophore decays to the free orbital of the receptor, and from this orbital to the HOMO of the fluorophore, as shown in Figure 16.

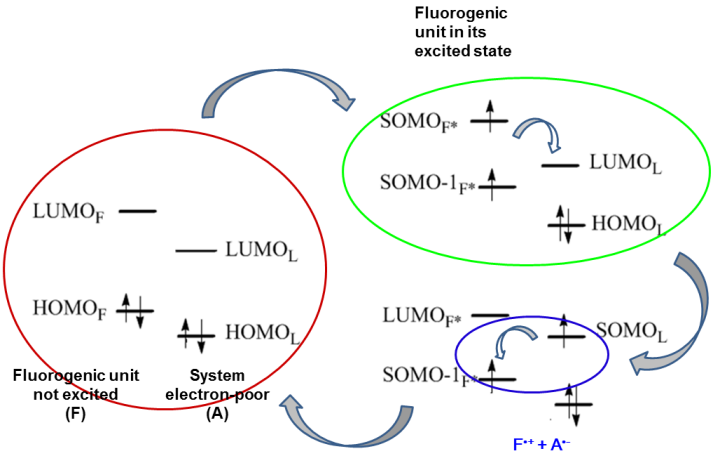

Figure 16. Oxidative Electronic Transfer.

Most of the PET sensors consists of a fluorophore linked with a polyamine receptor by a methylene spacer. Depending on the type of the amine groups, we can consider two cases as follows:

1) - the amine groups are not involved in proton or metal binding (free receptor)

Upon excitation of the fluorophore, an electron moves from the HOMO to the LUMO, and this activates the electronic transfer from the HOMO of the donor to the HOMO of the fluorophore determining a decrease of fluorescence. This situation is the case of PET reductive that is described above.

2) - The amine groups are protonated or the ligand coordinates a metal cation.

The redox potential of the donor increases, while the energy level of the HOMO of the receptor decreases compared to the HOMO of the fluorophore, thus preventing the PET process. Therefore, the fluorescence increases because of quenching inhibition.

In other words, a system constituted by and electron-donor receptor unit and a fluorophore generally originate a PET mechanism involving an electron transfer from the receptor to the excited fluorophore, whse emission is quenched. The involvement of the electron pairs of the receptor in protna or metal binding inhibits the PET effect giving rise to an enhancement of the emission fluorescence and the chemosensor 'turns on' (see Figure 17).

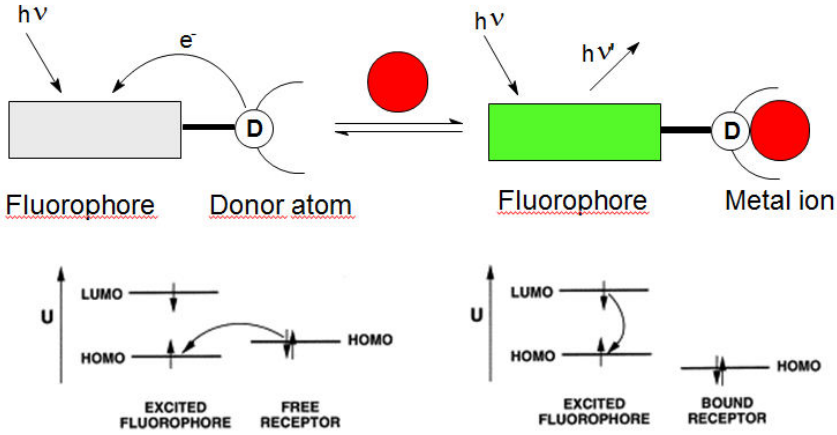

Figure 17. Fluorophore " Turns on ".

1.2.3.2- Electron energy transfer, or excitation energy transfer EET

Energy transfer processes can also changes the emission of the fluorophore. Generally speaking, both heterotransfer (energy transfer between two different molecules or sections of the same molecule) and homotransfer (energy transfer between two identical molecules or sections of the same chemosensor) processes may occur. A necessary condition for EET processes is the at least partial overlapping of the emission spectrum of the donor (excited molecule) with the absorption spectrum of the acceptor molecule.

$$\text{Heterotransfer: } D^* + A \rightarrow D + A^*$$

$$\text{Homotransfer: } D^* + D \rightarrow D + D^*$$

This effects generally occurs when HOMO and LUMO of the receptor are at intermediate energy between HOMO and LUMO of the fluorophore. Upon excitation by light, an electron is transferred from the HOMO to the LUMO of fluorophore. The system comes back to the ground state *via* non radiative decay involving the simultaneous transfer of an electron from the LUMO of the fluorophore to the LUMO of the receptor and then from the HOMO of the receptor to the HOMO of the fluorophore. Finally, the ground state is restored through the transition between LUMO and HOMO of the receptor (see Figure 18).

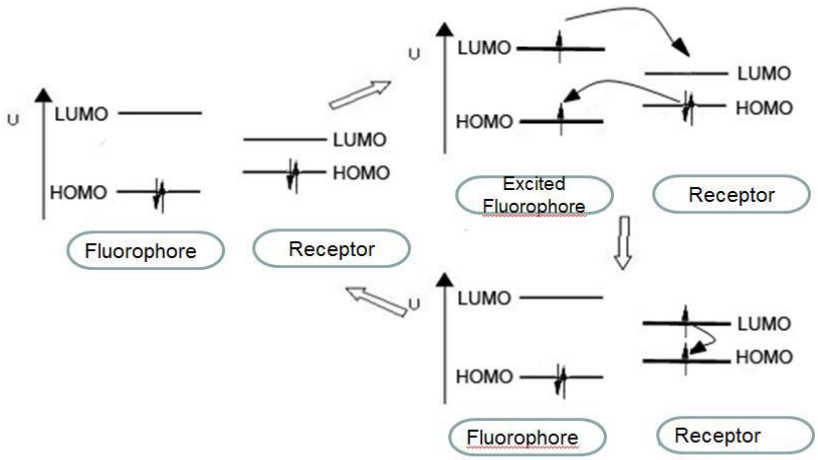

Figure 18. Electron Energy Transfer EET.

Energy transfer can occur with two different mechanisms, radiative and non-radiative, which may have different effects on the characteristics of fluorescence emission.

1.2.3.2.1- Radiative Transfer

This type of transfer does not require any interaction between A and D, i.e. it occurs without any interaction between the D and A is absent and normally occurs when the average distance between D and A is larger than the wavelength. It also depends on the concentration and the spectral overlap between the emission spectrum of D and the absorption spectrum of A.

The mechanism consists in two consecutive steps:

$$D^* \rightarrow D + h\nu$$

$$h\nu + A \rightarrow A^*$$

1.2.3.2.2- Non-radiative Transfer. This process takes place when the average distance between D and A is lower than the wavelength and it occurs without emission of photons. In this case, several vibronic transitions in the donor and in the acceptor have practically the same energy (see Figure 19).

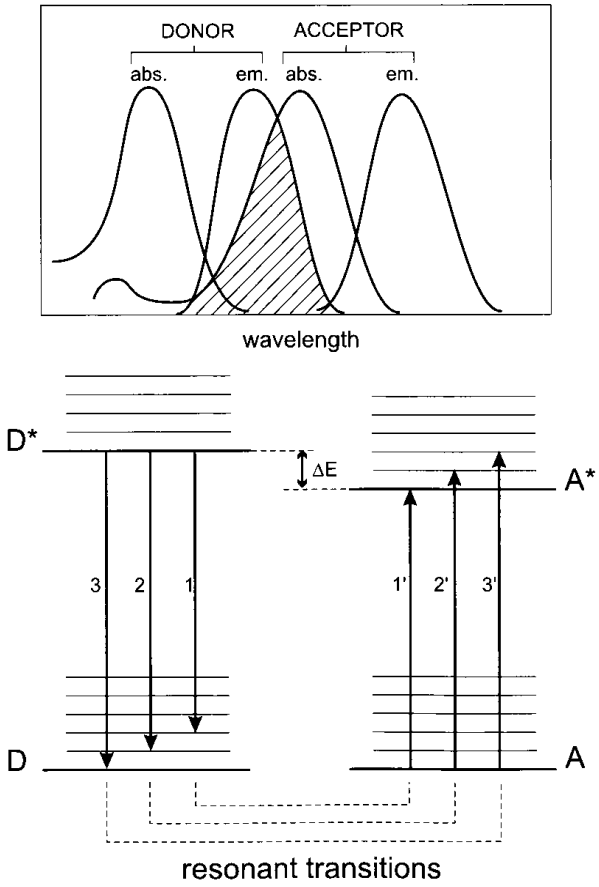

Figure 19 Energy level scheme of donor and acceptor molecules, showing the integral overlap between the emission spectrum of the donor and the absorption of the acceptor.

Non-radiative transfer can occur via two different mechanism, which gives rise to two different contributions to the overall process, a coulombian contribution, mainly electrostatic in nature

and a contribution form the overlap of the molecular orbitals of the donor and acceptor.

1.2.3.2.3- The Columbian contribution

The coulombian contribution is due to both long-range dipole–dipole interactions and short-range multi-polar interactions. It corresponds to the energy associated with an exchange of two electrons between the donor and the acceptor. The energy transfer takes place through the simultaneous transfer of an electron from the excited state to the ground state of D, and of an electron from the ground state to the excited state of A (see Figure 20).

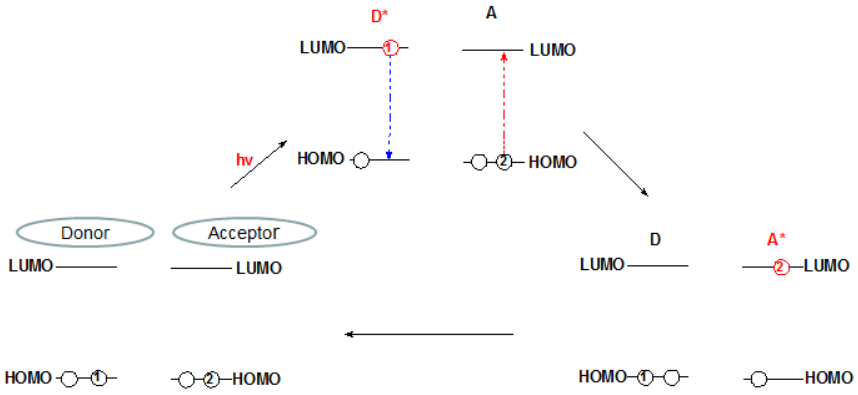

Figure 20. Coulombic mechanism.

This electrostatic contribution is the only active for long distance between the two molecules A and D, and it may result in an excitation energy transfer even at long distances (up to 80-100 Á). This mechanism is prevalent in spin-allowed non-radiative processes of electron transfer: $S_1(D^*) \rightarrow S_0(D)$ or $S_0(A) \rightarrow S_1(A)$, while it is absent not spin-allowed: $T_1(D^*) \rightarrow S_0(D)$ o $S_0(A) \rightarrow T_1(A)$.

1.2.3.2.4- The contribution due to orbital overlap

This contribution is due mainly to the electrostatic interaction between the two clouds of electronic charge of donor and acceptor. It is active just at short distances, because it envisages an overlap of the electron clouds of the two molecules A and D. Energy transfer is associated to the simultaneous passage of a first electron from the LUMO of D to the LUMO of A, and of a second electron from HOMO of A to the HOMO of D*(exchange mechanism), as depicted in Figure 21.

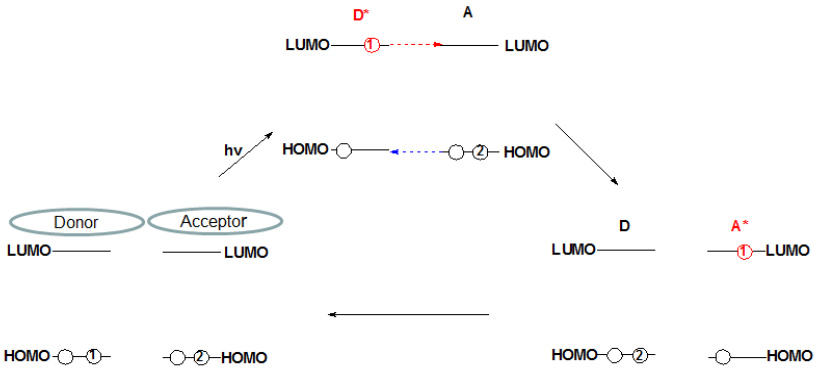

Figure 21. The contribution due to orbital overlap.

This process is predominant in not spin-allowed process: $T_1(D^*) \rightarrow S_0(D)$ or $S_0(A) \rightarrow T_1(A)$.

1.2.3.3- Photoinduced charge transfer PCT

When a fluorophore contains an electron-donor group (generally amine) conjugated to an electron-withdrawing group, the excitation can induce a process of intramolecular charge transfer from the donor to the acceptor. The consequent variation of the dipole moment in the excited state causes a shift of the wavelengths of the bands in the emission and absorption spectra (Stokes shift). The supramolecular interaction of the receptor with an ionic guest

may alter the efficiency of the charge-transfer process, determining changes in the photophysical properties of the fluorophore.

1.2.3.3.1- Interaction with the donor group

In this case the fluorophore, which contains an electron-donor group, interacts with a metal cation, thus reducing the electron-donor character of the donor and the overall conjugation in the excited state.

The coordination of a metal ion with the electron-donor group of the fluorophore (case A of the Figure F) reduce the electron-donor ability. This leads to a reduction of the charge separation and, consequently, of the dipolar moment of the molecule in its excited state. The reduction of charge separation in the fluorophore mainly destabilizes the excited state compared to the ground state, leading to a shift of the wavelengths toward greater energies of the absorption and emission spectrum (blue shift). In addition, the donor group of the molecule in the excited state has a lower tendency to the coordination of a metal ion (the electronic pair of the donor atom is less available to be used for the coordination) leading to a partial decomplexation in the excited state.

1.2.3.3.2- Interaction with the acceptor group

In contrast to the previous case, the coordination of a metal ion with the electron-acceptor group of the fluorophore, the case B of the Figure 22, occurs with an increase in the electron-acceptor character. The increased charge separation enhances the dipolar moment of the molecule in its excited state, stabilizing the excited state compared with the ground state, leading to a shift of the wavelengths toward lower energies of the absorption and emission spectrum (red shift).

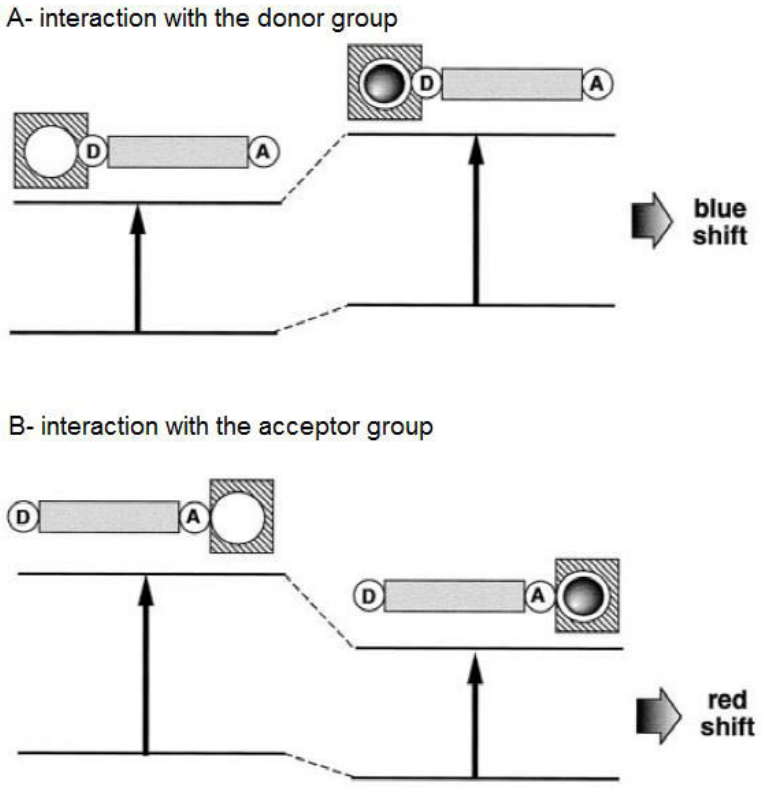

Figure 22. PCT when the cation interacts A)- with an electron-donor group or B)- with an electron-acceptor group of the fluorophore.

The effects of the coordination of metal ions to a donor group on the absorption and the emission spectra can be resumed as follows:

1) - The absorption spectra are shifted towards shorter wavelengths (higher energies) and are characterized by lower values of absorbance (the probability of a transition depends on the variation of the dipole moment).

2) - The absorption and emission characteristics depend on the metal ion, and the absorption/emission spectra are normally more

enhanced in the case of metal with with higher charge/dimension ratio

3) - The blue Shift in the absorption spectra is more marked than in the emission spectra.

4) - The stokes shift is often enhanced.

5) – The absorption and, overall, the emission intensity decrease.

1.2.3.4- Photoinduced proton transfer PPT

When a molecule absorbs photons, its acid-base properties are often different between the ground state and the excited state. In the acidic form, the pK_a^* of a proton donor group in the excited state is much lower than the pK_a in the ground state, because the acidic character can be increased by excitation. In contrast, the pK_a^* of a proton acceptor group in the excited state is much higher than in the ground state, because the acidic character can be decreased by the excitation. In fact, a redistribution of electron density in the fluorophore can occur upon absorption of light, changing the acid-base properties in the ground state and the excited state. In this case, proton transfer that normally does not occur in the ground state at a given pH, may take place in the excited state at the same pH values. The most simple case is proton transfer in aqueous solution from the excited species of a proton donor, AH *, to the surrounding water. This is the case of phenolic functions, whose acidity increases upon excitation. Consequently, the pK_a^* of the -OH group in the excited state will become lower than the pK_a reported in the ground state. Actually, this is the working principle of pH fluorimetric indicators.

1.2.3.5- Formation of excimers and exciplexes

Excimers (excited dimer) are dimers in the excited state. They are formed by the association between a molecule in its excited state and an equal molecule in its ground state, according the reaction:

$$M^* + M = (M\text{-}M)^*$$

Exciplexes (excited complexes). They are formed by the association between a molecule in its excited state and a different molecule in its ground state. The formation of exciplexes generally occurs when a molecule has electron-donor characteristic while the other one presents an electron-acceptor character.

$$D^* + A = (D\text{-}A)^*$$

$$D + A^* = (D\text{-}A)^*$$

The formation of excimers and exciplexes leads to the formation of a new band at lower energy, due to the stabilizing effect generated by the interaction between the two molecules. In same cases, the guest species may lead to the formation of exciplexes in a chemosensor. This occurs when the chemosensor contains two fluorogenic units. For instance, the coordination of a metal ion can lead to a structural change of the receptor that leads the two fluotrogenic groups at short distance, thus allowing for the formation of excimers or exciplexes.

1.2.4- Fluorescent pH indicators

The fluorimetric pH indicators provide greater sensitivity compared with the most common colorimetric indicators (the classical dyes based on color changes). They are widespread in the analytical and bioanalytical chemistry, cellular biology, and also in the medical field.

The value of pH is not defined by the concentration of H^+, but through the activity of protons H^+, as shown in the relationship below:

$$pH = - \log a_{H^+}$$

Their use in optical methods is based on visual determination of the concentrations of the acid form [A], and the basic form [B], of the indicator. A rearrangement of the equation of Henderson – Hasselbach is generally used:

$$pH = pK_a + \log [B]/[A]$$

Which leads in the fluorometric measurements to the expression:

$$pH = pK_a + \log [I - I_A]/[I_B - I]$$

where:

I: intensity of fluorescence at a given wavelength.

I_A: intensity of fluorescence measured at the same wavelength when the sample is in the acid form.

I_B: Intensity of fluorescence measured at the same wavelength when the sample is in the basic form.

In most of applications, these indicators are used in a range of pH around the pK_a and exploit the fact that the pK_a in the excited state is different.

These indicators can be divided into three classes according to the elementary processes occurring in the decay process

1.2.4.1- Class A

Fluorophores that undergo a photoinduced proton transfer, without the involvement of electron transfer processes. In general this type of fluorophores is much more acidic in the excited state (pK_a is lower) than in the ground state. Therefore, the emission in a pH range close to the pK_a in the ground state, is due to the basic form of the indicator because the excitation of the acidic form is followed by the deprotonation of the excited state. An example can be the indicator pyranine(1-hydroxypyrene-3,6,8-trisulfonic acid trisodium salt, DHPDS (see Figure 23) and hydroxycoumarin.

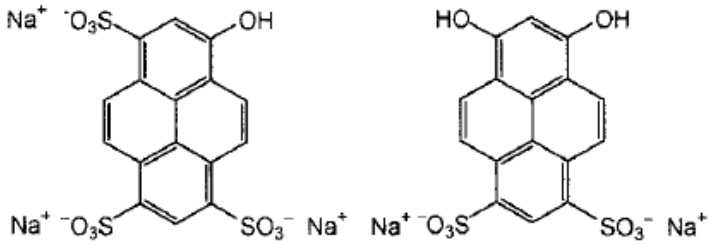

Figure 23. Examples of class A fluorescent pH indicators.

1.2.4.2- Class B

Fluorophores that do not undergo photoinduced proton transfer or photoinduced electron transfer. By increasing the pH, the absorption bands and the emission bands of the acidic form decrease in intensity, while at the same time, those of the basic form increase. In other words, the evolution of the spectrum of fluorescence and absorption *vs* pH are be similar. An example can be the indicator SNAFL, fluorescein (see Figure 24) and eosin Y**.**

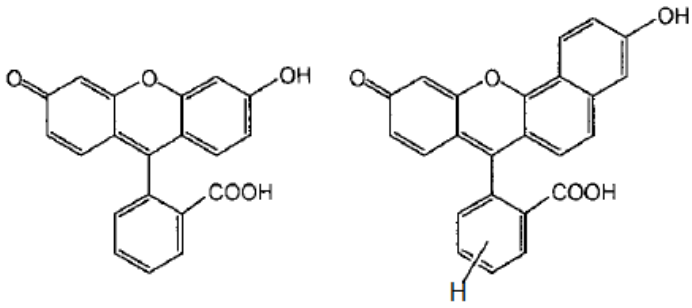

Fluorescein **SNAFL-1**

Figure 24. Examples of class B fluorescent pH indicators.

1.2.4.3- Class C

Fluorophores that undergo a photoinduced electron transfer, without any photoinduced proton transfer. When these fluorophores are in their non-protonated form, the emission of fluorescence is very low, because of the quenching due to the internal PET process. Protonation suppresses electron transfer, Thus leading to leads to a marked increase of the fluorescence emission. Therefore, the forms of the bands of the excitation and fluorescence spectra are dependent on the pH. An example can be the indicator perylene bisimide (PBI) dyes, as shown in Figure 25.

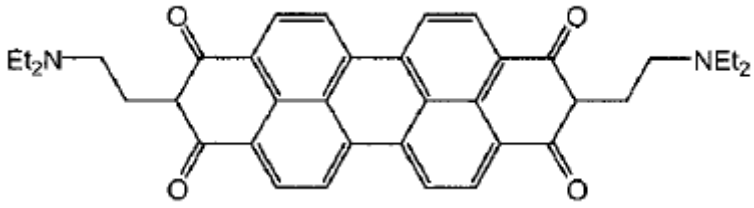

Figure 25. Examples of class C of fluorescent pH indicators perylene bisimide (PBI) dyes.

1.2.5- Fluorimetric sensors

In a fluorimetric chemosensor, the fluorogenic group acts as sensing agent analyte detection. In fact, the binding event changes the photophysical characteristics of this sub-unit, generating a detectable variation of the luminescence emission.

The fluorophore acts as transducer of the signal monitoring the interaction of the receptor with the substrate. A fluorimetric indicator offers great advantages given the wide range of usable fluorophores with different of wavelengths, together with a very rapid response as a result of complexation of the targeted species. These characteristics, joined to the properties already cited for supramolecular sensors (selectivity, velocity, reversibility, etc.) making the investigations with fluorescence sensors effective with a variety of chemical species, as shown in Figure 26:

a- Metal cations.
b- Inorganic and organic anions (it is a very widespread technique in biochemistry).
c- Neutral molecules and gas.

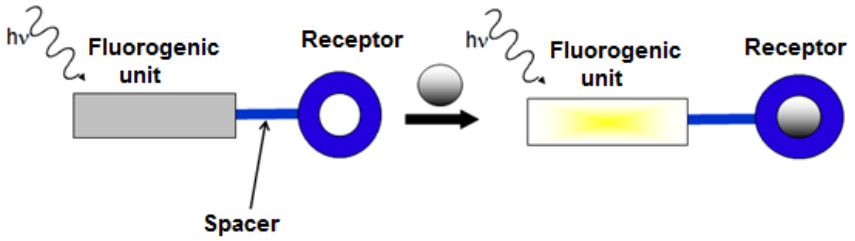

Figure 26. Fluorescence sensors effective with a chemical species.

1.2.5.1- Fluorimetric sensors for metal cations

Metal cations may have an important role in many biological processes and/ or can have profound effects at the environmental level[37,38]. The growing interest towards tools able to determine the

[37] A. X. Trautwein, Bioinorganic Chemistry, Wiley-VCH, Weinheim (1997).

concentration of these analytes (separately or simultaneously) in samples of biological or clinic relevance, as well as towards analytical methods for the in-situ determination of metal ions lead to the development of fluorescent molecular sensors capable to quantitatively detect these ions. As far selectivity is concerned, measurements based on the enhancement of the emission signal upon binding of the targeted species are analytically favored compared to those which induce emission quenching. In the first case, in fact, the Signal-to-Noise ratio is not only greater (making possible also the detection at the level of single molecules)[39,40] but the fluorescence increase is also accompanied by a new and characteristic lifetime, which can be exploited for discrimination between analytes with different lifetimes. Commonly the cations of heavy metals and transition metals have intrinsic properties that cause quenching of the emission of organic fluorophores.

The observable variations in the absorption spectrum (ipso- or bathochromic Shift) are similar for all the metal ions and the bands of the complexes often overlap[41]. The shifts induced by the ion reflect the electrostatic interaction between the free electron pairs of the donor atoms and the metal cation.The molar extinction coefficient of the free ligand and of the complex are often similar. In contrast to the invariability in the absorption characteristics, the emission featues strong variations as a result of the complexation of the metal ion.

---

[38] E. Merian, VCH, Weinheim (1991).

[39] W. P. Ambrose, P.M. Goodwin, J.H. Jett, A. Van Orden, J.H. Werner, R.A. Keller, Chem. Rev., 99 (1999), 2929.

[40] M. Prummer, C. G. Hübner, B. Sick, B. Hecht, A. Renn, U. P. Wild, Anal. Chem., 72 (2000), 443.

[41] C. Bazzicalupi , A. Bencini, A. Bianchi, C. Giorgi, V. Fusi, B. Valtancoli, M. A. Bernardo, F. Pina, Inorg.Chem., 38 (1999), 3806.

There are three situations that result directly related to the periodic properties and the electronic configuration of the targeted metal ions:

• The complex is more fluorescent than the free ligand (CHEF): only small diamagnetic transition metals, such as Zn^{2+}, give rise to this effect with most part of these sensors.

• The complex is weakly fluorescent (partial CHEQ): it is the typical case of the diamagnetic ions such as Hg^{2+} or Pb^{2+}, which can be considered "heavy metals" in terms of the heavy atom effect[42] and that determine a more or less pronounced quenching of the fluorescence[43,44].

• The complex doesn't fluoresce (CHEQ total): it is typical of paramagnetic ions with an orbital d not completely filled[45,46], for example Cu^{2+} or Ni^{2+}.

While the effects of quenching are substantially related to the nature of the metal ion, the increase in fluorescence can arise from changes in the geometry or in the flexibility of the ligand. They can also be induced by the coordination of the ion in the complex, due to the different availability of certain functional groups involved in the processes of deactivation of the free ligand. In addition, the induced variations by the coordination in the relative position of energy levels with similar energy centered on the ligand can preclude a channel for non radiative deactivation. In the case of flexible ligands, the coordination generally suppresses non

[42] D. S. McClure, J. Chem. Phys., 20 (1952), 682.

[43] A. Harriman, J. Chem. Soc., Faraday Trans. 2, 77 (1981), 1281.

[44] H. Masuhara, H. Shioyama, T. Saito, K. Hamada, S. Yasoshima, N. Mataga, J. Phys. Chem., 88 (1984), 5868.

[45] T.L. Banfield, D. Husain, Trans. Faraday Soc., 65 (1995), 1969.

[46] A.W. Varnes, R.B. Dodson, E.L. Wehry, J. Am. Chem. Soc., 94 (1972), 946.

radioactive processes of decay of the excited state, such as torsional movements of the molecule[47].

1.2.5.1.1- General features of fluorescent sensors for metal ions

Fluorescence involves the photon emission that occurs nanoseconds after the absorption. A fluorescence microscope takes advantage of the shift in the wavelength between the absorbed and emitted light by filtering the light due to the excitation source without blocking the emitted light[48].

Fluorescent sensors for metals should possess two essential features: a metal chelating or binding moiety, and at least one fluorophore capable of absorbing and emitting light. Metal binding should change either the electronic structure or the molecular structure of the sensor.

1.2.6- Photophysical Properties of Fluorophores

In a fluorimetric sensor, the most important property is its ability to be detected within the complex environment of real matrices, including living cell and tissues. The brightness and stability of fluorophore(s) affects on the sensitivity and signal-to-noise ratio of the sensor. The theoretical brightness of a fluorophore is defined as the product of the extinction coefficient and the quantum yield[49]. The extinction coefficient is the efficiency with which a chromophore absorbs light, while the quantum yield represents the efficiency with which a fluorophore emits light after absorption. Because many metal sensors involve a change in brightness upon metal binding, the brightness is reported in the metal-free and

[47] K. Rurack, R. Radeglia, Eur. J. Inorg. Chem. (2000), 2271.

[48] Lichtman, J. W.; Conchello, J. A. Nat. Methods 2005, 2, 910.

[49] Shaner, N. C.; Steinbach, P. A.; Tsien, R. Y. Nat. Methods 2005,2, 905.

metal bound state. The differences in viscosity, pH, solvent, accessibility to oxygen, or other factors associated with the environment and between the vitro (in a cuvette) e in situ (inside a real matrix, such as a cell) can generate differences in the photophysical properties of the sensor[50,51,52].

The wavelength of excitation and emission is an important factor that impacts detection sensitivity in real matrices. Considering, for instance, the cellular environment, many biomolecules absorb light in the UV and visible spectrum. Because excited molecules can react with molecular oxygen to produce free radicals, exposure to electromagnetic radiation can produce reactive oxygen species, which can damage biological samples[53,54,55]. Generally, higher energy, lower wavelength light causes greater photodamage than lower energy, longer wavelength light[56,57]. Light is also scattered when it encounters matter, and this scattering depends on the nature of the tissue and wavelength of light[58]. As a general rule, a fluorescent sensor that absorbs and emits at longer wavelengths leads to less phototoxicity, decreased background autofluorescence, and are subject to decreased scattering.

---

[50] Tsien, R. Y. Annu. Rev. Neurosci. 1989, 12, 227.

[51] Roe, M. W.; Lemasters, J. J.; Herman, B. Cell Calcium 1990, 11, 63.

[52] Poenie, M. Cell Calcium 1990, 11, 85.

[53] Grzelak, A.; Rychlik, B.; Bartosz, G. Free Radical Biol. Med. 2001, 30, 1418.

[54] Dixit, R.; Cyr, R. Plant J. 2003, 36, 280.

[55] Hoebe, R. A.; Van Oven, C. H.; Gadella, T. W., Jr.; Dhonukshe, P. B.; Van Noorden, C. J.; Manders, E. M. Nat. Biotechnol. 2007, 25, 249.

[56] Godley, B. F.; Shamsi, F. A.; Liang, F. Q.; Jarrett, S. G.; Davies, S.; Boulton, M. J. Biol. Chem. 2005, 280, 21061.

[57] Pattison, D. I.; Davies, M. J. EXS 2006, 131.

[58] Cheong, W.-F.; Prahl, S. A.; Welch, A. J. IEEE J. Quantum Electron. 1990, 26, 2166.

Often referred to detection sensitivity as the contrast between signal and background, this depends on the inherent properties of the sensor, the biological specimen and on the instrumentation available. The factors that influence the intensity of a measured fluorescence signal are: excitation source (intensity and nature of the source), filter sets, camera sensitivity,etc[59].

1.2.7- Chemosensor

A chemosensor is a molecule capable of determining the presence or the concentration of a targeted analyte interacting with it[60]. The interaction must be selective, not destructive and reversible, it must also determine a significant change of some characteristics of the sensor in order to be identified by the operator.
A chemosensor is generally composed by three subunits:
1) - Receptor: a subunit involved in the interaction with the substrate. This unit should show selectivity and reversibility in substrate binding.
2) - Active unit: the molecular fragment responsible for the variation of a characteristic that signals the presence of the substrate.
3) - Spacer: the linker between the two subunits above mentioned (receptor and active unit) when this is necessary.

The receptor generally should be able to bind the substrate, *via* a molecular recognition event, (lock and key principle), in other words a selective interaction should occur with respect to possible competing species. The selectivity is determined by the complementarity between the size, the shape and the disposition of the binding sites of the substrate and the receptor, in order to obtain the largest possible number of non-covalent interactions between the two partners. Possibly, the receptor should be pre-organized for substrate recognition, in order to minimize the energy required to achieve the final conformation and to increase the

[59] Lichtman, J. W.; Conchello, J. A. Nat. Methods 2005, 2, 910.
[60] B. Valeur; Molecular Fluorescence, Wiley-VCH Weinheim 2002.

stability of the adduct. In addition, the surface of contact between the receptor and the substrate should be as greatest as possible. In addition, the interaction should be kinetically fast and reversible.

Useful properties for substrate detection can be variations in color, variations in electrochemical nature (for example, the variation of the reduction potential) or, in the case of a photochemical sensor, variations in the emission of fluorescence.

1.2.7.1- Polyamine chemosensors

Overall, polyamine receptors, in particular of macrocyclic type, play a major role in chemistry of chemosensors for metal cations and anions. In fact, polyamine can give protonated species in aqueous solutions, optimal receptor for anionic species, and, at the same time, they can form stable complexes with transition metal in aqueous solution. Therefore, these ligands can be used as receptor units in fluorescence chemosensors. Furthermore, polyamines are normally highly soluble in water. This property often ensures a good solubility in aqueous solutions to fluorescence chemosensors formed by a polyamine binding unit and a fluorogenic sensing moiety, overcoming one of the mayor problem that often affects the mosts common fluorophore, e.g, their scarce solubility.

1.2.8- Utilized fluorophores

In this thesis we have synthesized new ligands containing one or two macrocyclic compounds as binding sites. Fluorogenic units have been either appended to a single macrocyclic unit or used as bridging linker between two macrocycles. We have used four different types of fluorogenic units, derived from quinoline, 8-OH quinoline, acridine and bipyridyl. For a better comprehension of our

results we summarize below the main photophysical properties of these fluorophores as such.

1.2.8.1- Quinoline

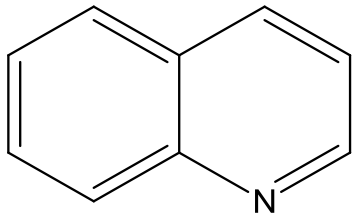

Figure 27. Quinoline.

Quinoline is an heterocyclic compound featuring a very high quantum yield in fluorescence emission. In addition, it possesses a nitrogen donor available for the interactions with metal cations. It gives an acid-base equilibrium in an aqueous solution, with pK_a= 4.79 (see Figure 28).

Figure 28. Equilibrium acid-base of the quinoline.

Considering the UV-Vis spectrum, quinoline shows a wide band with a maximum at 318 nm, while the cation of quinoline deriving from the protonation of the heteroaromatic nitrogen atom shows a blue-shifted structured band with a maximum at 305 nm, as shown in Figure 29 .

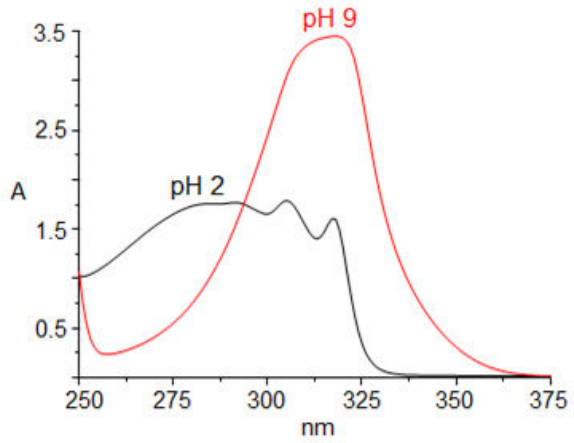

Figure 29. UV-Vis spectra of quinoline in solution of water-ethanol (5×10^{-4} M) 70:30 (V:V) at pH 2 (quinolinium cation) and at pH 9 (neutral form).

Fluorescence emission spectra of the protonated and non-protonated form of quinoline are substantially different. Figure 30 reports the emission spectra obtained with a 315 nm excitation wavelenght. Quinoline shows an emission band with a maximum at about 425 nm, while the band of the quinolinium cation is shifted toward shorter wavelengths at 350 nm.

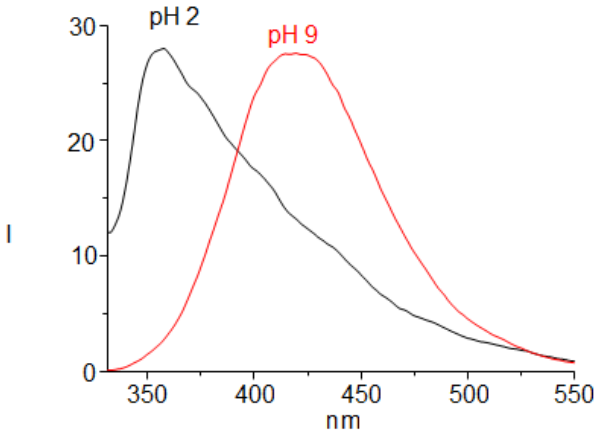

Figure 30. fluorescence emission spectra of quinoline in solution of water-ethanol (5×10^{-4} M) 70:30 (V:V) at pH 2 (quinolinium cation) and at pH 9 (neutral form), λ_{exc} = 315 nm.

The fluorescence intensity of quinoline depends on the interactions through hydrogen bonding between the solute and the solvent. In particular, the quinoline emits in apolar solvents more than the polar solvents. In fact, the excited state of singlet at lower energy is n,π * in polar solvents, while in apolar or scarcely polar solvents is π,π*. The decay from the state n,π* to the ground state is forbidden for symmetry, and this inhibits the process of radiactive decay. Therefore, the decay to the ground state in polar solvents takes place preferentially through non radiative processes, such as intersystem crossing and/or internal conversion, rather than through radiative emission, as shown in Figure 31.

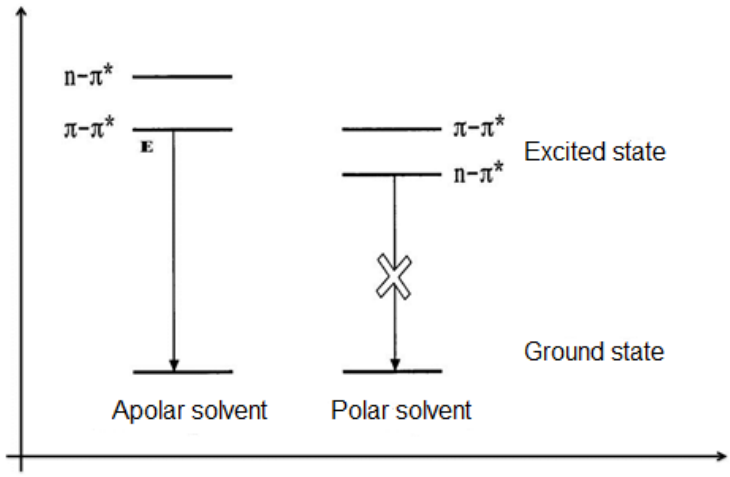

Figure 31. The decay to the ground state of the excited states of quinoline in polar and apolar solvent.

1.2.8.2- 8-Hydroxyquinoline

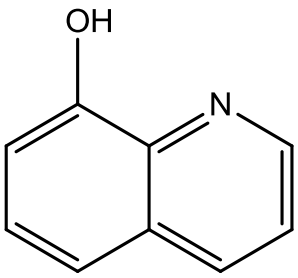

Figure 32. 8-Hydroxyquinoline.

8-Hydroxyquinoline is a derivative of quinoline, that is formally obtained by substitution of the hydrogen in position 8 with a hydroxyl group. Similarly to quinoline this fluorophore possesses a good quantum yield of fluorescence, but the emission band is more shifted towards the visible region than the quinoline.

8-hydroxyquinoline behaves as a bidentate chelating agent, using both the hydroxyl group and the heteroaromatic nitrogen atom in the process of coordination of metal ions.
In aqueous solution, there are two acid-base equilibria, as shown in Figure 33; the first involves the oxygen atom of the hydroxyl group, with a pK_a of 9.89.
the second involves the heteroaromatic nitrogen atom, with a pK_a of 5.13.

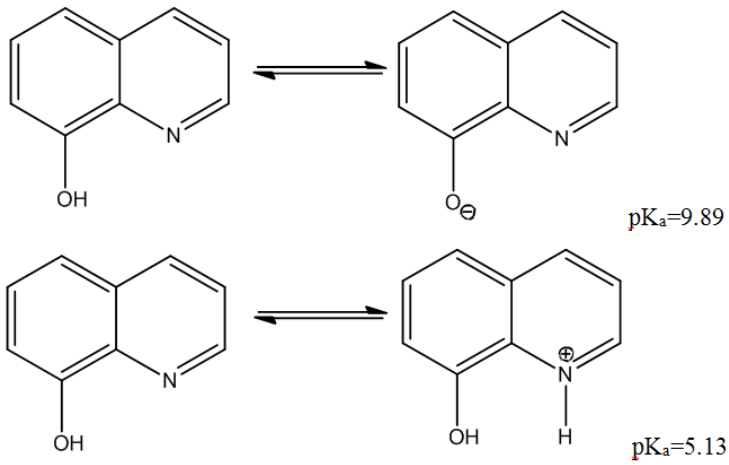

Figure 33. Equilibria of protonation and deprotonation of 8-hydroxyquinoline.

8-hydroxyquinoline in aqueous solution gives rise to a photoinduced proton transfer process (PPT) from the -OH group to the heteroaromatic nitrogen atom, and actually, the molecule is in its zwitterionic form in the excited state (see Figure 34).

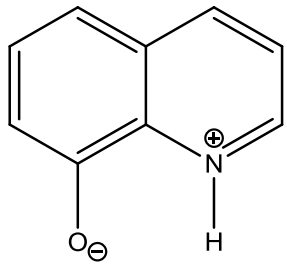

Figure 34. The zwitterionic form 8-hydroxyquinoline.

The PPT process makes the molecule scarcely emissive in aqueous environment. Only at strongly acidic pH values, where 8-hydroxyquinoline is in its protonated and positively charged form (8-hydroxyquinolinium cation), and at strongly basic pH values, pH> 12, where the fluorophore is present in monoanionic form, the molecules becomes emissive. Metal coordination induce deprotonation of the –OH group and, therefore, metal binding can be accompanied by an increase of the fluorescence emission. This

aspect makes this fluorophore very promising for the achievement of chemosensors for the detection of metal ions *via* an OFF-ON mechanism.

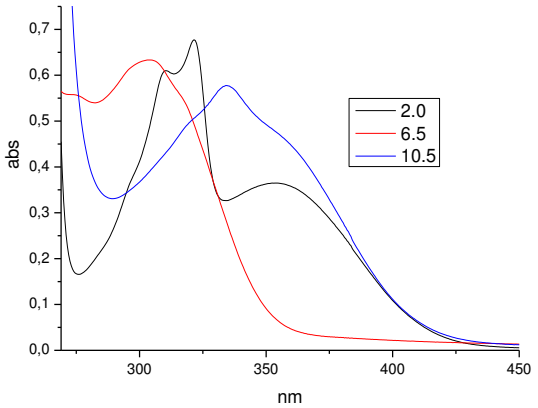

Figure 35. UV-Vis spectra of 8-hydroxyquinoline in aqueous solution at different values of pH.

Considering the characteristics of UV-Vis absorption of 8-hydroxyquinoline, Figure 35 shows that in very acid environment, where in aqueous solution the cation 8-hydroxyquinoliniumcation, the spectra are characterized by two bands with maximum at 321 and 354 nm, resepctively. By increasing tpH, the band at 354 nm disappears and the spectra feature a single band at 303 nm attributable to the neutral form of 8-hydroxyquinoline, containing a protonated -OH group and a not-protonated nitrogen atom. This band undergoes a red-shift up to 334 nm at alkaline pH values due to the presence of the anionic specie of 8-hydroxyquinoline in solution.

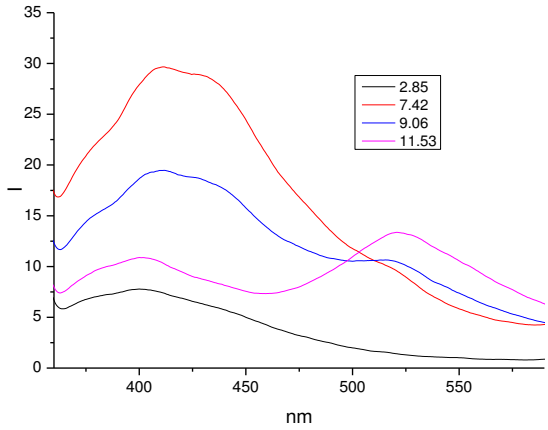

Figure 36. Emission spectra of 8-hydroxyquinoline at different values of pH.

The 8-hydroxyquinoline fluorescence emission spectra, shown in figure 36, are recorded at various pH values. At acidic pH value (pH=2.85), when the fluorophore is in its cationic monoprotonated form, the emission spectrum features a very weak band at ca 400 nm. By increasing pH, the band shape changes and presents an emission maximum at 410 nm, whose intensity increases up to pH 8.6 (pH 11.53). This spectral features are typical of the neutral form of 8-HQ. A more alkaline pH values, the emission intensity at 410 nm decreases and simultaneously a second band appears in the spectra, due to the formation of the monoanionic form of 8-HQ.

1.2.8.3- 2,2'-bipyridyl

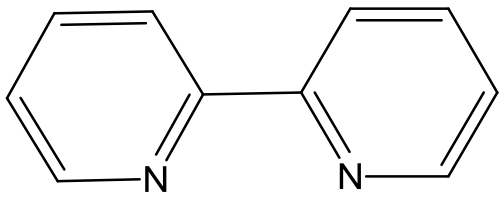

Figure 37. 2,2'-dibyridyl can be considered as a simple dimer of pyridine and it is widely utilized such as a ligand for cations.

The widespread use of this molecule as a ligand depends on its great affinity demonstrated for various metal ions, due to the ability of this ligand to act as bidentate chelating agent[61]. This molecule is not particularly emissive and normally featrure a low quantum yield of fluorescence[62]; nevertheless, some metal complexes with 2,2'-bipyridyl are strongly emissive[63].
bipyridyl is a weak base with a pK_a relative to the bipyridyl protonation of 5.3 log units.
The absorption spectrum shows two bands at 282 and 235 nm, which are typical of non-protonated form of the molecule, see figure 38. The spectrum of its protonated form shows a marked red-shift, with peaks centered to 301 and 241 nm.

[61] P. A. Lay, A. M. Sargeson, H. Taube, Inorg. Synth., 24, (1986), 291–299.

[62] M. S. Henry, M. Z. Hoffman, J. Phys. Chem., Vol. 83, No 5, (1979), 618-625.

[63] 39 G. P. McDermott, P. Jones, N. W. Barnett, D. N. Donaldson, P. S. Francis, Anal.Chem., 83, (2011), 5453–5457.

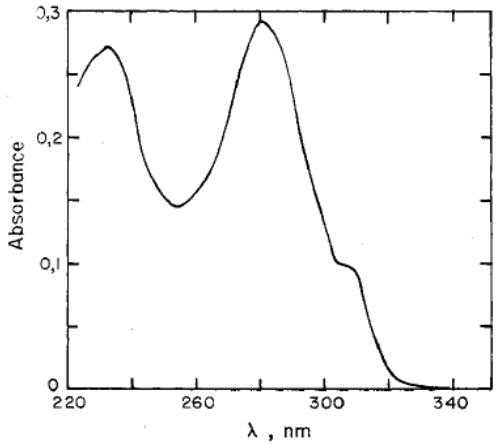

Figure 38. UV-Vis spectrum of 2,2'-bipyridyl.

The emission spectrum is also pH-dependent, due to the protonation equilibrium. This heterocycle display an emission band at 443 nm when not protonated , as shown in Figure 39. This band undergoes a marked red-shift upon protonation of the heterocycle, due to the different conformation that the 2,2'-bipyridyl assumes at different pH values. Below pH 5.3, bipyridyl is in its protonated form and the acidic proton, is shared by the two nitrogens via hydrogen bonding, thus stabilizing the cis conformer of the molecule; in neutral or basic solution, bipy is not protonated and the trans conformer is energetically favored.

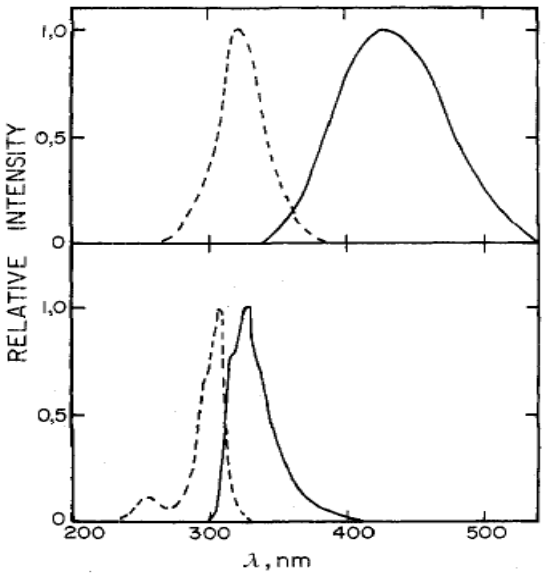

Figure 39. Emission spectrum (____) and UV-Vis spectrum (- - -) of 2,2'-bipyridyl in aqueous solution. The spectrum: above at pH=1.7; below at pH=8.2.

1.2.8.4- Acridine

Acridine is a heterocyclic compound, which presents three condensed rings. Acridine possesses a particularly high quantum yield of fluorescence emission, making this molecule a potential candidate as a fluorescent unit for the realization of fluorimetric chemosensors.

In addition, it posseses a nitrogen donor available for the interactions with metal cations. Acridine also gives an acid-base equilibrium in an aqueous solution, with pK_a= 5.4 (see Figure 40).

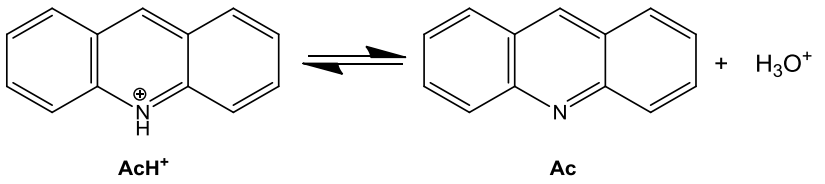

AcH^+ Ac

Figure 40. Protonation equilibrium of acridine.

Considering the UV-Vis spectral features, acridine presents a structured band with maximum at 356 nm in aqueous solution (Figure 41). Protonation of the nitrogen atom to give the acridinium ion leads to an enhancement of this band and to the appearance of a shoulder at ca 400 nm[64].

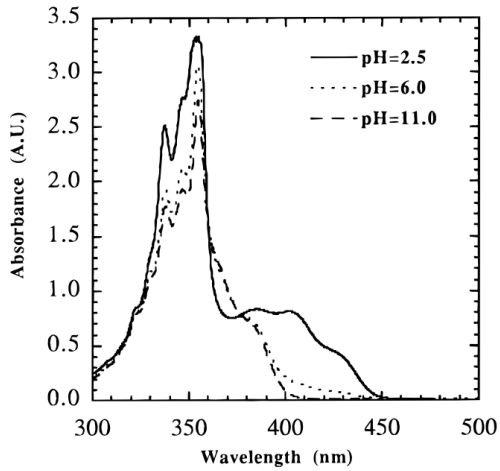

Figure 41. Absorption spectra of solutions of acridine (1 $\times 10^{-4}$ M)in aqueous solution (1 $\times 10^{-4}$ M) at room temperature, at pH 2.5, 6.0 and 11.0, respectively.

The fluorescence emission spectra in aqueous medium are also strongly affected by the protonation state of nitrogen atom. While not protonated acridine presents an emission band with a maximum at about 425 nm, the acridinium cation band is red shifted with a maximum at about 475 nm, as shown in Figure 42.

[64] E. T. RYAN, T. XIANG, K.P. JOHNSTON, M.A. FOX, J. Phys. Chem. A, 101(1997), 1827-1835

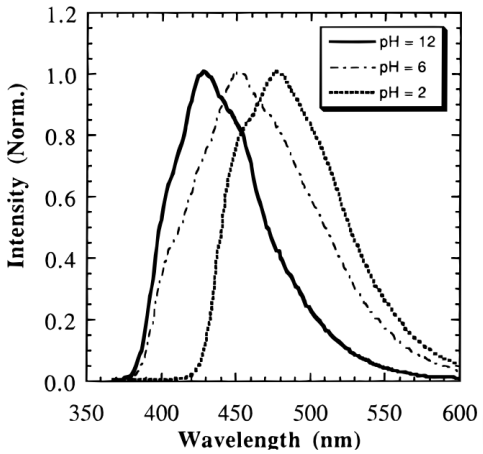

Figure 42. Fluorescence spectra of acridine (1×10^{-4} M) in aqueous solution at ambient temperature, at pH 2, 6 and 12, respectively.

The emission of acridine is also strongly dependent on the solvent, and in particular by the ability of the solvent to interact *via* hydrogen bonding with the nitrogen atom of the heterocycle. Indeed acridine emits in both protic and aprotic solvents. The interpretation of this phenomenon can be attributed to the fact that the lowest excited singlet state for many nitrogen heterocycles is of $n \rightarrow \pi^*$ in aprotic solvents but of $\pi \rightarrow \pi^*$ in solvents that donate hydrogen bonds. The decay of $n \rightarrow \pi^*$ of the ground state is forbidden by symmetry as is shown in Figure 43, the processes of radiative decay will be inhibited, then the return to the ground state will be almost exclusively by non-radiative process because of efficient intersystem crossing and/or internal conversion.

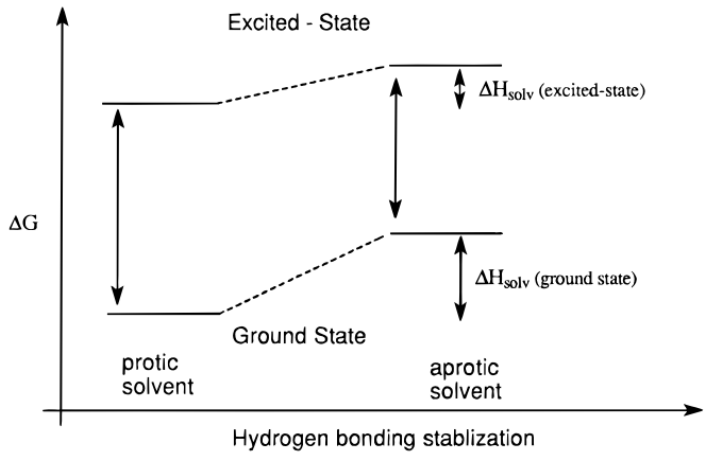

Figure 43. Effect of hydrogen bonding on the n-π* transition energy typical of nitrogen containing acridine

1.3- Objectives of the thesis project

The objective of this research is the realization of receptors able to bind selectively and reveal the metal ions of environmental or biological interest through quantifiable variations of their fluorescence emission. For this purpose we have made some chemosensors of fluorescence containing one or more polyamine units as coordination sites for metal ions and we started the study of their coordinative properties.

The chemosensores usable in vivo could allow to monitor some metabolic processes and determine the position of the ion metal inside the cell. Therefore, based on this fact and on previous researches in this field, in this thesis they have been achieved several chemosensors of fluorescence, that are capable of recognizing Zn^{2+} in the solution, in cells and tissues, where most of these chemosensores are capable of coordinating just with Zn^{2+}. So, this thesis is targeted towards the synthesis and characterization of five fluorescent chemosensors to evaluate their luminescent properties in the presence of bipositive ions of the

transition metals and post-transition metals, also for the selective recognition of Zn^{2+}.

We used as the reagents derived bis-aminal of type tetraaza macrocycle cyclen = (1,4,7,10-tetraazacyclododecane) (for: H_2L1, H_4L2, L3 and L4) and [12]aneNS_3 macrocyclic system (for L5) as coordinating. Also, they were used quinoline, 8-OH quinoline, 2'2-bipyridyl and acridine as fluorogenic units, where in addition to their luminescent properties, are also well known for their capacity to coordinate metal ions.

They were synthesized and characterized five new ligands, one was made by a cyclen with two quinoline units and two carboxyl groups in trans position H_2L1. The second ligand H_4L2 was synthesized through substitute the quinoline in H_2L1 with 8-hydroxy quinoline, while the third ligand was constituted from a unit of bipyridyl connected with two units of cyclen in position 4,4 ; L3. We synthesized the system L4, formed by two units of cyclen connected by two units of 2'2-bipyridyl, arranged in a manner that to form a cavity capable of hosting both metal ions and other chemical species. At each ligand, the fluorogenic unit was bound to a nitrogen atom of the macrocycl through a methylene bridge.

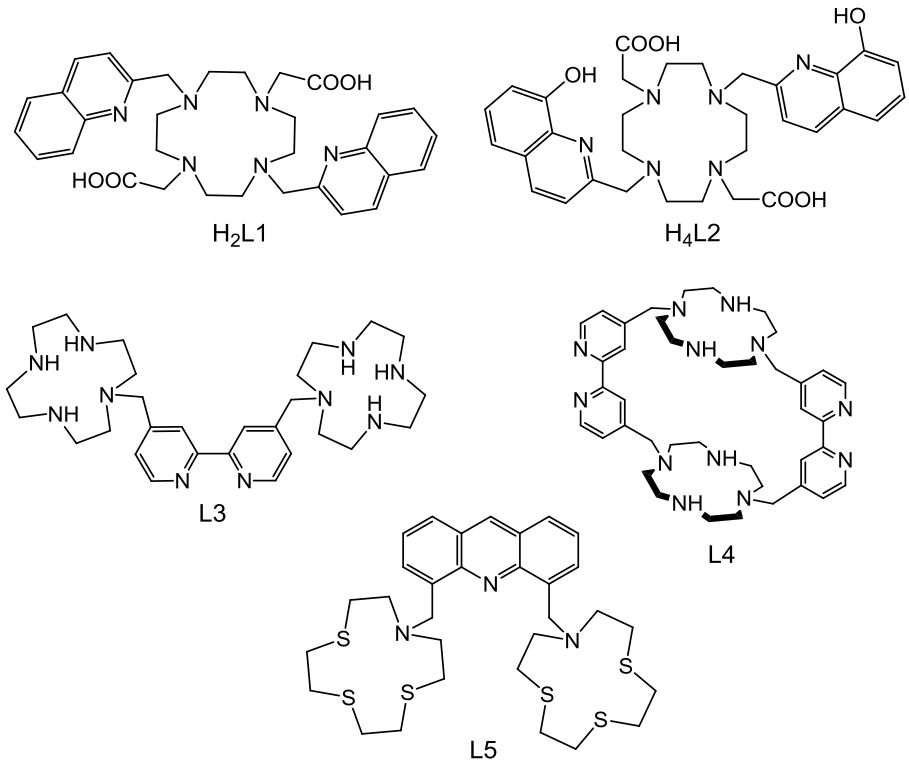

Figure 44 Synthesized ligands.

The great importance of these ligands due to their solubility in water and to their good affinity for the transition metal cations and post-transition metals. Also, the presence of fluorescent units (quinolone, 8-OH quinolone, 2'2-bipyridyl and acridine) make these ligands work as potential fluorescent chemosensors. The photochemical characteristics of these systems could be affected by the coordination with metal ion or by the protonation of the nitrogen atoms of the macrocyclic system or of the fluorescent unit.

The study of the ligands H_2L1, H_4L2, L3, L4 and L5 has been addressed through ^1H NMR, potentiometric, spectrophotometric and spectrofluorimetric titrations of coordinate properties of the

system in aqueous solution against different metal ions such as: Zn^{2+}, Cd^{2+}, Cu^{2+} and Pb^{2+}, where the potentiometric measures allow to determine the species that are formed in solution and also determine their stability. The coordination was analyzed by four metal ions aforementioned, the coordination of Zn^{2+} and Cd^{2+} generally leads to increase the fluorescence emission of chemosensors (their complexes are often fluorescent), that they are containing polyamine units as sites of "binding", while the coordination of Cu^{2+} and Pb^{2+} leads to decrease the fluorescence emission of chemosensors(their complexes are not fluorescent), this is because of Cu^{2+} is paramagnetic, while Pb^{2+} for the heavy-atom effect. Through the variations of fluorescence emission, showed that these receptors are capable to coordinate and indicate in a selective manner the ion Zn^{2+}, making sure that these systems are potential fluorescent chemosensors for Zn^{2+}.

2 – EXPERIMENTAL

2.1 – Synthesis

2.1.1 – Synthesis of fluorophores

2.1.1.1 – Synthesis of 2-(chloromethyl) quinoline

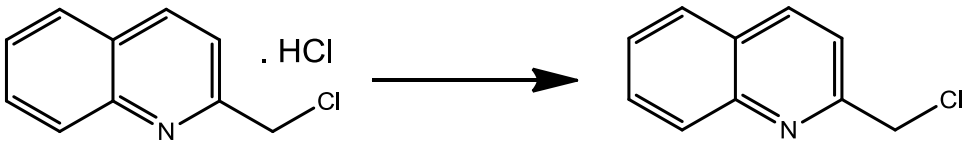

1 **2**

It is dissolved (1.5 g, 7.1 mmol) of **1** in 250 ml of distilled water in a beaker. Then, it is added a dropwise of K_2CO_3 20% until reaching to pH=7. After obtaining the required pH, the product extracted with dichloride methane (5x100 mL). The organic layer was dried over Na_2SO_4 and evaporated under reduced pressure (1.15 g, 93%).

2.1.1.2 – Synthesis of 8-hydroxyl quinoline

2.1.1.2.1 – Reduction of 8-hydroxy quinolone-2-carbaldehyde to 8-hydroxy-2-hydroxy methyl quinolone

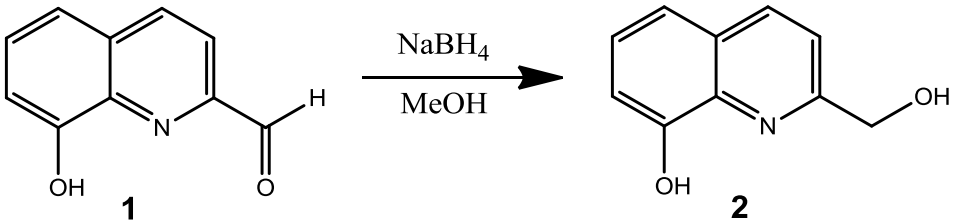

1 **2**

To a solution obtained by dissolving the compound 1 (2g; 11.56

m.mol) in 120 mL of MeOH, it was added dropwise of the solution of $NaBH_4$ (0.25 g; 13.22 m.mol) in 60 mL of MeOH. The reaction was followed with TLC evidence in support of silica (eluent: ethyl acetate / hexane 1: 1). Then it was evaporated under reduced pressure for eliminating most part of the solvent, after that it is added 80 mL of H_2O to the reaction mixture, next HCl 1M (about 10 ml) is added for neutralizing and extracted with ethyl acetate (4x50 ml). The collected solution in the flask is dried by addition of Na_2SO_4 and is evaporated under reduced pressure for removing the solvent. The obtained solid was ricristallizzo with hot ethyl acetate and hexane, the solid is recovered by filtration on a Büchner.
The yield : 1.94 g (97%).

2.1.1.2.2 – Synthesis of 8-hydroxy-2-chloro methyl quinoline

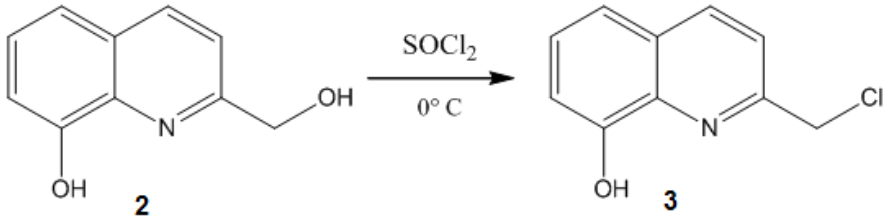

In an ice bath of 0 °C, they are put 1.94 g (11.09 mmol) of compound 2, then they are added dropwise 20 mL of $SOCl_2$. Eventually of the addition waiting for 30 minutes, after that it is placed the reaction mixture in a beaker with H_2O and ice to hydrolyze the thionyl chloride which is not reacted. The solution is neutralized with the addition of a saturated solution of Na_2CO_3 to obtain pH 5.5-6.
The product was recovered by extraction with dichloromethane (4x25ml). The organic phases are combined and dried with Na_2SO_4, the solvent removed using the rotavapore.
The product obtained is purified by a chromatographic column in silica utilizing an eluent: ethyl acetate/hexan (1:1) and the fractions are controlled through TLC.
The yield: (1.93 g, 99%).

^{1}H-NMR(400MHz,$CDCl_3$): δ=8.29ppm (1H, d, H_{quin}); δ=7.67ppm (1H, d, H_{quin}); δ=7.46ppm (1H, t, H_{quin}); δ=7.39 ppm (1H, dd, H_{quin}); δ =7.14ppm (1H, dd, H_{quin}); δ=4.91ppm (2H, s, H_{link}).

2.1.1.3 – Synthesis of 4,4 '- bis ((1,4,7,10 - tetraazacyclododecane) methyl) - 2,2' dipyridyl

2.1.1.3.1 – Synthesis of (4,4 'dimethyl) 2,2' dipyridyl

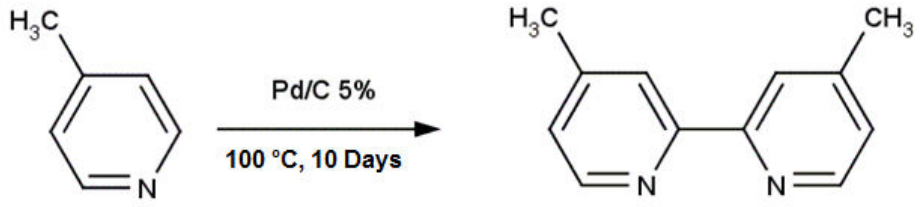

1 2

The solution of ϒ-picoline (250 ml, 2.57 mmol); the compound **1** that was stirred in an oil bath at 100°C for 10 days, in the presence of a catalyst of Pd/C 5% (10g). Subsequently, benzene is added to the mixture, leaving at reflux for minutes.
The reaction is filtered twice, the first washing the filtrate with hot benzene, and the second through a folded filter to remove the catalyst. Then, the residual liquid is evaporated to dryness using the rotating evaporator. It is thus obtained an impure yellow product, that is purified by recrystallizing in ethyl acetate (12.3 gr, 2.6%).

^{1}HNMR(400MHz, $CDCl_3$): δ=8,54ppm (2H, d, H_6); δ=8,24ppm (2H, s, H_3); δ=7,14ppm (2H, d, H_5); δ=2,44ppm (6H, s, H_{met}).

2.1.1.3.2 – Synthesis of 4,4' – dicarboxylic - 2,2 '-dipiridil

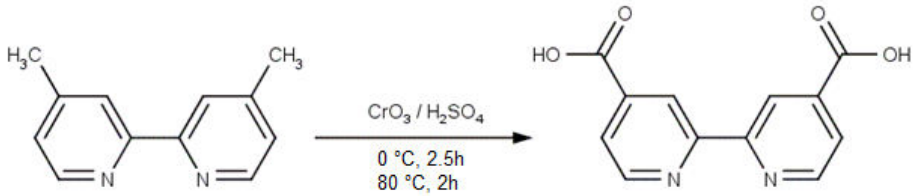

2 3

(12.30 g, 66.76 mmol) of **2** in a flask three neck of 0.5 litre with mechanical agitator. The flask was immersed in an ice bath, and is added 150 ml of H_2SO_4 97%. Then, they were added 47 g of CrO_3 for 3 hours. The solution is heated to 80 °C and is kept under stirring for 2 hours. It is obtained a solution dark green, that was allowed to cool at room temperature, and thereafter is poured 1 kg of ice and 400 mL of water, keeping always the stirring. It is obtained a suspension of a grey product. After that, it is filtered in vacuo, it is achieved a yellow-green precipitate, which is the compound **3**. It is separated from the solution of black color. Recrystallization of the product is obtained in 250 mL of NaOH 0.3 M. The solution is diluted up to 2 dm^3 with water, then acidified with HCl 37%. The product precipitates again, and it can be separated by filtration. The filtrate is washed with water-ethanol, and then it is placed in the desiccator (15.45 g, 95%).

^{1}HNMR(400MHz, DMSO): δ=8,90ppm (2H, d, H_6); δ=8,83ppm (2H, s, H_3); δ=7,90ppm (2H, dd, H_5).

2.1.1.3.3 – Synthesis of 2,2 '- (4,4' dicarboxy methyl) – dipyridyl

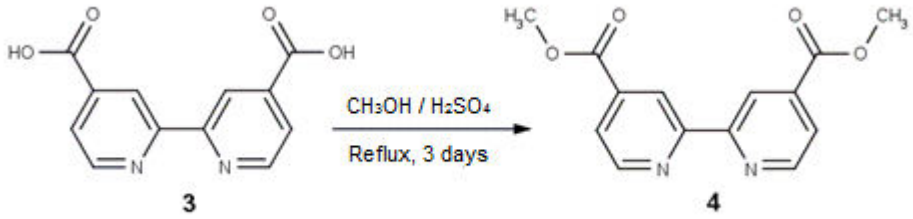

3 **4**

They were dissolved (15.45 g, 63.8 mmol) of **3** in 450 mL of CH_3OH, in a flask of 1 litre, the flask is immersed in an ice bath, before adding a dropwise of 12 cm^3 of H_2SO_4. The reaction mixture is heated to reflux, and it is held under stirring for 3 days. The color solution is pink. The mixture is allowed to cool to the room temperature, before reducing the volume using the rotating evaporator. They were 200 mL water, and the solution is carried a pH=8, using NaOH 40%. The extraction of the product **4** has taken place in the aqueous phase with $CHCL_3$. They came together the organic phases, then it is added Na_2SO_4 anhydrous to remove the residual water. The solution is filtered, and the liquid is collected in a flask, which is evaporated to dryness the rotating evaporator. It is thus obtained an impure product of **4**, that is recrystallized by hot - cold toluene (14.97 g, 87%).

^{1}HNMR(400MHz, $CDCl_3$): δ=8,96 ppm (2H, s, H_3); δ=8,87ppm (2H, d, H_6); δ=7,91ppm (2H, dd, H_5); δ=4,00ppm (6H, s, H_{met}).

2.1.1.3.4 – Synthesis of 2,2 '- (4,4' dihydroxymethyl) - dipyridyl

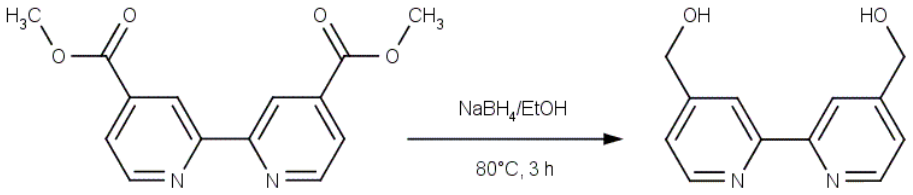

4 **5**

They were added (14.97 g, 54.98 mmol) of the compound **4** to 40 g of $NaBH_4$ in a flask four necks of 2 litres, then it is added 1 litre of ethanol. The solution is kept under reflux with stirring for 3 hours at 80 °C, under a nitrogen atmosphere, and with a cap of $CaCl_2$ to maintain the anhydrous environment. The flask is allowed to cool to the room temperature, before reducing the volume to about 0.2 litre using the rotating evaporator. Meanwhile, a saturated solution of NH_4Cl is prepared, which is added to the flask to make the solution acidic. Then, the volume is reduced, and is filtered to remove H_3BO_3, washing with ethyl acetate. They came together the various liquid phases, and an extraction is carried out with ethyl acetate. They joined together the organic phases, and it is added Na_2SO_4 anhydrous to remove the residual water. The solution is filtered, which is evaporated to dryness the rotating evaporator (6.95 g, 59%).

^{1}HNMR(400MHz, MeOD): δ=8,59ppm (2H, d, H_5); δ=8,27ppm (2H, s, H_3); δ=7,44ppm (2H, d, H_6); δ=4,78ppm (4H, s, H_{bridge}).

2.1.1.3.5 – Synthesis of 2,2 '- (4.4' dibromo methyl) – dipyridyl

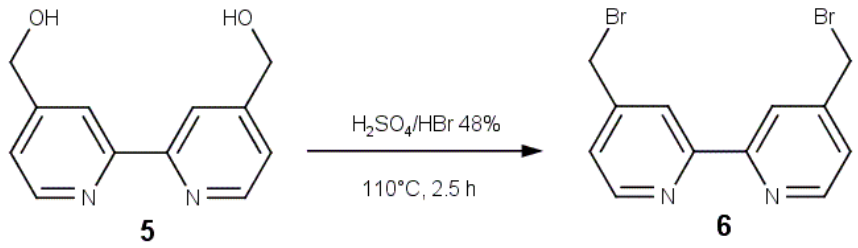

5 **6**

They are inserted (960 mg, 4.44 mmol), and 50 mL of HBr 48% of **5**, in a conical flask of 100 mL. The solution is kept under reflux at 110°C for 2.5 hours, adding a catalytic amount of H_2SO_4 97% to a hot environment. It is allowed a cool to room temperature, before that the conical flask placed in an ice bath. The solution is put in a beaker, and is added Na_2CO_3 until reaching to a neutral pH. The pink precipitate is filtered, and is washed with water. Finally, it is placed in the desiccator. For purification of the compound 6, it is used the chromatography column, with a stationary phase of silica, and using a mixture of hexane and ethyl acetate as eluent. Starting with the first fractions with pure hexan, then increasing the amount of ethyl acetate, as follows: (1/5, 1/1, 5/1, 1/0), (186 mg, 12.12%).

^{1}HNMR (400MHz, $CDCl_3$): δ=8,68ppm (2H, d, H_6); δ=8,45ppm (2H, s, H_3); δ=7,37ppm (2H, dd, H_5); δ=4,49ppm (4H, s, H_{bridge}).

2.1.1.4 - Synthesis of 4,5-bis (bromomethyl) acridine

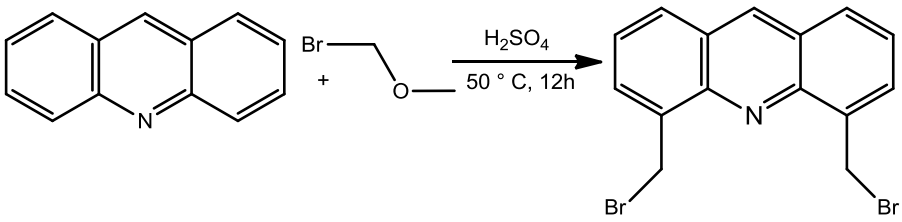

Depending on the previous article[110], it was prepared the compound 4,5-bis (Bromomethyl) acridine that is used as a fluorophor unit in synthesis of ligand L5.

They are added 6 mL of bromomethyl methyl ether (d = 1.531 g/mL a 25 °C, 73,2mmol) to 3 g (16.7 mmol) of acridine solution in 38 mL of sulfuric acid. The solution was maintained below nitrogen flux at 50 ° C for 12 h. After That, they are added to the mixture 150 g of ice and it is filtered and dissolved in chloroform $CHCl_3$ (450 mL) the yellow precipitate that is formed. The insoluble part is eliminated and the organic phases are combined and dried with Na_2SO_4, the solvent removed using the rotavapore. The residue after evaporation of the solvent is crystallized by a mixture ethyl ether / cyclohexane to give a yellow solid (2.5 g, yield 41.7%, MW: 365.06 g/mol).

^{1}H-NMR (300 mHz, $CDCl_3$): δ H 5.34 (s, 4H), 7.41-7.46 (m, 2H), 7.86-7.92 (4H), 8.69 (s, 1H).

^{13}C-NMR (75 mHz, $CDCl_3$): δ C 29.91, 125.56, 126.87, 128.84, 131.0, 136.11, 143.20.

2.1.2 – Synthesis of the ligands

2.1.2.1 – Synthesis of the ligand H_2L1

2.1.2.1.1 – Synthesis of cyclen-glioxal – 2a,4a bis(methyl-quinoline), compound 3

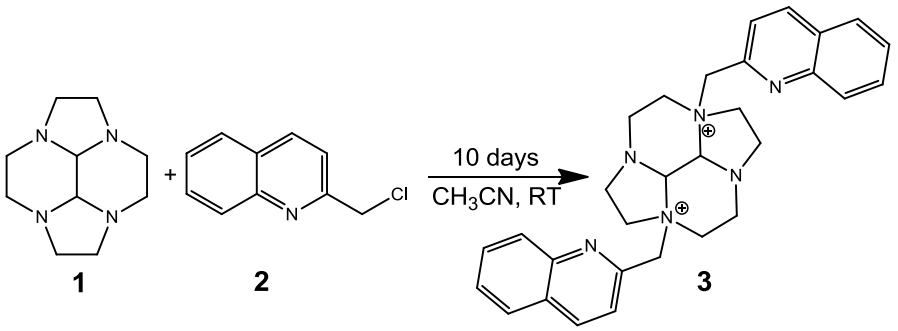

A solution of 2-(chloromethyl) quinoline (900 mg, 5.07 mmol) in CH_3CN (10 mL) was added dropwise to a stirred solution of **1** (395 mg, 2.03 mmol) in CH_3CN (8 mL). The solution was stirred at room temperature for ten days. During the reaction, the formation of a white precipitate at the end is filtered and washed with CH_3CN thus obtaining the product **3.** (557 mg, 81%).

*d*H (400 MHz, MeOD): 8.51(d, 1 H), 8.16 (s, 1 H), 8.05 (d, 1 H), 7.88 (t, 1 H), 7.74 (d, 2 H), 5.32(t, 1 H) , 7.93(t, 1 H) , 8.10(t, 2 H) , 8.62(d, 1 H); *d*C (125 MHz, D_2O): 150.22, 148.25, 138.68, 131.04, 129.56, 128.48, 128.38, 128.31, 123.08, 84.61, 72.25, 63.63, 61.25, 59.50, 52.03, 49.42, 48.75, 43.93.

2.1.2.1.2 – Deprotection of compound 3

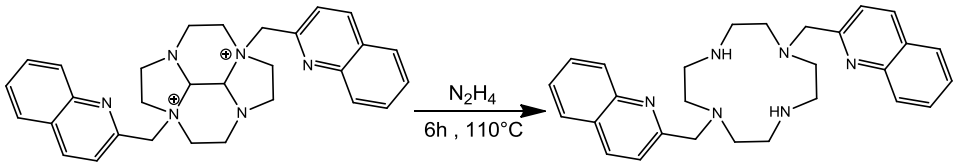

3 4

Deprotection of **3** is obtained with hydrazine (N_2H_4). 1.28 g of **3** is dissolved in 25ml of N_2H_4 and 5 ml of EtOH, the mixture is stirred at 110 ° C for 3h. The resulting solution was cooled at room temperature, addition of a 5 M NaOH aqueous solution (15 mL), and the product extracted with chloroform (5x50 mL). The organic layer was dried over Na_2SO_4 and evaporated under reduced pressure. The crude product was dissolved in ethanol and salified by adding concentrated HBr, it is filtered to give the compound H_2L1 as a light yellow powder (1.88 g, 73%).

*d*H (400 MHz, D_2O pD = 2.4): 3.12 (m, 8 H), 3.23 (t, 4 H), 3.28 (t, 4 H), 4.28 (s, 2 H), 7.66 (d, 1 H), 7.76(t, 1 H) , 7.93(t, 1 H) , 8.10(t, 2 H) , 8.62(d, 1 H); *d*C (125 MHz, D_2O): 153.86, 147.71, 138.68, 135.50, 130.14, 129.22, 128.51, 122.69, 120.32, 55.08, 48.33, 44.55, 41.99, 41.58.

2.1.2.1.3 – Synthesis of H_2L1

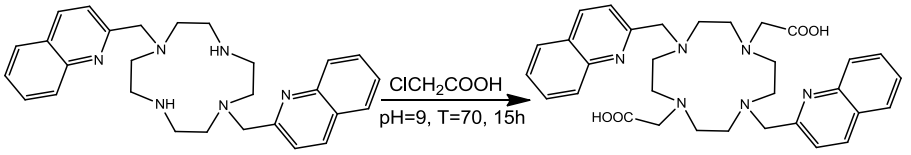

4 L1

A solution of **4** (1 g, 1.18 mmol) in 74 ml H_2O, and (1.12 g, 11.8 mmol) of chloride acetic acid in 5 ml H_2O, then we added both together in a flask three necks. The solution was stirred in an oil bath at 70°C for 15 h adjusting the pH with NaOH 1-5 M keeping it about 9 during all the reaction. The resulting solution was cooled at

room temperature, and evaporated under reduced pressure (w=2.620 g).

2.1.2.1.4 – Purification of the ligand H_2L1

- Cation column using exchange resin of type Amberlite IR120 Na^+ form, using an aqueous solution of NH_4OH (0.5 M) and evaporated under reduced pressure (w=1.15 g).
- Anion column using exchange resin of type Amberlite IR-900 chloride form, using an aqueous solution of HCl (0.1-5 M) and evaporated under reduce pressure for salified product **H_2L1** (w=0.95 g, 96%).

dC (125 Mz,D_2O pD=2.27) 9.12(d , 2H) , 8.37(d , 2H) , 8.29(d , 2H) , 8.24(t,2H),8.22(d,2H),7.97(t,2H).
4.16(s,2H), 4.12(s), 3.58(s,4H), 3.48(s), 3.48(s,4H), 3.26(s,3H) 3.18(s,3H).

2.1.2.3– Synthesis of the ligand H_4L2

2.1.2.3.1– Synthesis of cyclen-glioxal – 2a,4a bis(methyl-8-hydroxyquinoline)

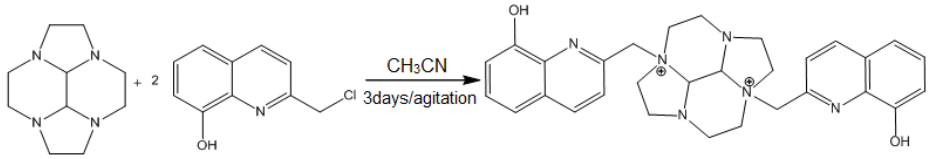

1 2 3

The reaction is carried in a flask of 100 mL dissolving in stoichiometric ratio 1: 2.5 the reagents: 0.8g of 1 (4.10 mmol) in 25 mL of CH_3CN and 2g of 2 (11.7 mmol) in 25 mL of CH_3CN, then the resulting solutions are placed together. The resulting solution is maintained under agitation for 3 days in a flask of 50 ml with stopper of $CaCl_2$. During the reaction, it is observed the formation of a yellow precipitate (product 3) that is eventually separated by

filtration on a büchner and washing it with acetonitrile to eliminate any trace of the reagents.
The yield : (2.01g, 97.1%).

^{1}H-NMR(400MHz,CD3OD): δ=8.53ppm (2H, d, Hquin); δ=7.84ppm (2H, d, H_{quin}); δ=7.61ppm (2H, t, H_{quin}); δ=7.54 ppm (2H, d, H_{quin}); δ =7.27ppm (2H, d, H_{quin}); δ=5.28ppm (4H, m, H_{link}).

2.1.2.3.2– Deprotection of the product 3

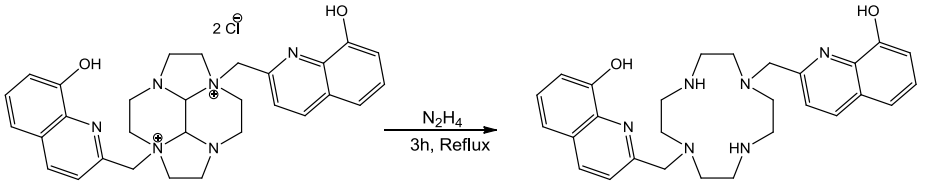

3 4

In the same reaction flask, they are added 2.01 g of 3 and a dropwise 5 mL of EtOH, then 25 mL of N_2H_4 aqueous 65%. The solution is maintained under at reflux for 3 hours and is brought to dryness with rotovapor. The obtained residue is taken up with 25 ml of 40% NaOH and extracted with $CHCl_3$ (5x150 ml). The organic phases are combined and dried with Na_2SO_4 and the solvent removed using the rotovapor. The purification of compound **4** from hydrazine in excess is carried out by salification with HBr in EtOH dropwise until complete precipitation of the hydrobromide amine as a yellow solid.
The yield: (1.9g, 94.5%).

^{1}H-NMR(400MHz,D_2O, pH=2.5): δ=7.80ppm (2H, d, H_{quin}); δ=7.24ppm (2H, d, H_{quin}); δ=7.14ppm (2H, t, H_{quin}); δ=7.03ppm (2H, d, H_{quin}); δ =6.75ppm (2H, dd, H_{quin}); δ=4.25ppm (4H, s, H_{link}); δ=3.38ppm (8H,H_{cyclen}); δ=3.20ppm (4H, H_{cyclen}); δ=3ppm (4H, t, H_{cyclen}).
^{13}C-NMR(100MHz, D_2O, pH=2.5): δ=156ppm, 149ppm, 139ppm, 134ppm, 128ppm, 127ppm, 121ppm, 119ppm, 113ppm (C_{quin}); δ=56ppm (C_{link}); δ=49ppm, 42ppm, (C_{cyclen}).

2.1.2.3.3- Acetylation of 1,7- (bis-8-hydroxy quinoline) 1,4,7,10-tetraazateradodecane

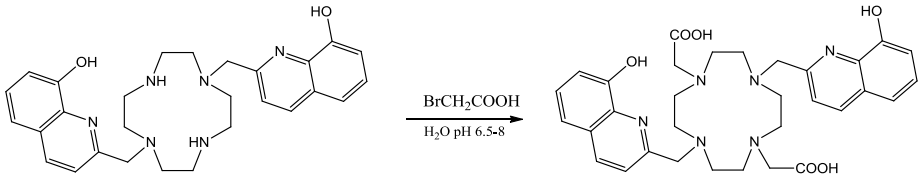

4 H_4L2

They are introduced 320 mg of compound 4 (0,66 mmol) in a two-neck round-bottom flask containing a magnetic armature and refrigerant in 95 mL of H_2O. Then, they are added a dropwise 800 mg of $BrCH_2COOH$ (5.76 mmol) in 5 mL H_2O. The flask is put in an oil bath of 70° C and the pH is maintained between 6.5 – 8.0 using small additions of solution of NaOH 5m for 3 days. pH tends to decrease during the reaction, for this we have to control it at a regular time intervals, reporting it between pH 6.5 and 8.0. Later, it is dried using the rotavapor. The weight of the obtained solid is 1.67 g with yield of 71%. The obtained solid is dissolved in H_2O and passed first on cation-exchange column (Amberlite IR 120, in the form Na^+) conditioning HCl 0.1 M, using NH_4OH 0.5 M as eluent. Afterwards, The obtained solution is passed on anion-exchange column (Amberlite IRA 900, forma Cl^-) conditioned with NaOH 0,1 M, using initially eluent HCl 5 M and 0.1 M HCl, and finally using H_2O. Obtaining the product in the form of hydrochloride.

^{1}H-NMR(400MHz, D_2O, pH=2.3): δ=9.06ppm (2H, d, H_{quin}); δ=8.33ppm (2H, d, H_{quin}); δ=7.6 ppm (4H, d+d, H_{quin}); δ=7.52ppm (2H, d, H_{quin}); δ=4.27ppm (4H, s, H_{link}).

2.1.2.3– Synthesis of the ligand L3

2.1.2.3.1 – Synthesis of compound 3

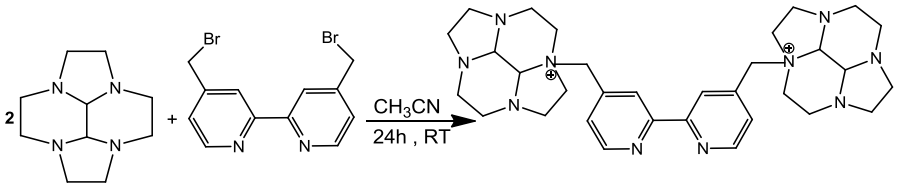

1 2 3

We dissolved (540 mg, 2.8 mmol) of compound **1**, and (500 mg, 1.4 mmol) of compound **2** in a little amount of CH_3CN, separately. After that, we added both together to the same flask 2:1, and we completed the volume to 30 ml of CH_3CN. The solution was stirred at room temperature for 24 hours. During the reaction, the formation of a white precipitate at the end is filtered and washed with CH_3CN thus obtaining the product **3**, which is placed in the desiccator (750 mg, 74%).

^{1}HNMR(400MHz, MeOD): δ=8,90ppm (2H, d, H_6); δ=8,72ppm (2H, s, H_3); δ=7,81ppm (2H, dd, H_5); δ=5,21-4,97ppm (2H, m, H_{bridge}), δ=4,45-2,58ppm (10H, m, $H_{cyclen\ protected}$).

2.1.2.3.2 – Deprotection of compound 3

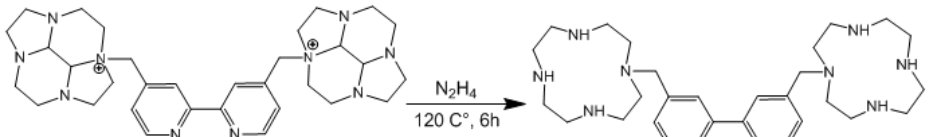

3 L3

Deprotection of **3** is obtained with hydrazine (N_2H_4). (300 mg, 0.410mmol) of **3** is dissolved in 7 ml of N_2H_4 and 1 ml of EtOH, the mixture is stirred at 120 °C for 6h. The resulting solution was cooled at room temperature, addition of a 5 M NaOH aqueous

solution (15 mL), and the product extracted with chloroform (5x50 mL). The organic layer was dried over Na_2SO_4 and evaporated under reduced pressure. The crude product was dissolved in ethanol and salified by adding concentrated HBr, it's filtered to give the compound **L3** as a light yellow powder (210 mg, 98%).

^{1}HNMR(400MHz, MeOD): δ=8,79ppm (2H, d, H_6); δ=8,42ppm (2H, s, H_3); δ=7,86ppm (2H, d, H_5); δ=4,10ppm (2H, s, H_{bridge}); δ=3,30-2,89ppm (6H, m, H_{cyclen}).

2.1.2.3.3 – Purification of the ligand L3

- Column chromatography alumina, the used eluent is CH_3Cl/ MeOH /NH_3: (80:15:5).
- The reference of TLC is the compound **L3** + $CHCl_3$.

2.1.2.4 – Synthesis of the ligand L4

2.1.2.4.1 – Synthesis of the compound 4

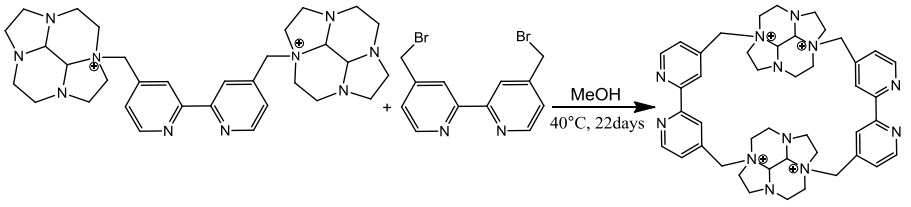

3 2 4

We dissolved (1.02 g, 1.34 mmol) of compound **3** and (764 mg, 2.23 mmol) of compound **2** in a little amount of MeOH, separately. After that, we added both together to the same flask 1:1.60 and we completed the volume to 150 ml of MeOH. The solution was stirred in an oil bath at 40°C for 21 days. The resulting solution was cooled at room temperature, and evaporated under reduced pressure, thus obtaining the product **4**, which is placed in the desiccator (1.32 g, 92%).

2.1.2.4.2 – Deprotection of compound 4

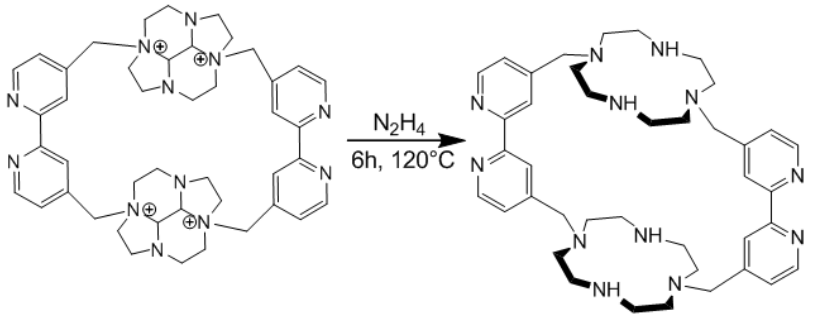

4 L4

Deprotection of **4** is obtained with hydrazine (N_2H_4). (0.9 g, 0.84 mmol) of **4** is dissolved in 20 ml of N_2H_4 that it was added dropwise to the compound **4**, and it was added 1 ml of EtOH, the mixture is stirred at 120 °C for 6h. The resulting solution was cooled at room temperature, addition of a 5 M NaOH aqueous solution (25 mL),

and the product extracted with chloroform (5x50 mL). The organic layer was dried over Na_2SO_4 and evaporated under reduced pressure. The crude product was dissolved in ethanol and salified by adding concentrated HBr, it's filtered to give the compound **L4** as a light yellow powder (0.56 mg, 95%).

2.2 – Potentiometry

The potentiometric measures are carried out using an automatic potentiometric system (Figure 2.1), that made from the following parts:

1) - Potentiometer for the research Orion Mod.701A.

2) - Automatic burette Mettler Mod. DV10 graduated in 2-10 cm.

3) - Mechanical agitator Mettler Mod. DV70.

5) - Thermostatic cell of the capacity around 25 cm^3, that is thermoregulated by circulation of water.

6) - Electrode glass for research Orion Mod. 91-01.

7) - Reference electrode of type Ag / AgCl in a saturated solution of KCl.

8) - A salt bridge of type Wilheim, that is filled with a solution of NaCl 0.15 M.

9) - Computer with video, hard disk and printer.

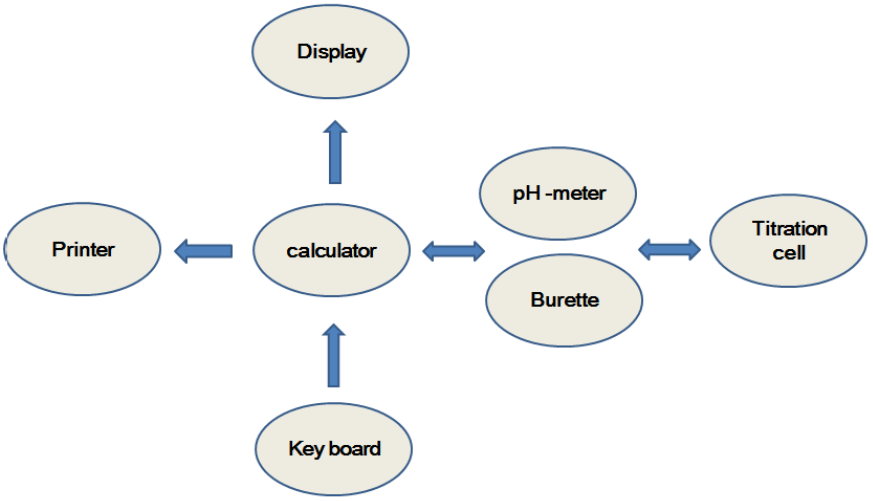

Figure 2.1. - Scheme of a potentiometric system.

Each solution is prepared with bidistilled deaerated water, cooled in an inert atmosphere (under nitrogen), then is passed through a purification system of type Millipore to eliminate the ionic species and the organic compounds.

The used solutions of NaCl, HCl and NaOH are prepared using commercial products of a high purity, and their concentrations are determined by following a standard analytical procedure.

All measures are carried out at 25±0,1°C.

During all the measures, it was used a continuous flux of nitrogen, that is kept inside of the cell for avoiding the carbonation of the studied solutions. Before reaching for the cell, the gas of nitrogen is passed through a wash bottle, where this bottle contains a concentrated solution of NaOH. In this manner, any traces of carbon dioxide found in the nitrogen are removed, and the gas in water vapor is saturated before introducing it in the potentiometric cell.

All measures are carried out at ionic strength constant, using solutions of of NaCl 0.1 M. The computer controls the measuring

system, adjusting the additions of titrant solution and performing the readings of the values of electromotive strength. Latter operation is made possible by the interface, that connects the personal computer to the potentiometer.

The program before starting the measure asks initial parameters of inputs, that affect the characteristics of the potentiometric acquisition:

1) - Maximum number of readings.

2) - Time interval between two readings.

3) - Tolerance on the standard deviation.

4) - Tolerance on the drift.

5) - Volume of added titrant initially.

6) - The volume of titrant to add overall.

7) - Increase of volume of titrant.

When these data inserts, the computer starts to collect the values of f.e.m that are measured by the potentiometer.

According to the parameter 2, ten values of f.e.m are collected, where the average value is calculated. The determined average (reading) is stored and displayed in the video next to a progressive number.

This procedure is repeated until to obtain a group of ten readings. With regard to the parameter 3, the computer calculates the average value and checks if the standard deviation of the average value is greater or minor than the imposed tolerance. Two cases are differentiated as follows:

2.2.1- The first case

If the number of performed readings and the preset maximum number of the parameter 1 are equal, the computer stores and prints on the same row the volume of added titrant, the average value of the last ten readings, the number of performed readings and a graphic signal which indicates that the standard deviation of the average value is is higher than the tolerance setting.

2.2.2- The second case

If the number of performed readings is minor than the preset maximum number, the system carries out another reading, calculates the average value of the last ten readings and performes again the control on the standard deviation. This sequence Can continue until to achieve the maximum number of imposed readings.

With regard to the parametr 4, when the standard deviation of the average value is lower than the imposed tolerance, the difference between the first value and tenth value of f.e.m is calculated, they are used to calculate the average value and is checked that the absolute value of this difference does not exceed the fixed value for the tolerance on the drift. In this manner, those values respecting the conditions imposed on the standard deviation are discarded and they represent the result of a series of readings of f.e.m, where the last is very different from the first.

If the condition is not met, another reading is performed, the new average value is checked and the values of the standard deviation and of the drift are checked. Otherwise the computer considers it a good measure, it stores the data and it proceeds to another addition.

The obtained data elaborate with the calculation program HYPERQUAD2003.

2.2.3 – Methods of calculation

If we are able to do a direct measure of the equilibrium concentration for any type of the species present in solution, the problem of determining the equilibrium constants in solution will be solvable. It is obvious that this is not in general possible.

In general, it is possible to put a concentration relation for one type of the species with the equilibrium constants in solution and the initial concentrations in solution. Basically, the measure of the variation of concentration of one species with the total composition of the system can be allowed to determine the equilibrium constants. The determination can be done by the potential difference measurements (potentiometric measures), between a reference electrode and another electrode, where this potential is a function of the concentration of the considered species.

The determinations of the equilibrium constants can be carried out by measurs with a glass electrode, using the concentration of hydrogen ions, this is in a case of equilibrium of complexation, where a ligand participates with a protonable anion.

The concentration of hydrogen in the solution and the measured potential can be linked through Nernst equation:

$$E = E° + \frac{RT}{F}\ln[H^+]$$

E - is the electrode potential (V).

R - is the gas constant (8.314 J / mol • K).

T - is the absolute temperature (K).

F - is the Faraday constant (96,458 Coulomb).

E° - must be experimentally determined for the special conditions of the required potentiometric measures and to achieve short temporal distance.

The calibration of the reference electrode happens under the experimental conditions, through a titration experience of an amount that is treated with a strong acid (HCl) and with a strong base (NaOH). The equivalence point, in our case, is determined by the method of Gran, it is thus obtained the value of E° and the ionic product of water K_w.

The method of data processing differs depending the system where the ligand interacts with a metal ion or with an anion. The formed complex from the interaction of a metal ion M with a protonable ligand L in aqueous solution can be expressed by the following by the equation below:

$$pM + qL + rH = MpLqHr$$

Note: the charges have been omitted for simplicity.

The formation constant of the species MpLqHr is quantitatively determined in the relative constant in the above equation:

$$\beta pqr = [MpLqHr]/[M]p[L]q[H]r$$

The constant βpqr in the case of hydroxylated species will be reported in the following equation:

$$pM + qL + rH_2O = MpLq(OH)r + rH$$

The constants βpqr and β' are linked together according to the equation:

$$\beta' = [MpLq(OH)r]/[M]p[L]q[OH]r$$

Reported to the equilibrium:

$$pM + qL + rOH = MpLq(OH)r$$

By the ionic product of water K_w:

$$\beta pqr = \beta' Kwr$$

The solution in the course of a potentiometric measure will compose of a certain amounts of metal at any point, the total concentrations of ligand and acid are defined by:

$$TM = [M] + \sum pqr\ p\ [MpLqHr]$$

$$TL = [L] + \sum pqr\ q\ [MpLqHr]$$

$$TH = [H] + \sum pqr\ r[MpLqHr] - [OH]$$

Through the provision of expressions βpqr, will get the following:

$$TM = [M] + \sum pqr\ p\beta pqr[\ M]p[L]q[H]r$$

$$TL = [L] + \sum pqr\ q\beta pqr\ [M]p[L]q[H]r$$

$$TH = [H] + \sum pqr\ r\beta pqr\ [M]p[L]q[H]r - [OH]$$

The concentration of free hydrogen ions H^+ is measured and the experimental titration curve is obtained bringing back the electrode potential versus volume of added titrant. At each experimental point, a system of three equations corresponds in (n + 2) of unknown factors; n- the number of formed species, that correspond to n constants of stability and to the concentrations of the free ligand and metal.

For N experimental points, it will be formed a system of 3N equations in (n + 2N) unknown factors. The mathematical treatment is very hard and complicated, so it uses the calculators. There are several programs for calculation of stability constants of potentiometric measures. The results of this work are obtained using the calculation program HYPERQUAD 2003.

2.3 – UV - vis spectroscopy

The absorption spectra are obtained using the prepared solutions with a certain concentration of the ligand, and they are registered by Jasco V-670 spectrophotometer of a double beam with a quartz

cell of thickness 1 cm. Mother (Stock) solutions of the ligands are prepared dissolving a certain amount of ligand in a certain volume of distilled water, then are prepared the diluted solutions for the study. For determining the coordinative characteristics of the ligand, the spectra are registered at different values of pH in the absence and in the presence of a certain concentration of metal ions (1 or 2 eq compared with the ligand), and for each measure, the pH is adjusted through solutions of NaOH and HCl in different concentrations (0.1, 1, 5) M, using the glass electrode. For determining the changes in the absorption, the spectra of the solutions of ligand, that contained different amounts of metal ions, such as: Zn^{2+}, Cd^{2+}, Pb^{2+} and Cu^{2+}, are registered at pH-fix. Also, the prepared solutions are isolated at pH=7.5 by TRIS buffer and the spectra are recorded following progressive additions of 0.1 eq of ion metal, until reaching to a concentration that doesn't occur any change in the absorption.

UV-vis spectra of H_2L1 (and for all other ligands) were recorded with a Jasco V-670 Spectrophotometer double ray, with cuvette 1 cm of a thickness. The solutions were obtained by direct weight or through dilution of solutions mother prepared by direct weight. The solution mother of H_2L1 was prepared to the optimal concentration for the electron spectroscopy. It has a solution 1.16×10^{-4} M obtained by dissolving 5.78 mg of ligand salified (MW = 993.33) in 50 cm^3 of double-distilled and deaerated water. at various pH have been measured in the spectral range 200−600 nm. To analyze the acid-base properties of the ligand H_2L1 and the characteristic of the absorption varying pH, the spectra were recorded on solutions at different values of pH. The pH was adjusted for each measure by addition of solutions of HCl or NaOH (at various concentrations) and measured with a glass electrode. The purpose of this operation to see how it changes the absorption maximum at a variation of pH.

In the same manner, for the ligand H_4L2; $[H_4L2] = 1.7\times10^{-4}$ M, while $[L3]=8\times10^{-5}$ M, $[L4]=1.56\times10^{-5}$ M and $[L5]=8{\cdot}7\times10^{-6}$ M.

2.4 - Fluorescence emission spectroscopy

The fluorescence spectra were registered to perform the measurements of emission. It is used spectrofluorometer: PerkinElmer Luminescence Spectrofotometer LS 55m, with a cell of thickness 1 cm. The wavelength of excitation is 290 nm, and the input and output slits are 8 nm. Mother (Stock) solutions of the ligands are prepared dissolving a certain amount of ligand in a certain volume of distilled water, then the diluted solutions are prepared for the study. For determining the coordinative characteristics of the ligand, the spectra are recorded at different values of pH in the absence and the presence of a metal ions, and for each measure, the pH is adjusted through solutions of NaOH and HCl in different concentrations (0.1, 1, 5) M, using the glass electrode. In addition to, the spectra of the solutions of ligand, that contained different amounts of metal ions, such as: Zn^{2+}, Cd^{2+}, Pb^{2+} and Cu^{2+}, are registered at pH-fix. Also, the prepared solutions are isolated at pH=8 by TRIS buffer, and the spectra are recorded following progressive additions of 0.1 eq of ion metal, until reaching to a concentration that doesn't occur any change in the emission.

Fluorescence emission has been measured on the same solutions using a PerkinElmer LS 55 Luminescence Spectrofotometer with a cell of 1 cm thickness, using an excitation wavelength at 295 nm (the isosbestic point) or at 316 nm (the absorption maximum), depending on the experiment, and collecting the emission in the range 200−500 nm. The solution of H_2L1 in concentration 2.32×10^{-5} M was obtained by removing 10 cm^3 from the solution of UV-vis that was brought to 50 cm^3 using double-distilled and deaerated water. As the absorption spectra, to analyze the characteristics of emission of the ligand varying pH, the spectra were recorded on solutions at different values of pH. The pH was adjusted for each measure by addition of solutions of HCl or NaOH (at various concentrations) and measured with a glass electrode.

While the ligand H_4L2; [H_4L2] = 5.56×10^{-6} M, [L3]=8×10^{-5} M, [L4]=4.14×10^{-5} M and [L5]=9.92×10^{-6} M.

2.5 – Nuclear magnetic resonance spectroscopy NMR

To characterize the compounds, that are resulting from the reactions (intermediate and final), and to secure them, and to verify the purity, they were carried out spectra ^{1}H and ^{13}C, using an instrument Bruker TOPSPIN 2.1 NMR.

It is used as a reference either the signal of tetramethylsilane (δ = 0 ppm), or the signal of OD-H (δ = 4.79 ppm) in aqueous solutions, then the chemical shift of the solutions is brought in ppm.

pH of the solutions calculates in deuterated water D_2O as the relation below[109]:

$$pH = pD - 0.40$$

By measuring the pH, the value of Chemical Induced Shift (CIS) of a hydrogen atom can be determined through calculation the difference of chemical shift (Δδ), between the signal of this atom, that is in the spectrum of ^{1}H NMR of the complex type, and the signal of the atom in the spectrum of ^{1}H NMR of the uncoordinated type.

The value of Chemical Induced Shift (CIS) is calculated according to the relation:

$$CIS = \frac{\Delta\delta}{\%compl}$$

%comp - The percent of species of complex, that is in the solution under the conditions in which the spectra were registered (pH and temperature).

2.6 – X-ray diffractometry

It was obtained the crystalline structure of a single crystal by X-ray Diffraction. The single crystals of the complex are obtained with a slow evaporation of an aqueous solution containing the complex and Zn $(ClO_4)_2.6H_2O$ in a molar ratio 1:1 at pH=7.

2.7 - Acid-base properties of the ligands

The analysis of acid-base properties of the ligands are a necessary premise at each successive study of coordination of metal ions. The ligands are soluble in water and in aqueous solution, the amine groups of the ligands have the characteristic of giving rise to protonation equilibrium which compete with the coordination of the metal ions in the formation of the complexes. Therefore, we firstly studied the acid-base equilibria of the receptors. The optical properties depend on the pH, the study of the acid-base has been addressed matching potentiometric and spectroscopic measurements (UV-vis absorption and fluorescence emission)

3-RESULTS AND DISCUSSION

3.1- Synthesis of the ligands

To optimize the method of synthesis of ligands, we started from literature articles [65 , 66] that deal with the functionalization of macrocycles such as protected cyclen with aminals[67].

For the functionalization of the fluorophores, we used methods of synthesis already present in the literature. The fluorophore 2-(chloromethyl) quinolone (2) used in the synthesis of H_2L1, is obtained from the commercial product 2-(chloromethyl) quinoline as hydrochloride salt (1). The molecule of acid was neutralized by using potassium carbonate.

For the synthesis of ligand H_4L2, we used the commercial compound 8-hydroxyquinolin-2-carboxy aldehyde (1) The two carbonyl group were reduced to hydroxyl group using $NaBH_4$. The obtained alcohol (2) was reacted with thionyl chloride to obtain eventually 8-hydroxy-2-chloromethyl-quinoline (3).

2,2'-dibromomethyl-dipyridyl, used in the synthesis of L3 and L4, was obtained starting from 4-methyl pyridine (1). The latter is a commercial product, which has been dimerized.. Later, the two methyl groups on the product (2) are oxidized to the carboxyl group (3) using chromic anhydride, then they undergo to an esterification in methanol (4). After that, the groups are reduced to alcohols (5)

---

[65] Baker WC, Choi MJ, Hill DC, Thomson JL, Petillo PA. J. Org. Chem. 1999;64:2683 2689.

[66] Jan Rohovec, Robert Gyepes, Ivana Císařová, Jakub Rudovský, Ivan Lukeš, Tetrahedron Letters, 2000, 41,1249-1253.

[67] M. Le Baccon, F. O. Chuburu,Toupet, H. Handel, M.Soibinet, I. De-champs-Olivier, JP. Barbierc and M. Aplincourtc, New Journal of Chemistry, 2001, 25, 1168-1174.

using $NaBH_4$. Finally, a bromination process is carried out in concentrated hydrogen bromide HBr to obtain the product (6).

The use of cyclen protected with glyoxal is very important, where in this type of compounds only two of the four amine groups present in the macrocycle (in position trans) are reactive toward nucleophilic reagents, while the two remaining amine groups have their non-bonding doublets oriented towards the center of the cavity and this inhibits their reactivity. In consequence the nucleophilic substitution reactions occurs only on the amine groups in position 1,7 (see paragraph 1.1.4). In addition, the functionalization of the first nitrogen atom is usually faster than the nucleophilic addition on the second amine group, so the reaction time which allows the formation of di-functionalized is longer than that necessary for formation of mono-functionalized.

In the synthesis of the ligands H_2L1 and H_4L2 we chose acetonitrile as a solvent to exploit the scarce solubility of the two ligands to achieve an easy isolation of the final products.

The choice of cyclen and acetonitrile as reagents are determined to direct the functionalization reaction, to have an excellent selectivity and good yield. This type of reaction can be of interest for realization of systems containing different functional groups. On this basis, it could be also possible to insert within a polyamine macrocycle two different functional groups, simply by using a procedure in two steps, which leads firstly to the formation and isolation of the mono-functionalized product. This can be used as reagent to obtain a bi-functionalized product with two different constituents, as shown in Figure 3.1.

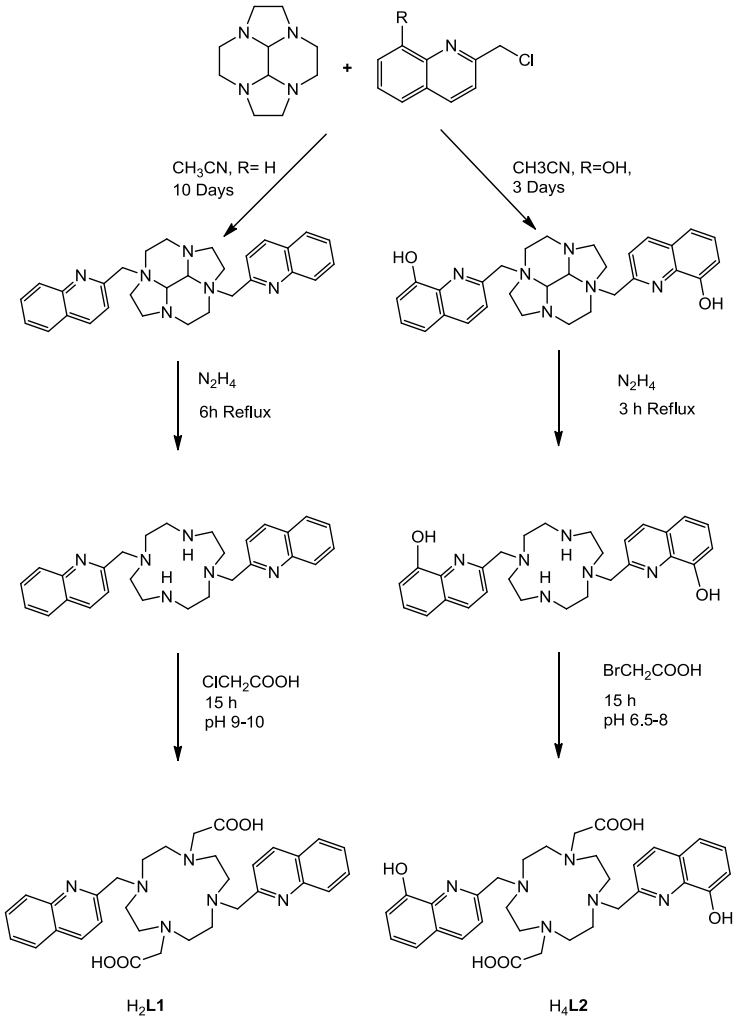

Figure 3.1 Synthesis procedure of H_2L1 and H_4L2.

The characteristic of the reactivity of bis-animals was exploited in the synthesis of the ligands L3 and L4 in both cases, to insert one group of 4,4'-dimethyl dipyridyl as a bridge between two units of cyclen avoiding any possible reaction on the nitrogen atom in position 7 of cyclen protected and without further functionalization of the receptor, or to insert two groups of 4,4'-dimethyl bipyridyl leading to the formation of the intermediate compound (Figure 3.2) which leads to the formation of the final compound L4.

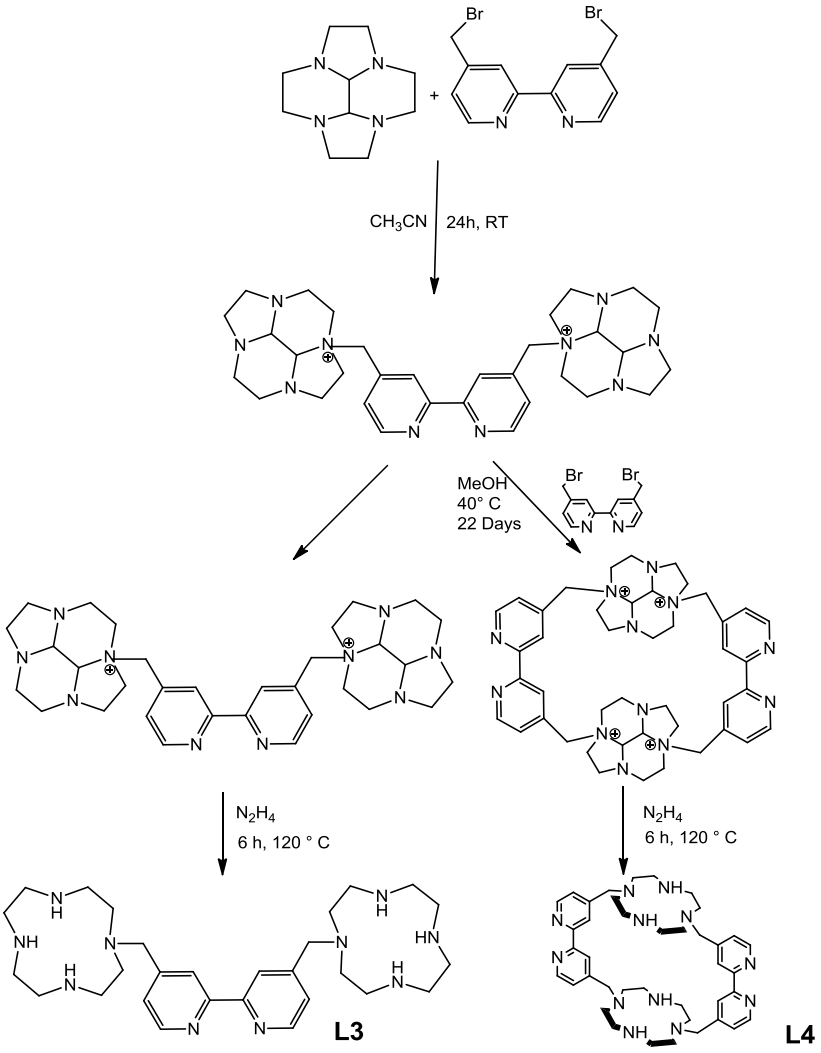

Figure 3.2 Synthesis procedure of L3 and L4.

3.2- Ligand H_2L1

3.2.1- Determination of the protonation constants of H_2L1

The protonation constants of the ligand were determined by potentiometric measurements in aqueous solution and their values are reported in Table 1.1. H_2L1 gives rise to five protonation equilibrium in the range investigated of pH (2-11). The first constant, relative to the equilibrium $L1^{2-} + H^{+} = HL1^{-}$, is not determinable by potenziometry because the equilibrium takes place in solution outside the studied pH range. H_2L1 can bind up to a maximum of six protons in aqueous solution, and these high number of acid-base equilibria is the result of the presence of multiple protonation sites, such as the amine groups of the macrocycle, the nitrogen atoms of the quinoline, and carboxyl groups.

Equilibrium	log K
$[L1]^{2-} + H^{+} = [HL1]^{-}$	> 12
$[L1]^{2-} + 2H^{+} = [H_2L1]$	22.20
$[H_2L1] + H^{+} = [H_3L1]^{+}$	7.05
$[H_3L1]^{+} + H^{+} = [H_4L1]^{2+}$	6.50
$[H_4L1]^{2+} + H^{+} = [H_5L1]^{3+}$	4.21
$[H_5L1]^{3+} + H^{+} = [H_6L1]^{4+}$	3.88

Table 1.1 Protonation constants of H_2L1, the error on constants in H_2O reported is lower than the 0.02 logarithmic units (298 K, I=0.1 M).

The distribution diagrams of the species, obtained the protonation constants in Table 1.1, are reported in Figure 1.1. As can be seen from the distribution diagrams, there is never a single prevalent species in a wide range of pH. The values of the protonation constants can be used to make hypothesis about the

corresponding protonation sites of the ligand by comparing them with the protonation constants of the constituent units of the receptor (cyclen, acetate groups, quinoline).

In fact, the first two protonation constants have high values, the first one being too high to be determined through potentiometric measurements. It can only be estimated as greater than 12 logarithmic units. This suggests that the first and second steps of protonation take place on the nitrogen atoms of cyclen. In fact, this macrocycle is particularly basic, its first two protonation constant being $\log K_{1\ Cyclen} = 11.27$, $\log K_{2\ Cyclen} = 9.96$[68]. However, the values of successive protonation constants are lower than the two previous constants and they may be due to the protonation of the remaining amine groups of cyclen, acetate groups ($\log K_{COOH}$ ca 4.5-5) or the nitrogen atoms of quinoline ($\log K_{Quinoline} = 4.79$).

The distribution diagram of the species shown in Figure 1.1 highlights the formation of several species in the solution.

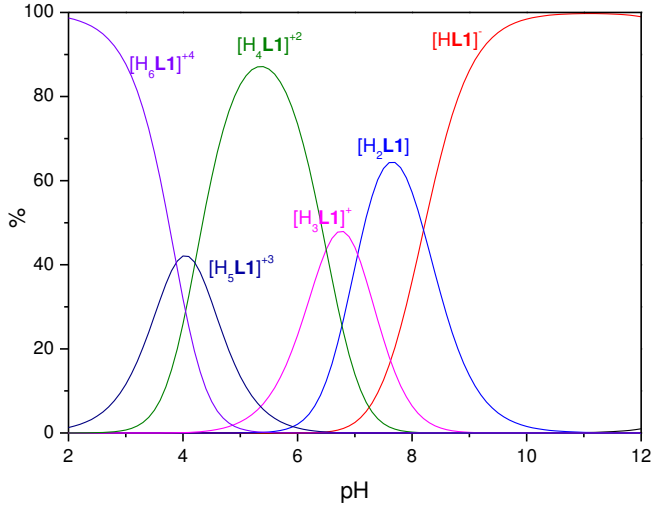

Figure 1.1 Distribution diagram of protonated species of H_2L1 (T=298 K, I=0.1 M).

[68] A.P. Leugger, L. Hertli, T.A. Kaden, Helv. Chim. Acta 61 (1978) 2296.

The species $[H_6L1]^{+4}$ is present at pH lower than 3, while the polyprotonated species $[H_5L1]^{+3}$, $[H_4L1]^{+2}$, $[H_3L1]^{+}$ are present in the pH range 4 - 7.5. However, the ligand at pH=7.5 is present in its neutral form $[H_2L1]$. Finally, the monoanionic species $[HL1]^{-}$ is formed at strongly alkaline pH values.

For more information on the protonation sites, UV-Vis and fluorescence emission spectra were registered at various values of pH, exploiting the fact that the protonation state of the nitrogen atoms of the quinoline can influence on the absorption and emission properties.

3.2.2- UV-Visible spectroscopic study of H_2L1

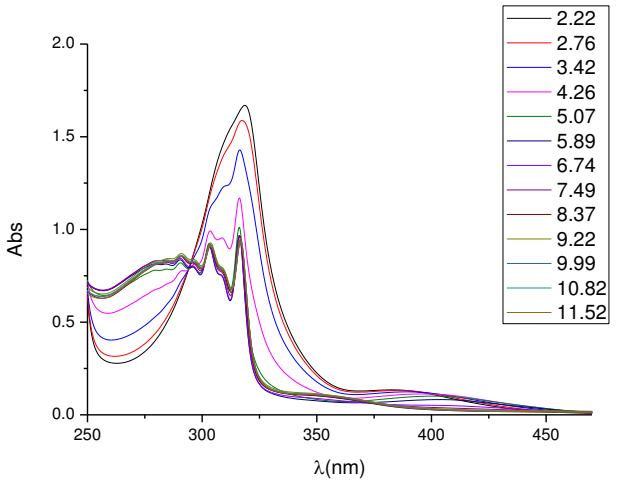

Figure 1.2. UV-Vis spectra of H_2L1 at different values of pH, ($[H_2L1]=1.16 \times 10^{-4}$ M, T =298 K).

Figure 1.2 shows the UV-Vis spectra of the ligand H_2L1 at various values of pH in aqueous solution. At acidic values of pH, we can observe two bands, an intense band with maximum at 318 nm and a second less intense band at 395 nm, while at basic pH, the intensity of the absorption band at 318 nm decreases and tends to

be structured in two bands, one at 318 nm and the other at 303 nm. In addition to, the band at 395 nm shifts toward the blue.

Figure 1.3 shows the absorbance at 318 nm at different values of pH, overlapped to the distribution diagram of the species. This figure obviously shows that the absorbance at 318 nm strongly increase for values of pH lower than 5, e.g., with the formation of species $[H_5L1]^{3+}$ and $[H_6L1]^{4+}$, while it does not significantly changes between pH 5 -12. and this allows us to conclude that the acidic protons in the last two steps of protonation are localized on the quinoline units.

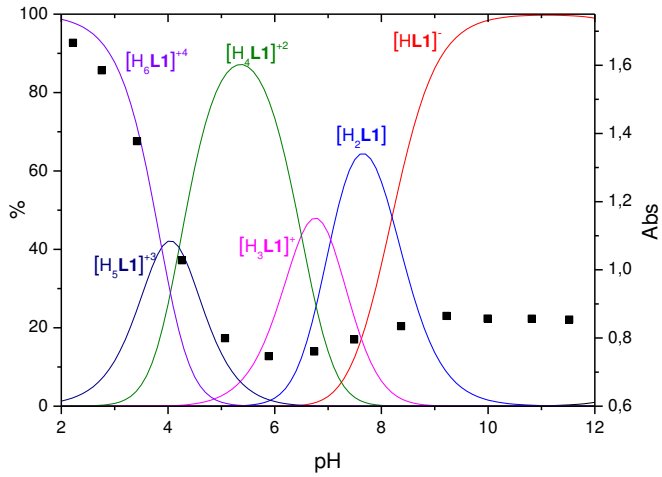

Figure 1.3 absorption intensity at 318 nm (■) of H_2L1 at different values of pH, overlapped to the distribution diagram of the species ($[H_2L1]=1.16 \times 10^{-4}$ M, T =298 K, I=0.1 M).

3.2.3- Fluorescence emission spectroscopic study of H_2L1

To analyze the characteristics of fluorescence emission of H_2L1, were registered emission spectra in aqueous solution at different values of pH. At acidic pH, the spectra are characterized by a band

at 410 nm. Moving towards alkaline pH, the intensity of this band decreases and it originates a new band shifted towards the blue with a maximum at 350 nm (Figure 1.4). This behavior is exactly the opposite of that of quinoline alone, which is characterized by a band at 360 nm at acidic pH, where it is present in solution in its protonated form and by a band shifted toward the red with a maximum at 425 nm at alkaline pH values.

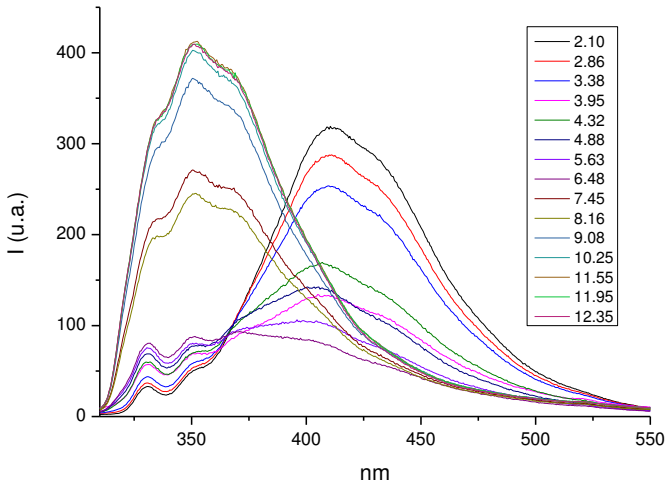

Figure 1.4 fluorescence emission spectra of H_2L1 at different pH values ($[H_2L1]=2.32 \times 10^{-5}$ M, T = 298K).

In order to determine the emission characteristics of the ligand, we have superimposed –the values of emission intensity at 410 and 350 nm at different values of pH with the distribution diagram of the species (Figure 1.5).

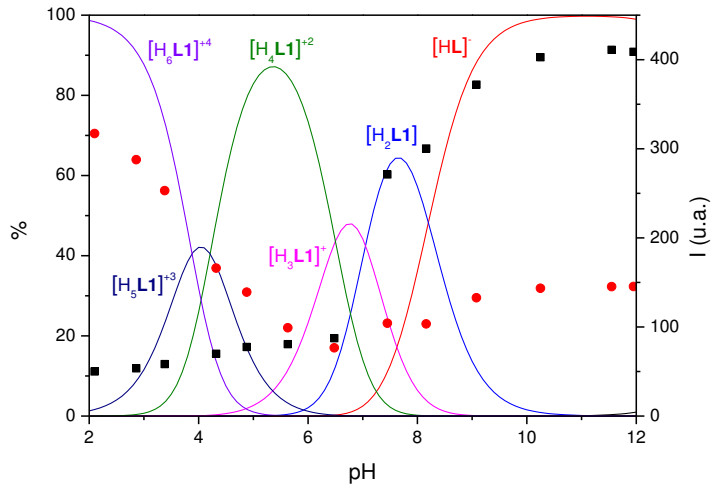

Figure 1.5 Emission intensity at 350 nm (▪) and 410 nm (●) of H_2L1 in function of pH superimposed to the diagram of distribution of protonated species, ($[H_2L1]=2.32 \times 10^{-5}$ M, T =298 K, I=0.1 M).

At alkaline pH values, between 7.5 and 11, where the species $[HL1]^-$ and $[H_2L1]$ are widely prevalent in solution (Figures 1.4 and 1.5) the ligand shows a marked fluorescence emission at 350 nm. This leads us to suppose that in these species, the acidic protons are localized on the amine groups of the macrocyclic system, in particular on the tertiary nitrogen atoms in position 1 and 7, thus inhibiting the eventual effect PET which could switch off the emission of the ligand. The emission intensity at 350 nm decreases for pH values between 7.5 and 6,-with the formation the species tri-protonate $[H_3L]^+$. This decrease is difficult to explain, but we can assume that in the tri-protonate species a "redistribution" of the acidic protons between the two carboxylate groups and the four amine groups of the macrocyclic system takes place in solution, leading to the reduction the positive charge localized on the two nitrogen atoms 1 and 7, making the latter able to switch off again the fluorescence of quinoline in its excited state via PET effect. At acidic pH, the formation of the species with a higher degree of

protonation $[H_5L]^{3+}$ and $[H_6L]^{4+}$ (pH < 5) leads to the appearance of a new band of emission at 410 nm, which can be attributed to the protonation of the two units of quinoline.

3.2.4- Determination of the stability constants of complexes with H_2L1

The formation constants of the complexes of the ligand with the metal cations were determined by potentiometric measurements and reported in the table 1.2.

The ligand H_2L1 presents kinetic inertia problems in the formation of the complexes and this prevents the complete speciation of the metal/ligand of systems in aqueous solution, especially at acidic pH.

All complexes are more stable than those obtained with the simple, non functionalized, macrocycle cyclen (for instance: logK = 15.3 for the formation of the complex $[Zn\text{-cyclen}]^{2+}$ compared to the logK = 21.2 (Table 2) of the complex [ZnL1]). This property is probably to be attributed to the involvement of the nitrogen of quinoline, and/or of the carboxylate groups in the coordination of the metal ion, which generally leads to a stabilization of the complexes. These considerations reflect in the diagrams of distribution of the species obtained carrying out the potentiometric measurements in the presence of metal cations at varying pH.

Table 1.2 shows that the stability of the complexes [ML1] increases in the order $Zn^{2+} < Cd^{2+} < Cu^{2+} < Pb^{2+}$. The greater stability of the complexes of Cu^{2+} compared to those of Zn^{2+} and Cd^{2+} is a fact normally observed in complexes with the polyamines and it can be attributed to the stabilizing effect of CFSE (crystal field stabilization energy) on the complex Cu^{2+}, being an ion d^9, while Zn^{2+} and Cd^{2+} have a similar stability, because they have both electron configuration d^{10}.

The high stability of the complex of Pb^{2+} is rather unexpected in a complex with a polyamine ligand. However, we can observe that the Pb^{2+} easily gives rise to complexes with coordination number greater than 6, which is rare for the other metals. Therefore we can assume that there may be a greater coordination number for the ion Pb^{2+} compared to the other three cations studied due to the presence of eight potential sites of coordination in the ligand, and this guarantees greater thermodynamic stability.

Equilibrium	**Zn^{2+}**	**Pb^{2+}**	**Cu^{2+}**	**Cd^{2+}**
$[L1]^{2-} + M^{2+} = [L1M]$	21.2(1)	24.47(8)	23.6(1)	22.0(1)

Table 1.2 Formation constants of the metal complexes of the ligand H_2L1 (308 K, 0.1 M NMe_4Cl).

Analyzing the figure 1.6, which reports the distribution diagram of the species in function of pH for the ion Zn^{2+} (taken as the model for the four metal ions investigated), we note that the metal cation only forms the complex [ML1], that is present in a percentage greater than 50% above pH 3 and it is the only species in solution above pH 4.

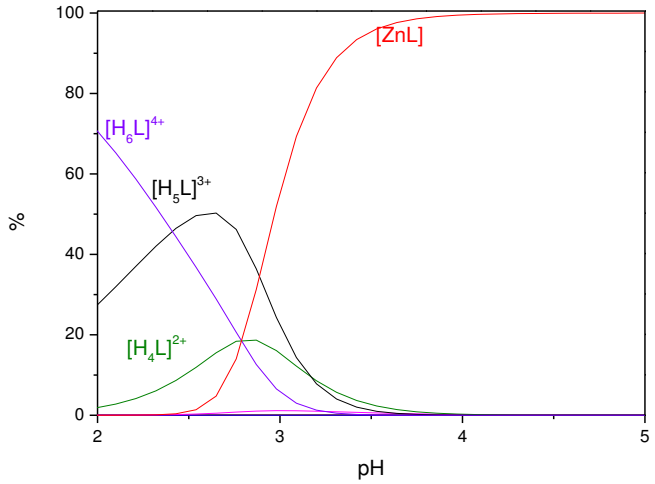

Figure 1.6 Distribution diagram of the complexed species of Zn^{2+} in the presence of an equivalent of H_2L1 ($[H_2L1] = [Zn^{2+}] = 1\times10^{-3}$ M, NMe_4Cl = 0.1M, 308 K).

3.2.5- UV-visible spectroscopic study of the metal complexes with H_2L1

To determine the coordinative characteristics of the ligand H_2L1, we recorded the UV-visible spectra of the ligand in the presence of some metal ions, in particular Zn^{2+}, Cd^{2+}, Pb^{2+} at different pH values. The purpose of this step is the analysis of the pH dependence of the UV-vis spectral featureWe also carried out measurements at a fixed pH value of 7.5 in Tris buffer by adding increasing amounts of different metal cations. Only the results with Cd^{2+} and Pb^{2+} will be showed, the results obtained with Cu^{2+} ad Zn^{2+} being very similar. The formation of the complexes resulted kinetically inert and therefore it was necessary to prepare with many hours in advance the solutions containing respectively 0.2, 0.4, 0.6, 0.8, 1.0, 1.2, 1.4 and 2.0 equivalents of each of the two metals. The solution were kept 18 hours in an incubator at 50 ° C and an hour in the air to return to room temperature before recording of the spectra.

In principle, the analysis of the UV-vis absorption spectra can give information the formed complexes in aqueous solution. The bands of absorption of the chromophore units are sensitive to eventual equilibria of protonation and deprotonation that they involve.

Figures 1.7, 1.9, 1.10, 1.1 show the spectra of the ligand H_2L1 in the presence of an equivalent of metal cations Zn^{2+}, Cd^{2+}, Pb^{2+} and Cu^{2+}, separately. We note that these spectra are not much diffrent, neither in the form of the bands, nor on the absorbance values. At pH lower than 4 the complexes present different characteristics of absorption with respect to those registered more alkaline at pH. At pH lower than 4 the complexes are not formed and the increase in the absorbance about at 318 nm is simply due to the protonation of the nitrogen atoms of the quinoline groups.

Figure 1.7 shows that the spectra recorded at strongly acidic pH values (pH 1.95 and 2.6) feature a strongly intense band at 318 nm and much less intense band at ca 400 nm. These spectral characteristics are simply typical of protonated quinoline. By decreasing pH from pH 2.68 to pH 5, the intensity of the band at 318 nm decreases and becomes more structured with the presence of the two maximums at 318 nm and 304 nm. Then, the band undergoes a shift toward the blue at 400 nm. For values of pH above 5, the spectral characteristics do not undergo further changes. This behavior is almost similar to that found for the free ligand.

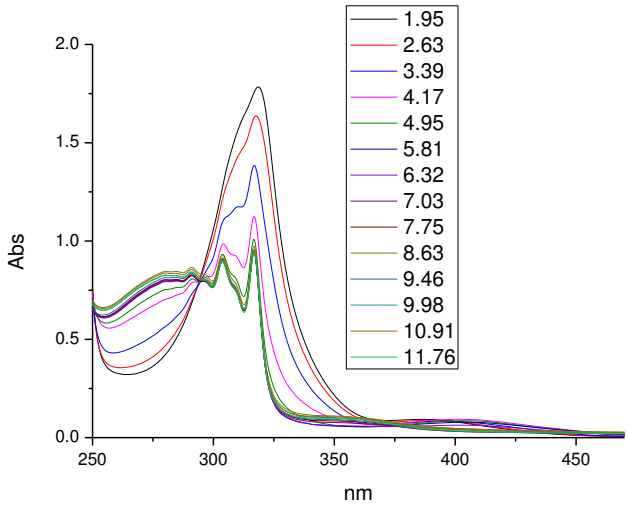

Figure 1.7 UV-Vis spectra of H_2L1 in the presence of one equivalent of Zn^{2+} at different values of pH ([H_2L1] = 1.16×10^{-4} M, T=298 K).

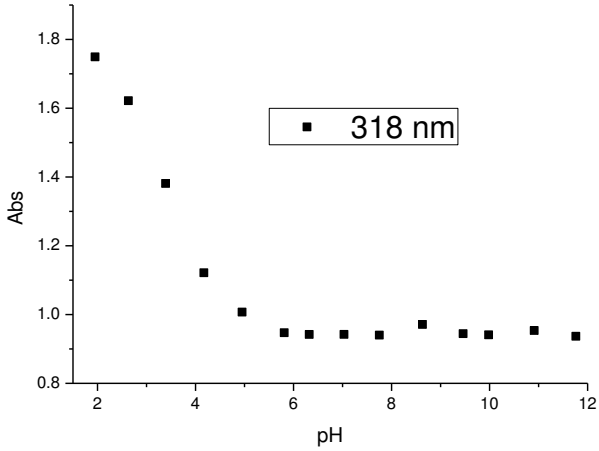

Figure 1.8 UV-Vis spectra of H_2L1 in the presence of one equivalent of Zn^{2+} at different values of pH at 318 nm ([H_2L1] = 1.16×10^{-4} M, T=298 K).

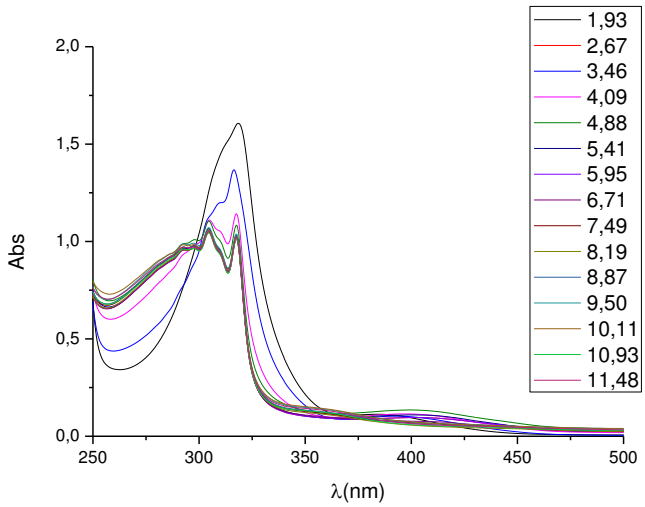

Figure 1.9 UV-Vis spectra of H_2L1 in the presence of one equivalent of Cd^{2+} at different values of pH ($[H_2L1] = 1.16\times10^{-4}$ M, T=298 K).

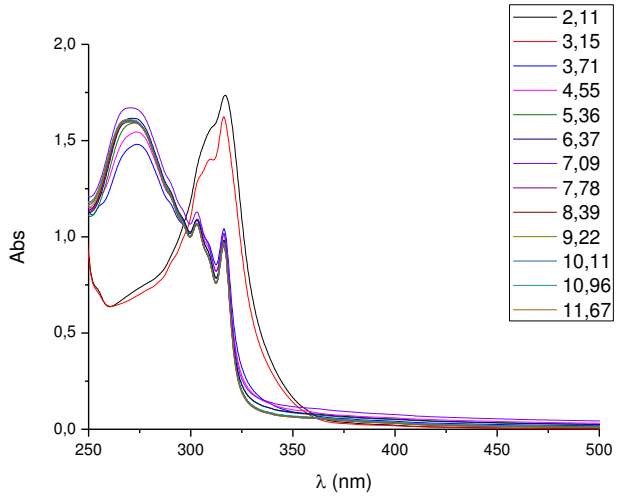

Figure 1.10 UV-Vis spectra of H_2L1 in the presence of one equivalent of Pb^{2+} at different values of pH ($[H_2L1] = 1.16\times10^{-4}$ M, T=298 K).

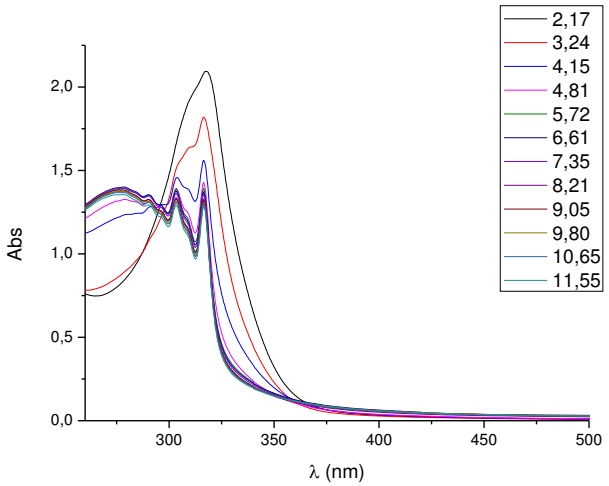

Figure 1.11 UV-Vis spectra of H_2L1 in the presence of one equivalent of and Cu^{2+} at different values of pH ([H_2L1] = 1.16×10^{-4} M, T=298 K).

Figure 1.12 shows the trend of the absorption maxima at 318 nm in function of the pH of the ligand-Free in the absence and presence of the four metal ions investigated: Zn^{2+}, Cd^{2+}, Pb^{2+} and Cu^{2+}. We note clearly a progressive decrease in the absorbance at 318 nm moving from pH 2 to pH 6 due to the proton release form the protonated nitrogen atom of quinoline. All complexes highlight a greater absorbance at 318 nm compared to the absorbance of the free ligand.

Analyzing the performance of the maximum of the absorption band at 318 nm in the presence of Zn^{2+}, Cd^{2+}, Pb^{2+} between pH 2 and 4, we note that the absorbance is analogous to those of the free ligand at the same pH, highlighting the absence of the coordination of the metal ions in this range of pH. However, at higher values of pH, the absorbance in the presence of metal ions results to be higher due to the effect of their coordination with the ligand. In

contrast to Zn^{2+}, Cd^{2+}, Pb^{2+}, in the presence of Cu^{2+} the absorbance is the highest in the whole investigated pH range of pH, even at strongly acidic pH values, suggesting that quinoline could interact with Cu^{2+} at a very acidic pH.

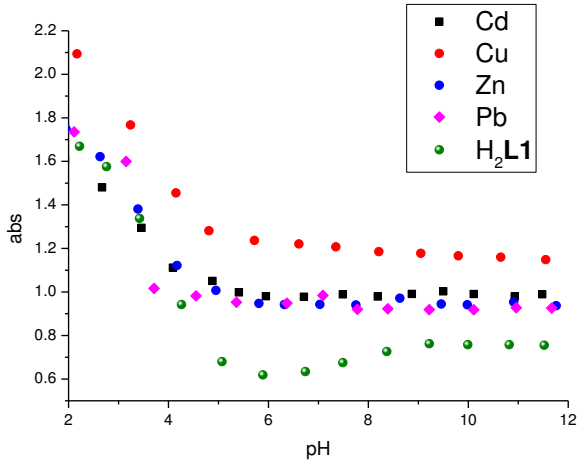

Figure 1.12 pH dependence of the absorption maxima at 318 nm for the metal ions Cu^{2+} (●), Cd^{2+} (▪), Zn^{2+} (●), Pb^{2+} (▪), H_2L1 (●).

3.2.6- Fluorescence emission spectroscopic study of the metal complexes with H_2L1

To determine the possible ability of the ligand to signal a metal cation in aqueous solution, we preliminary recorded fluorescence emission spectra on solutions at different values of pH in the presence of the Zn^{2+}, Cd^{2+}, Pb^{2+} and Cu^{2+} metal ions. In fact, $Zn^{2+}$and Cd^{2+} normally increase the emission of polyamine ligands, while Pb^{2+} and Cu^{2+} represent example of metal cations that normally quench the emission because of the heavy atom effect in the case of Pb^{2+} and of its paramagnetic nature in the case of Cu^{2+}.

The analysis was carried out by recording fluorescence emission spectra of an aqueous solution of the ligand H_2L1 in the presence of each metal ion both at a fixed pH and at a variable pH. We initially recorded the emission spectra of fluorescence of H_2L1 in the presence of an equivalent of each metal ion varying the pH in aqueous solution, in order to define the characteristics of emission of the different complex species formed by the ligand with each metal ion (Figures 1.13, 1.14, 1.15 and 1.16). In a similar way to that found in the case of the absorption spectra, the pH dependence of the spectral characteristics is similar for the four investigated metal ions[69].

At a given pH value, the spectra are similar in the presence of the different metal cations. At pH < 4 the recorded spectra are analogous to those of the free ligand at the same pH value, highlighting the absence of the coordination of the metal ion in this range of pH. In fact, the spectra are characterized by a single band with a maximum at 410 nm, whose intensity decreases with increasing pH, as clearly shown shown in Figure 1.13 in the case of Zn^{2+}. The intensity decrease is accompanied by a blu shift of the band and actually, the spectra recorded at alkaline pH values feature a weak emission at 367 nm.

[69] C. Bazzicalupi, A. Bencini, A. Bianchi, C. Giorni, V. Fusi, B. Valtancoli, M. A. Bernardo, F. Pina, Inorg. Chem., 38 (1999), 3806.

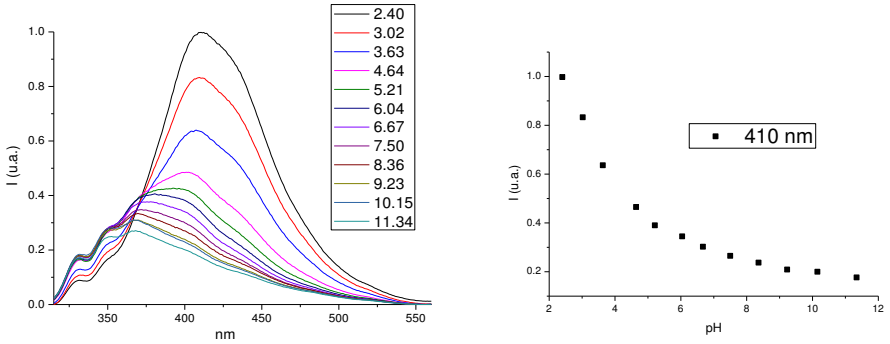

Figure 1.13 fluorescence emission spectra of H_2L1 and emission intensity at 410 nm in the presence of one equivalent of Zn^{2+} at different values of pH ([H_2L1]=2.32 × 10^{-5} M, T=298 K).

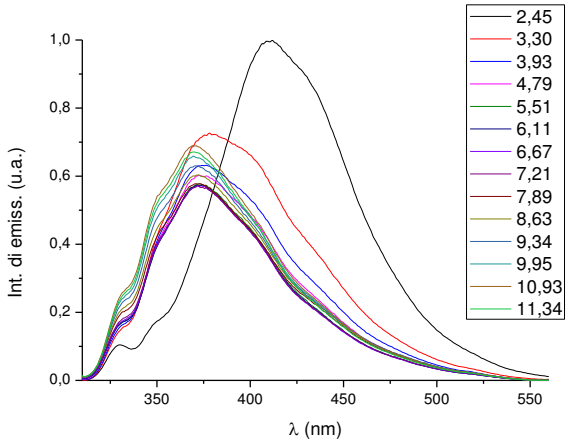

Figure 1.14 fluorescence emission spectra of H_2L1 in the presence of one equivalent of Cd^{2+} at different values of pH ([H_2L1]=2.32 × 10^{-5} M, T=298 K).

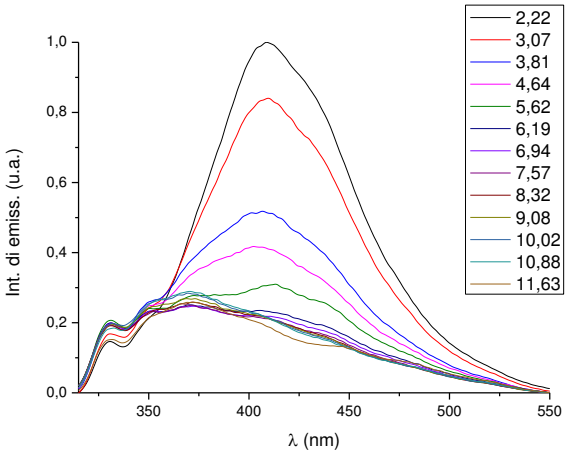

Figure 1.15 Emission intensity of H_2L1 in the presence of one equivalent of Pb^{2+} at different values of pH ($[H_2L1]=2.32 \times 10^{-5}$ M, T=298 K).

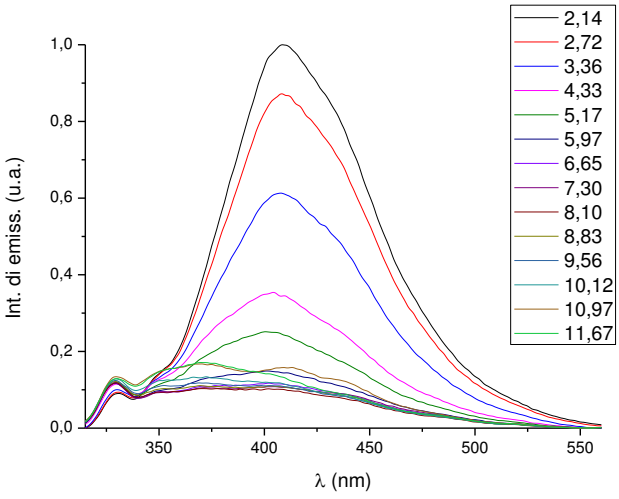

Figure 1.16 Emission intensity of H_2L1 in the presence of one equivalent of Cu^{2+} at different values of pH ($[H_2L1]=2.32 \times 10^{-5}$ M, T=298 K).

Figure 1.17 reports the emission intensity at 410 nm of the free ligand and of the complexes with the four metal ions as a function of pH. We can note that the coordination of the Zn^{2+} and Cd^{2+} leads to an increase of emission of the ligand, while Cu^{2+} and Pb^{2+} ' turn off ' the emission at any value of pH[70,71].

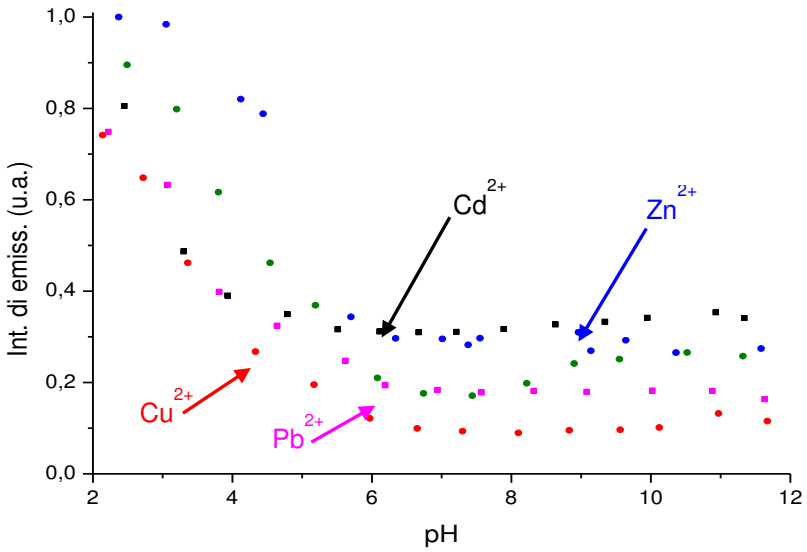

Figure 1.17 Emission intensity at 410 nm of H_2L1 in the absence *(●)* and in the presence of 1 equivalent of Cd^{2+} (▪),Cu^{2+} (●), Zn^{2+} (●) and Pb^{2+} (▪).

To elucidate the effect of metal coordination on the emission properties of the complexes, we recorded the emission spectra of the ligand in the presence of increasing amounts of the four metals at pH 6, using MES as buffer(Figure 1.18)) Addition of Zn^{2+} and Cd^{2+} leads an increase of the emission intensity as shown in Figure 1.18 for the case of Cd^{2+} (Figure 1.18).

[70] T. L. Banfield, D. Husain, Trans. Faraday Soc., 65 (1995), 1969

[71] A. W. Varnes, R. B. Dodson, E. L. Wehry, J. Am. Chem. Soc., 94 (1972), 946.

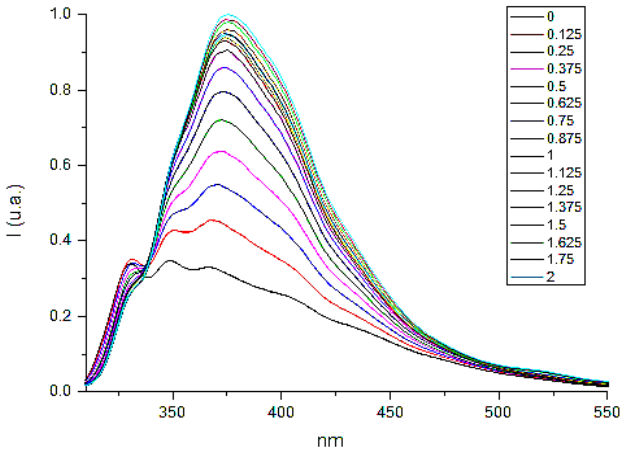

Figure 1.18 Fluorescence emission spectra of H_2L1 in the presence of increasing amount of Cd^{2+} at pH=6 ([H_2L1]=2.32 × 10^{-5} M, T=298 K).

Figure 1.19 reports the emission intensity of the ligand at 378 nm as a function of the added equivalents of Cd^{2+}. The coordination of the metal ion leads to a linear increase in the intensity of emission up to the addition of ca 0.9 equivalents of Cd^{2+}. The addition amounts of metal cation greater than 1.2 equivalents does not lead to further increase of the emission intensity, indicating the formation of stable complexes with 1:1 stoichiometry in solution.

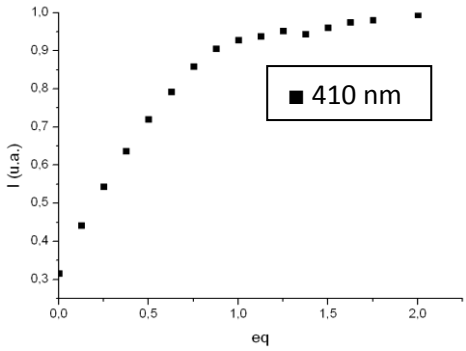

Figure 1.19 Emission intensity of H_2L1 at 410 nm in the presence of increasing amount of Cd^{2+} at pH=6 ([H_2L1]=2.32 × 10^{-5} M, T=298 K).

Figure 1.20 reports the fluorescence emission of the ligand alone and in the presence of one equivalent of different metal cations (Zn^{2+}, Cd^{2+}, Pb^{2+}, Hg^{2+}, Cu^{2+}, Mn^{2+}, Ca^{2+}, Ni^{2+}, Co^{2+}, Fe^{2+}, Na^{+} and Mg^{2+}).

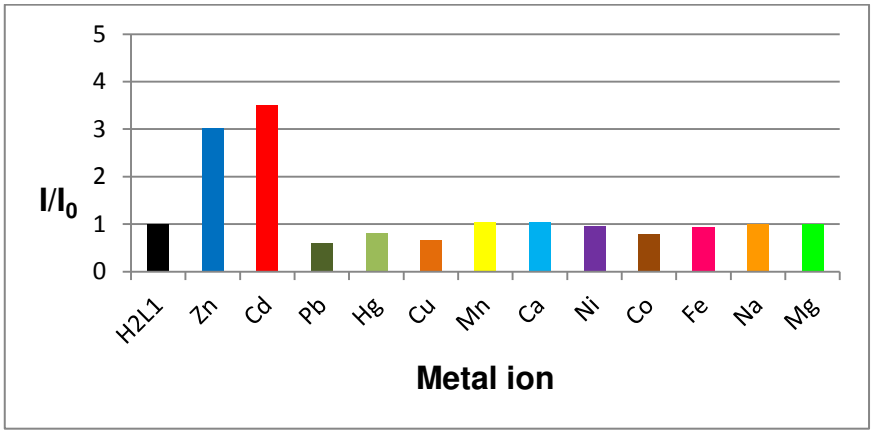

Figure 1.20 Value of I / I_0 of the ligand H_2L1 in the presence of different metal ions. I is the intensity of emission in the presence of one equivalent of metal ion and I_0 is the intensity of emission of H_2L1 (pH = 6, MES buffer).

The emission intensity increases only in the presence of Zn^{2+} and Cd^{2+}. The emission increases more than 3 times in the presence of one equivalent of Cd^{2+} and about twice in the presence of one equivalent of Zn^{2+}. The fluorescence substantially does not change in the presence of Mg^{2+}, Ca^{2+} and Na^{+}, and it decreases with the other ions investigated.

3.2.7- Crystal structure of the complex [ZnL1]

In the course of our study, we also obtained crystals of the [ZnL1] complex, thanks to a slow evaporation of an aqueous solution containing H_2L1 and $Zn(ClO_4)_2.6H_2O$ at pH=7. The structure of the complex was then solved by means of single crystal X-ray diffraction and it is shown in Figure 1.21. Bond distances and angles are reported in table 1.3 and 1.4.

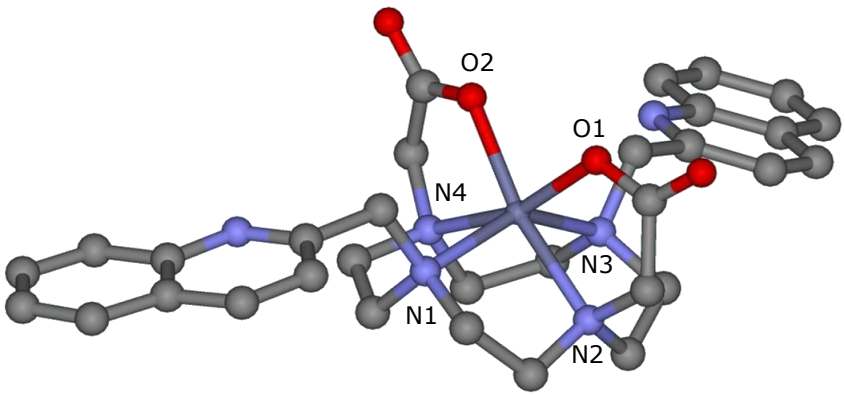

Figure 1.21 Crystal structure of [ZnL1].

Atom	Bond distance (Å)
N1	2.19
N2	2.29
N3	2.24
N4	2.19
O1	2.00
O2	2.11

Table 1.3 Bond distances of the complex [ZnL1].

Atoms	Bond angle (°)
N1-Zn-N2	82.6
N2-Zn-N3	80.0
N3-Zn-N4	79.4
N4-Zn-N1	79.6
N1-Zn-N3	142.2
N2-Zn-N4	117.9
N1-Zn-O1	108.2
N1-Zn-O2	104.2
N2-Zn-O1	79.7
N2-Zn-O2	164.7
N3-Zn-O1	98.4
N3-Zn-O2	104.4
N4-Zn-O1	161.4
N4-Zn-O2	77.4
O1-Zn-O2	85.1

Table 1.4 Bond angles of the complex [ZnL1].

The metal ion results hexa-coordinated by four nitrogen atoms of the unit of cyclen and two oxygen atoms of the two carboxylic groups in their deprotonated form. The geometry is substantially distorted octahedral. However, the two units of quinoline are not

involved in the coordination, to indicate the preference of the metal to the coordination of two groups of anionic carboxylate compared to the atoms of nitrogen heteroaromatics of the quinoline systems, at least in the solid state.

3.3- Ligand H_4L2

3.3.1- Determination of the protonation constants of H_4L2

Ligand H_4L2 contains several sites able to give acid-base equilibria in aqueous solution, e.g., the amine groups of cyclen, the carboxylic groups, the nitrogen atoms the hydroxyl groups in 8 position of quinoline linked to the macrocycle. Therefore, H_4L2 gives rise to several protonation equilibrium in the range investigated of pH (2-11). The protonation constants of the ligand were determined by potentiometric measurements in aqueous solution and their values reported in Table 2.1.

Equilibrium	log K
$[L2]^{4-} + H^+ = [HL2]^{3-}$	10.11
$[HL2]^{3-} + H^+ = [H_2L2]^{2-}$	10.3
$[H_2L2]^{2-} + H^+ = [H_3L2]^-$	8.38
$[H_3L2]^- + H^+ = [H_4L2]$	6.3
$[H_4L2] + H^+ = [H_5L2]^+$	4.5
$[H_5L2]^+ + H^+ = [H_6L2]^{2+}$	3.7
$[H_6L2]^{2+} + H^+ = [H_7L2]^3$	2.5
$[H_7L2]^{3+} + H^+ = [H_8L2]^{4+}$	2.2

Table 2.1 Protonation constants of H_4L2; the reported error on constants is lower than the 0.02 logarithmic units (T=298 K, I=0.1 M).

We can note that the ligand can bind up to a maximum of eight protons in aqueous solution, and this high number of acid-base

equilibria is the result of the presence of the multiple protonation sites mentioned above. We can speculate on the possible protonation site involved in each protonation equilibria considering the protonation constants of the different units that constitute the ligand. The first two protonation constants of cyclen are remarkably high for a polyamine ligand ($LogK_{1Cyclen}$ = 11.27, $LogK_{2Cyclen}$ = 9.96), while the third one is rather low ($LogK_{3Cyclen}$ = 1.6), Similarly deprotonation of the –OH groups of quinoline occurs only at strongly basic pH values ($LogK_{1quinoline}$ = 9.89), while the nitrogen atom is a very base ($LogK_{2quinoline}$ = 5.13). Finally, the acetate groups in polyamine-polycarboxilic acids present a protonation constants that range between 4.5 and 5 log. units. Considering these values, it can be suggested that the first four protonation steps of the L^{4-} ligand occur on two nitrogen atoms of cyclen and on the hydroxyl groups of quinoline. However, the data in Table 2.1 does not allow us to infer hypothesis of the remaining protonation steps. The protonation constants in Table 2.1 allows to calculate the diagrams of distribution of the species, which is shown in Figure 2.1. At pH < 4.5, there are various poly-protonate species ($[H_8L2]^{+4}$, $[H_7L2]^{+3}$, $[H_6L2]^{+2}$, $[H_5L2]^{+}$). The neutral species of the ligand $[H_4L2]$ is formed at pH 4.5 - 6.5. Finally, at pH > 7, H_4L2 gives rise to anionic species and, finally, at pH > 10, the formation of the species completely protonated $[L2]^{-4}$ occurs in solution.

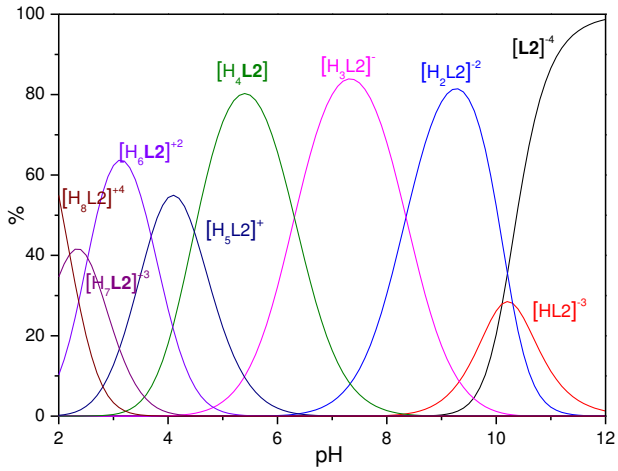

Figure 2.1 Distribution diagram of protonated species of H_4L2 (T = 298K, I = 0.1 M).

To obtain further information on the protonation sites involved in the different protonation steps, we recorded UV-vis and fluorescence emission spectra at various values of pH. In fact, the protonation state of the nitrogen atoms and the hydroxyl groups of the 8-hydroxy quinoline can influence both the absorption and emission properties.

3.3.2- UV-Visible spectroscopic study of H_4L2

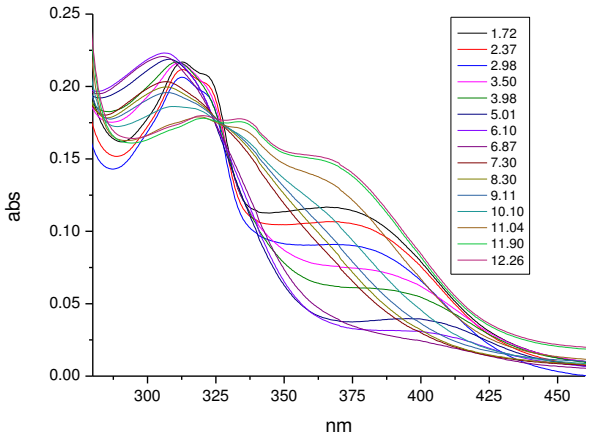

Figure 2.2 UV-Vis spectra of H_4L2 at different values of pH, ($[H_4L2]=1.7\times10^{-4}$ M, T = 298 K).

Figure 2.2 shows the absorption spectra of the ligand H_4L2 at different values of pH. The spectrum is different from ligand H_2L1 and feature different absorption maxima. To better visualize the spectral changes occurring by varying pH, we have reported in Figure 2.3 three spectra of H_4L2 that are obtained at three particular values of pH, e.g. at strongly acidic pH value, at pH 6.1 and finally at strongly basic pH value (greater than 12).

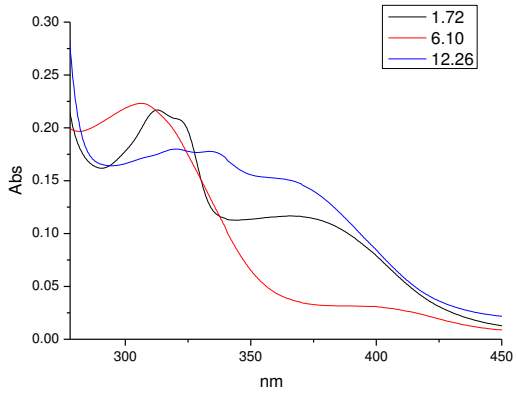

Figure 2.2 UV-Vis spectra of H_4L2 at pH 1.72, 6.10 and 12.26 ($[H_4L2]=1.7\times10^{-4}$ M, T = 298 K).

At pH=1.72, the spectrum presents two maxima of the absorption, at 306 nm and 374 nm, respectively, which are typical of the protonated form of 8-hydroxy quinoline.

The intensity of the band at 374 nm significantly decreases by increasing pH, while the band at 306 nm undergoes a slight shift toward shorter wavelengths. At pH 6.10, the spectrum is similar to this of neutral species of 8-hydroxy quinoline. At strongly alkaline pH value, the spectrum shows a broad band with a maximum at ca 320 nm a shoulder at ca 380 nm.

Figure 2.3 and 2.4 shows the spectral changes occurring at acidic and at alcline pH value. Figure 2.3 clearly depict the spectral changes occurring upon deprotonation of the quinoline nitrogens, e.g., a decrease of the absorbance at 375 nm accompanied by a blu shift of the band at ca 320 nm.

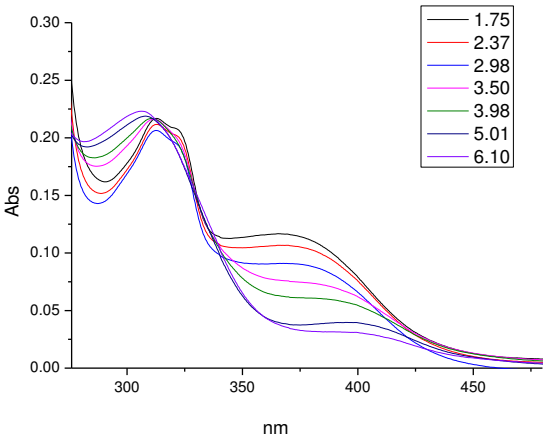

Figure 2.3 UV-vis spectra of H_4L2 between pH 1.75 and 6.10 ($[H_4L2]=1.7\times10^{-4}$ M, T = 298 K).

Figure 2.4 shows that the increase of pH from 6.1 to 12.26 leads to a decrease in intensity of the the band at 306 nm and to an enhancement of the intensity of the absorption band at 374 nm. At pH 12.26, the spectrum is very similar to that of the anionic form of 8-hydroxy quinoline. Therefore, the spectral changes observed for the ligand are similar to that of the single fluorophore.

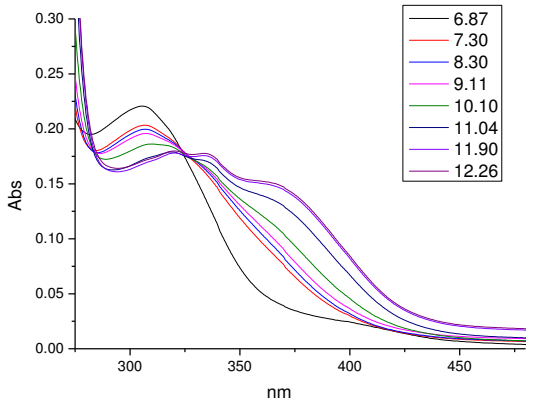

Figure 2.4 UV-vis spectra of H_4L2 between pH 6.87 and 12.26 ($[H_4L2]=1.7\times10^{-4}$ M, T = 298 K).

Figure 2.5 reports the absorbance at 306 and at 374 nm overlapped to the distribution diagram of the species at different values of pH. As a matter of fact, the absorbance at 306 nm is not significantly affected by pH. Conversely, the absorbance at 374 nm shows a marked increase below pH 5, where the species $[H_6L2]^{+2}$ and $[H_7L2]^{3+}$ are formed in solution. This suggest that the formation of these species may imply the protonation of the nitrogen atom of 8-hydroxyquinoline. An increase of the absorbance at 374 nm also accompanies the formation of the $[H_2L2]^{2-}$, $[HL2]^{3-}$ and $[L2]^{4-}$ species, indicating that two of three last protonation step occurring above pH 8 involve the –OH groups of 8-hydroxyquinoline.

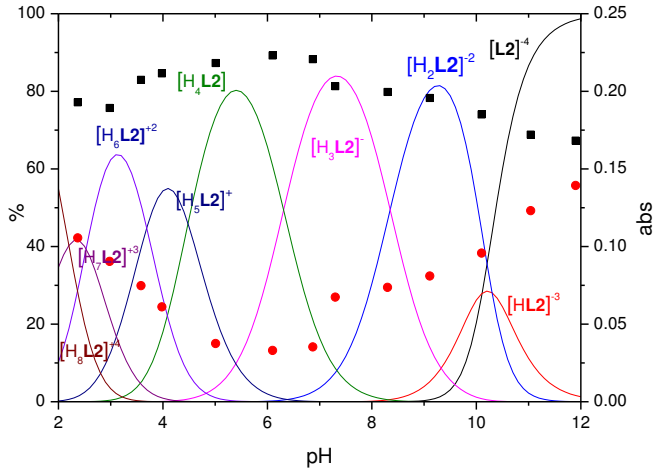

Figure 2.5 absorption intensity at 306 nm (■) and 374 nm (●) of H_4L2 at different values of pH, overlapped to the distribution diagram of the species ($[H_4L2]=1.7\times10^{-4}$ M, T = 298 K, I = 0.1 M).

3.3.3- Fluorescence emission spectroscopic study of H_4L2

To analyze the characteristics of fluorescence emission of H_4L2, were recorded the fluorescence emission spectra of the ligand in aqueous solution at different values of pH (Figure 2.6). The ligand was excited at 325 nm, in correspondence of the isosbestic point in the UV-Vis spectra (Figure 2.2).

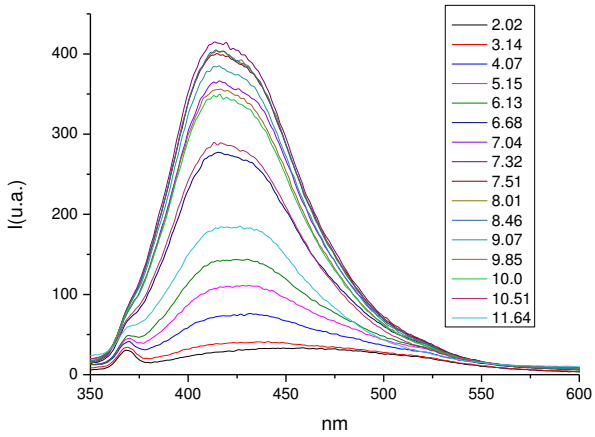

Figure 2.6 Fluorescence emission spectra of H_4L2 at different values of pH ($[H_4L2]= 5.56 \times 10^{-6}$ M, T = 298 K).

The emission spectra of the ligand H_4L2 show a marked pH dependence. Differently from ligand H_2L1, H_4L2 presents a single band with the emission intensity at 420 nm. Analyzing the pH dependence, it is clear that the ligand weakly emits between pH 2.02 and 5.15. Increasing pH from pH 6.13 to 7.32, we can note an increase of the emission, while at pH > 8.01 another decrease in the intensity is observed, which leads to the quenching the system, as shown in Figure 2.7 and Figure 2.8.

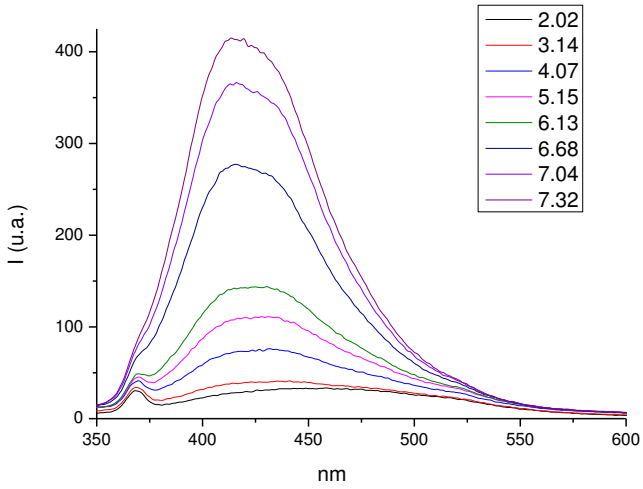

Figure 2.7 Fluorescence emission spectra of H_4L2 at acidic pH ($[H_4L2]= 5.56 \times 10^{-6}$ M, T = 298K).

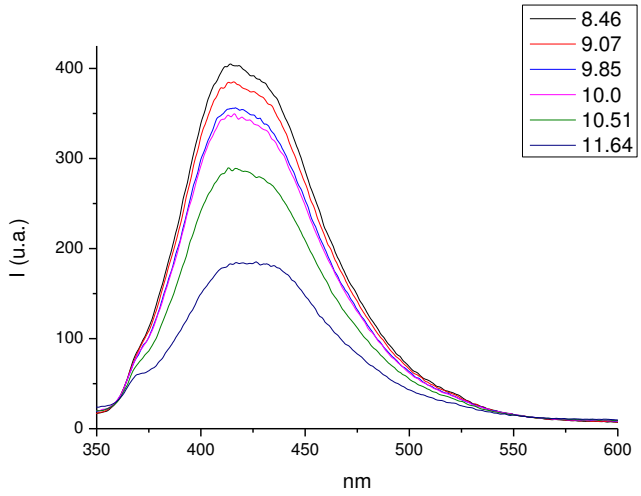

Figure 2.8 Fluorescence emission spectra of H_4L2 at alkaline basic pH ($[H_4L2] = 5.56\times10^{-6}$ M, T=298 K).

In order to determine the emission characteristics of the protonated forms of the ligand, we have superimposed the values of emission

intensity at 420 at different values of pH with the distribution diagram of the species (Figure 2.9).

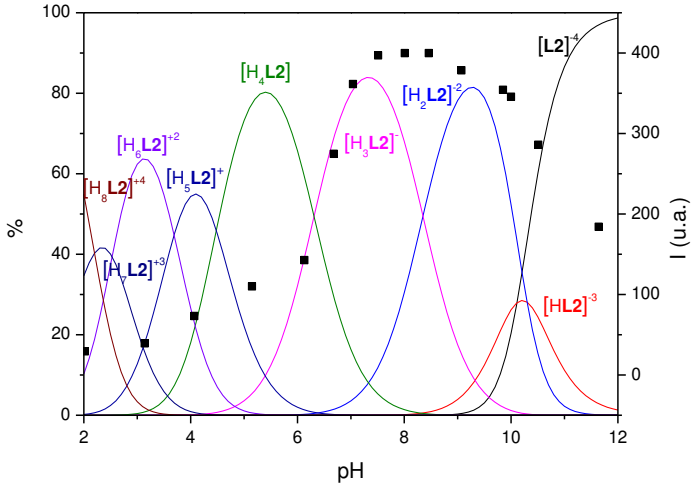

Figure 2.9 Emission intensity at 420 nm (▪) of H_4L2 as a function of pH superimposed to the diagram of distribution of protonated species, ($[H_4L2]= 5.56 \times 10^{-6}$ M, T = 298 K, I = 0.1 M).

Figure 2.9 shows that the most emissive species are $[H_3L2]^-$ e $[H_2L2]^{-2}$. This leads us to suggest that in these species two nitrogen atoms of cyclen can be protonated, i. e. the acidic protons are localized on the amine groups of cyclen, in particular on the nitrogen atoms in 1 and 7 positions, thus inhibiting the PET process to the fluorophore in its excited state. Most likely in the $[L2]^{-4}$ and $[HL2]^{-3}$ at least one of the amine groups of in 1 or 7 position of cyclen are not protonated, leading to the activation of a PET effect, which quenches the emission of the fluorophore. The decrease of the emission observed for the species with higher protonation degree can be attributed to the protonation of the nitrogen atoms of the 8-hydroxy quinoline, which leads to a quenching of the fluorescence.

3.3.4- Coordination of metal ions with H_4L2

It can be of interest to make comparisons between the coordination characteristics of the ligand H_4L2 with those of H_2L1, in order to determine the effects of the substitution of quinoline groups with the 8-hydroxyquinoline units. We first analyzed the effects of the coordination of Zn^{2+} and Cd^{2+} on the absorption characteristics in the UV-Vis region and on the fluorescence emission. The ligand presents several donor atoms of different nature. The high number of donors could suggests the formation of complexes with metal to ligand 1:1 and 2:1 stoichiometry. Therefore, we carried out measurements at different pH value in the presence of one or two equivalent of these metals.

3.3.5- UV-Vis spectroscopic study of the metal complexes with H_4L2

3.3.5.1- UV-Vis spectroscopic study of Zn^{2+}

Figure 2.10 shows the UV-Vis spectra of the ligand H_4L2 in the presence of an equivalent of Zn^{2+} in aqueous solution at various values of pH.

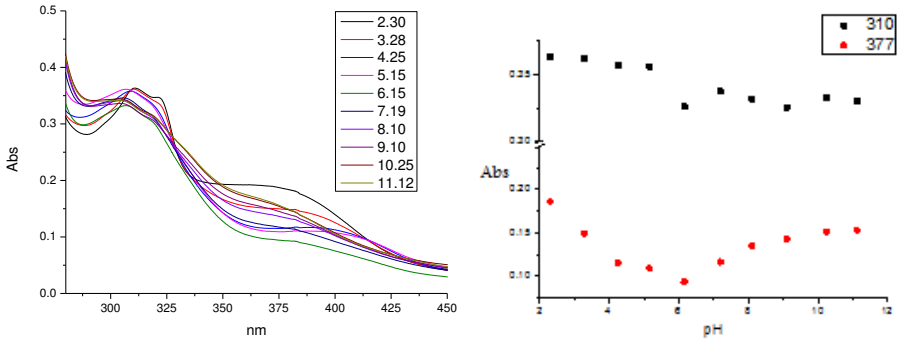

Figure 2.10 UV-Vis spectra of H_4L2 in the presence of an equivalent of Zn^{2+} at different values of pH and absorbance values measured at 310 nm(■) and 377 nm(●) ($[H_4L2] = 1.7\times10^{-4}$ M, T = 298 K).

At acidic pH, the spectra feature two bands at 310 and 377 nm, respectively, the first one being more intense. By increasing pH, the absorption of the band at 310 decreases nm up to pH 5. Above this pH, the absorbance at 310 nm remains almost constant. The absorbance of the band at 377 nm shows a decrease from pH 2 to pH 6, to subsequently increase from neutral to alkaline pH values. The same behavior was found in the presence of two equivalents of Zn^{2+} (Figure 2.11).

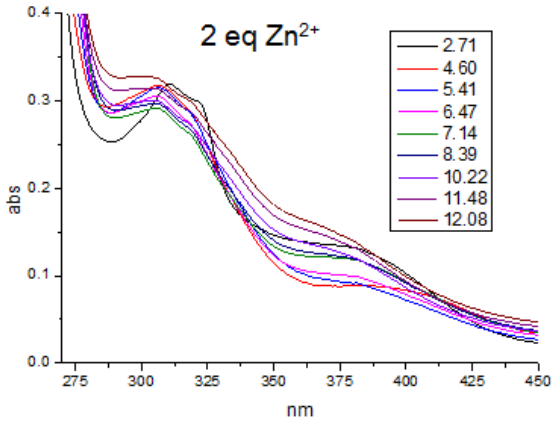

Figure 2.11 UV-Vis spectra of H_4L2 in the presence of 2 eq of Zn^{2+} at different values of pH ($[H_4L2] = 1.7\times10^{-4}$ M, T = 298 K).

Figure 2.12 reports the absorbance measured at 310 and 377 nm of the free ligand and of the ligand in the presence of one or two equivalents of metal cation (Figure 2.12). The measured absorbance values appear to be not much affected by the presence of Zn^{2+}. Only the band at 377 nm is more intense at basic pH in the presence of 1 or 2 equivalents of the metal ion, suggesting that 8-hydroxiquinoline could be involved in metal coordination at alkaline pH values.

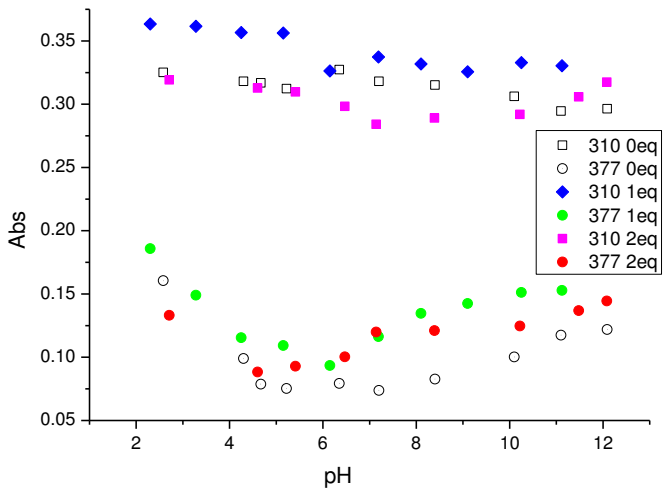

Figure 2.12 pH dependence of the absorbance at 310 nm with 0 eq (□), 1 eq (♦) and 2 eq (■) and at 377 nm with 0 eq (○), 1 eq (●) and 2 eq (●) of Zn^{2+} as a function pH ($[H_4L2] = 1.7\times10^{-4}$ M, T=298 K).

3.3.6- Fluorescence emission spectroscopic study of the metal complexes with H_4L2

3.3.6.1- Fluorescence emission spectroscopic study of Zn^{2+}

The fluorescence emission spectra were registered either at different values of pH in the presence of 1 or 2 equivalents of Zn^{2+} or at fixed pH value in the presence of increasing amount of Zn^{2+}.

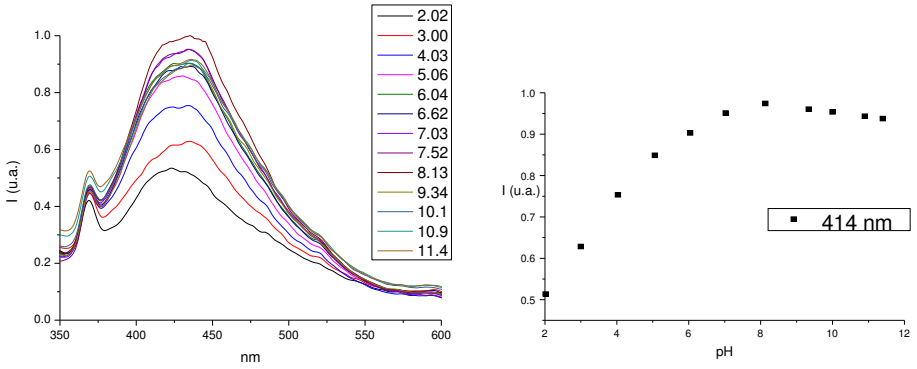

Figure 2.13 fluorescence emission spectra of H_4L2 and emission intensity at 414 nm in the presence of one equivalent of Zn^{2+} at different values of pH ([H_4L2] = 5.56×10^{-6} M, T=298 K).

As shown in Figure 2.13, the fluorescence emission spectra of the ligand in the presence of an equivalent of Zn^{2+} show a marked pH dependence. In fact, we can note an increase of the emission intensity at 414 nm from pH 3 to pH 8. At more alkaline pH value the emission does not show significant changes. The same experiment was also performed in the presence of two equivalents of Zn^{2+} and the results are summarized in Figure 2.14, where we have reported the emission intensity at 414 nm in the absence and in the presence of one or two equivalents of metal cation.

Figure 2.14 clearly shows that the presence of Zn^{2+} does not affect the emission from pH 2 to 5, where the metal cation is likely to be not bound by the ligand. Conversely, above pH 6 Zn^{2+} coordination

induces a marked quenching of the ligand emission, independently on the amounts of Zn^{2+} present in solution.

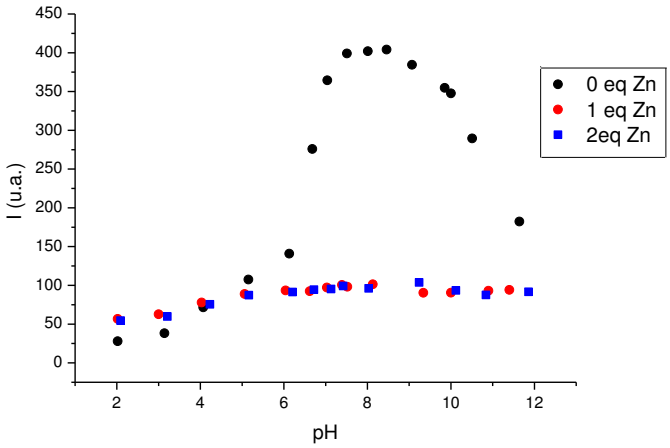

Figure 2.14 pH dependence of the emission intensity at 414 nm in the absence of Zn^{2+} 0 eq (●) and in the presence of 1 eq (●) and 2 eq (■) of Zn^{2+} in function pH ([H_4L2] = 5.56×10^{-6} M, T=298 K).

We also recorded fluorescence emission spectra of H_4L2 in the presence of increasing amounts of Zn^{2+} at pH 7.2, and the results are shown in the Figure 2.15. We can note that additions of Zn^{2+} cause a progressive quenching of the system. The emission remains almost constant in the presence of Zn^{2+}amounts greater than 1 equivalent. This suggests the formation of a stable complex with 1:1 metal to ligand stoichiometry in the solution.

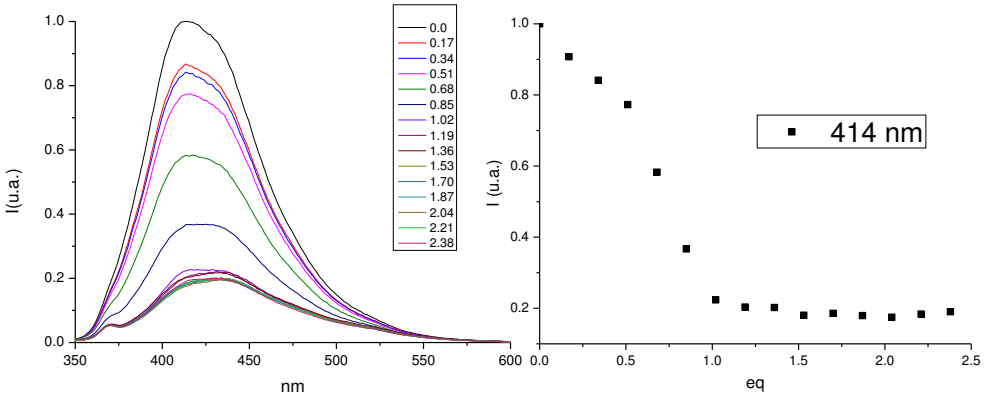

Figure 2.15 Fluorescence emission spectra of H_4L2 registered at pH=7.2 and emission intensity at 414 nm in the presence of increasing amount of Zn^{2+} ($[H_4L2] = 5.56\times10^{-6}$ M, T=298 K).

3.3.6.2- Fluorescence emission spectroscopic study of Cd^{2+}

As in the case of Zn^{2+}, the coordination of the Cd^{2+} does not significantly alter the absorption spectra but alters considerably the fluorescence emission of the ligand. We have reported the fluorescence emission spectra in the presence of 1 equivalent of Cd^{2+} at different values of pH in Figure 2.16. At strongly acidic pH values, the ligand shows an emission band at 438 nm similarly to the free ligand. By increasing pH, we can observe a considerable increase of the emission intensity up to pH 5.14. At higher pH values the emission band does not undergo significant changes and the emission remains almost constants as depicted in Figure 2.17.

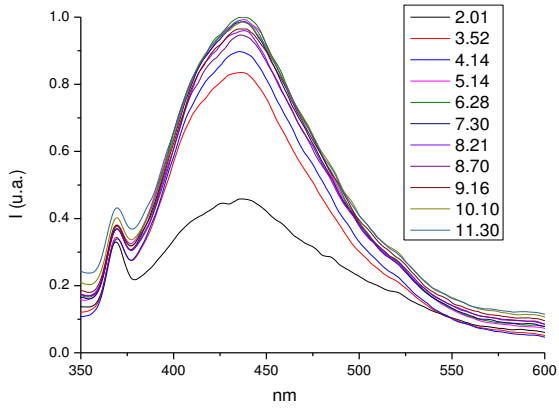

Figure 2.16 fluorescence emission spectra of H_4L2 in the presence of 1 eq of Cd^{2+} at various values of pH ($[H_4L2] = 5.56\times10^{-6}$ M, T=298 K).

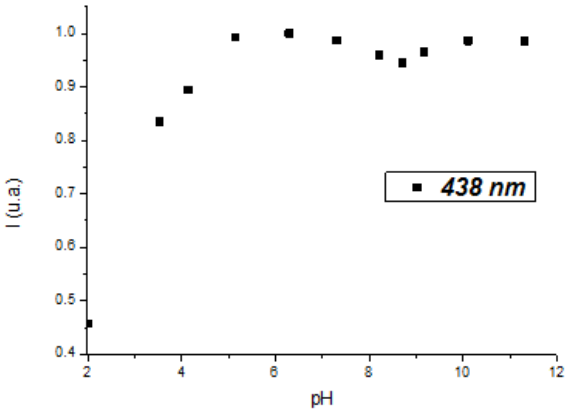

Figure 2.17 Emission intensity of H_4L2 measured at 438 nm in the presence of 1 eq of Cd^{2+} at different values of pH ($[H_4L2] = 5.56\times10^{-6}$ M, T=298 K).

Figure 2.18 compare the pH dependence of the ligand in the absence and in the presence of one or two equivalents of Zn^{2+} and Cd^{2+}. As in the case of Zn^{2+}, the presence of one or two

equivalents of Cd^{2+} leads to an quenching of the emission at pH > 6, while almost no effect is observed below pH 6.

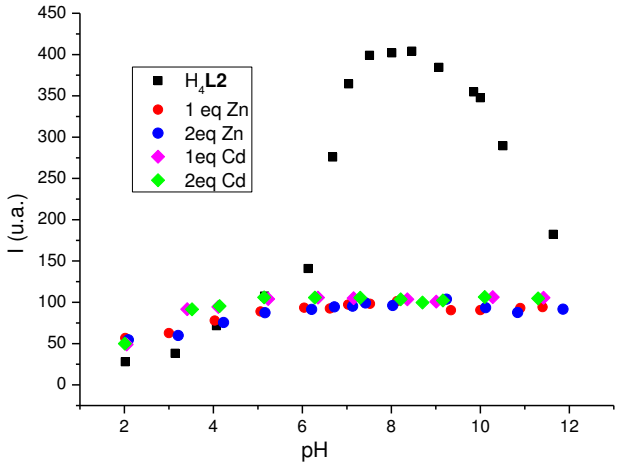

Figure 2.18 pH dependence of the emission intensity at 420 nm of H_4L2 in the absence of metal ion (■). in the presence of 1 eq (●) and 2 eq (●) of Zn^{2+} and in the presence of 1 eq (♦) and 2 eq (♦) of Cd^{2+} as a function of pH ($[H_4L2] = 5.56\times10^{-6}$ M, T=298 K).

Finally we recorded emission spectra of the ligand in the presence of increasing amounts of Cd^{2+} at pH 7.3 and the results are shown in Figures 2.19 and 2.20.

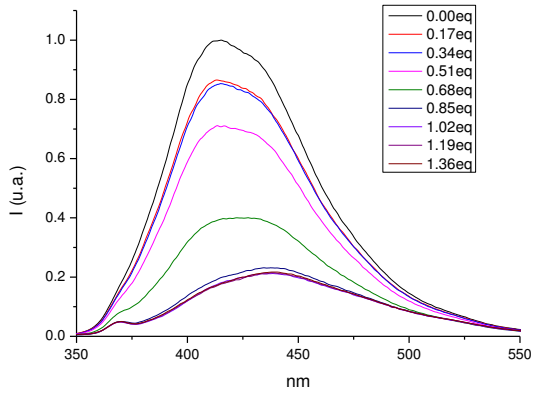

Figure 2.19 Fluorescence emission spectra of H_4L2 recorded in the presence of increasing amount of Cd^{2+} at pH=7.3 ($[H_4L2]$ = 5.56×10^{-6} M, T=298 K).

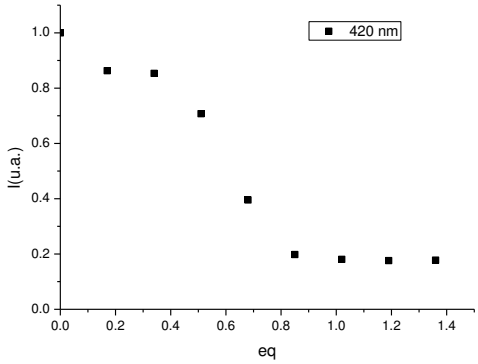

Figure 2.20 Emission intensity of H_4L2 measured at 420 nm in the presence of increasing amount of Cd^{2+} at pH=7.3 ($[H_4L2]$ = 5.56×10^{-6} M, T=298 K).

As in the case of Zn^{2+}, Cd^{2+} quenches the emission of the receptor at pH 7.3. Additions of increasing amounts of Cd^{2+} to the ligand lead to a progressive decrease in the fluorescence intensity, which achieves a constant value for $[Cd^{2+}]$ / [ligand] molar ratios greater than 1. This result suggests, once again, the formation of a stable complexes with 1:1 metal ion to ligand stoichiometry in solution.

Finally, we analyzed the variation of the emission of the ligand in the presence of different metal ions, including paramagnetic metal cations (Cu^{2+} and Mn^{2+}) and heavy metal cations (Pb^{2+} and Hg^{2+}). As shown in Figure 2.21, the emission intensity of the ligand H_4L2 in the presence of 1 equivalent of metal ions at pH 7 is quenched by all metal ions investigated.

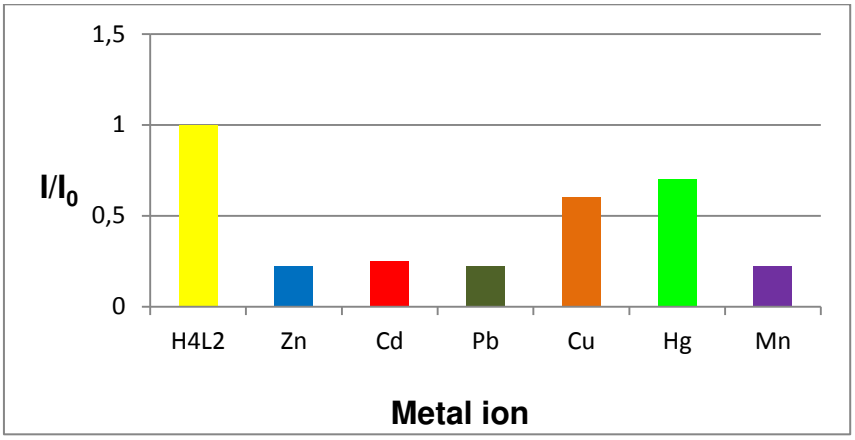

Figure 2.21 emission intensity at 438 nm in the presence of one equivalent of H_4L2 (■), Zn^{2+}(■), Cd^{2+}(■), Pb^{2+}(■), Cu^{2+} (■), Hg^{2+} (■) and Mn^{2+} (■) at pH=7 ([H_4L2] = 5.56×10^{-6} M, T=298 K).

3.4- Ligand L3

3.4.1- Acid-base properties of ligand L3

The structure of the ligand presents two cyclic polyamine-based receptor moieties and a dipyridyl photoactive unit, both possessing nitrogen atoms which give rise to protonation equilibria in competition with the coordination of the metal ions in the formation of the complexes in aqueous solution.

As the previous ligands, the protonation constants obtained for this receptor (4,4'-bis ((1,4,7,10-tetraazacyclododecane)methyl)-2,2'-dipyridyl, named L3) were determined by potentiometric measurements in aqueous solution and their values are reported in Table 3.1.

Equilibrium	log K
$L3 + 2H^+ = L3H_2^{2+}$	20.69
$L3H_2^{2+} + H^+ = L3H_3^{3+}$	8.92
$L3H_3^{3+} + H^+ = L3H_4^{4+}$	8.70
$L3H_4^{4+} + H^+ = L3H_5^{5+}$	6.90
$L3H_5^{5+} + H^+ = L3H_6^{6+}$	3.35
$L3H_6^{6+} + H^+ = L3H_7^{7+}$	2.06

Table 3.1 Protonation constants of L3 in aqueous solution, Errors on constants are lower than the 0.02 logarithmic units (T=298 K, NaCl=0.1 M).

The ligand L3 gives rise to six protonation equilibria in the investigated pH range (2 – 11). Considering the formation of the cation LH_2^{2+}, it was not possible to separately determine the constants relative to the addition of a single acidic proton to the species L3 and $L3H^+$. This is probably due to the fact that the equilibria $L3 + H^+ = L3H^+$ and $L3H^+ + H^+ = L3H_2^{2+}$ take place in a

very similar range of pH and therefore the measurement system is not capable to detect the two protonation equilibria separately.
Although the ligand has eight potential sites of protonation, it can only bind in aqueous solution seven acidic protons in the pH range investigated.
We can note from Table 3.1 a marked decrease of the constants increasing the degree of protonation of the ligand. This is a typical characteristic of the polyamine structures, which can be explained considering the electrostatic repulsion between protonated groups which become more intense as the overall charge of the receptor increases.
By using the protonation constant values, the distribution diagram of species at different pH values can be obtained and is reported in Figure 3.1.

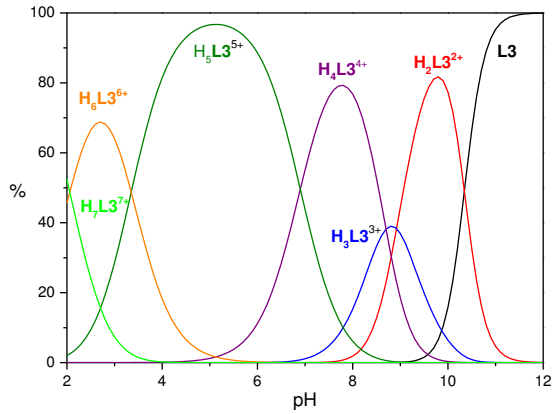

Figure 3.1 Distribution diagram of protonated species of L3 (NaCl= 0.1 M, T = 298K).

The ligand forms several species with different degrees of protonation as the pH changes in solution. The species $[H_7L3]^{+7}$ and $[H_6L3]^{+6}$ are present at pH < 3, while the polyprotonated species poly- $H_5L3]^{5+}$, $[H_4L3]^{4+}$, $[H_3L3]^{3+}$ and $[H_2L3]^{2+}$ prevails in solution between pH 4 and 9.5. However, the free ligand is present in solution only at strongly alkaline pH values.

UV-vis and fluorescence emission spectra were registered at different values of pH to achieve more information on the protonation sites.

3.4.2- UV-Visible spectroscopic study measurements of L3

UV-Vis spectra of the ligand L3 were recorded at various values of pH in aqueous solution and are shown in Figure 3.2.

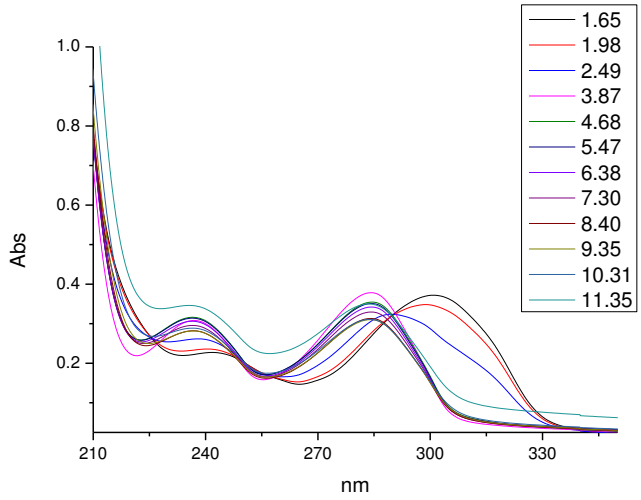

Figure 3.2. UV-Vis spectra of L3 at different values of pH ([L3]=8×10^{-5} M, T = 298 K).

We note that the ligand is characterized by two bands, at 237 and 284 nm, respectively. These bands are typical of not-protonated dipyridyl. At acidic values of pH (pH < 3) the absorbance of these bands decreases and a new band, shifted at ca 300 nm, appears in the spectra. This bathochromic effect is due to protonation of the dipyridyl unit, which leads to a marked conformational rearrangement of the molecule, the two nitrogen atoms passing from a "trans" to a "cis" reciprocal disposition. This effect is due to protonation of a nitrogen atom of dipyridyl unit protonated and to

the consequent formation of a strong hydrogen bond with the adjacent nitrogen atom.

Figure 3.3 shows the maximum absorbance at 300 nm, 284 nm and 237 nm at different values of pH, overlapped to the distribution diagram of the species. This figure shows that the absorption band at 284 nm undergoes the previously highlighted red-shift when the specie LH_7^{+7} is formed in solution. This suggests that the protonation of dipyridyl unit occurs with the formation of the species LH_7^{+7}.

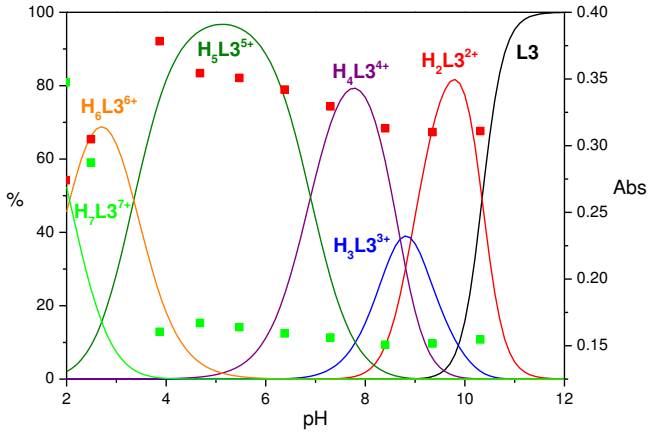

Figure 3.3 Absorbance at 300 nm (■) and 284 nm (■) of L3 at different values of pH, overlapped to the distribution diagram of the species ([L3]=8×10^{-5} M, NaCl= 0.1 M, T = 298K).

3.4.3- Fluorescence emission spectroscopic measurements of L3

To elucidate the characteristics of fluorescence emission of L3, were recorded emission spectra in aqueous solution at different values of pH, as shown in Figure 3.4.

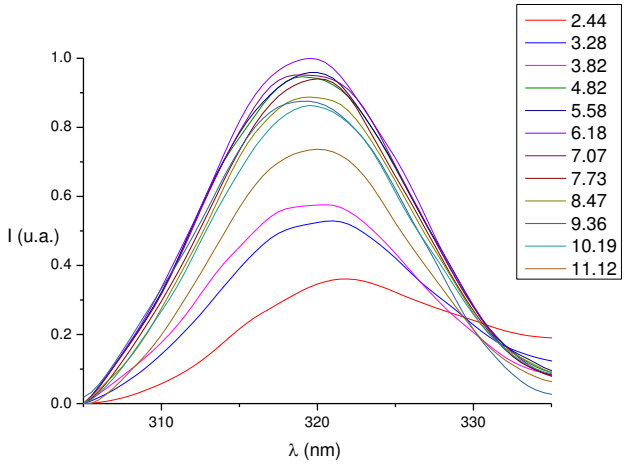

Figure 3.4 fluorescence emission spectra of L3 at different values of pH ([L3]=8×10^{-5} M, T = 298 K).

At acidic pH, the emission spectra undergo a clear quenching in the fluorescence intensity. This effect probably due to the protonation of a nitrogen atom of dipyridyl in the $L3H_7^{7+}$ species. As mentioned above, in this species hydrogen bonding between the two dipyridyl units allows for the stabilization of the cis conformer of dipyridyl, causing a change in the optical properties of the system.

In order to further clarify the emission properties of the ligand, we have superimposed the values of emission intensity at 320 nm at different values of pH with the distribution diagram of the species (Figure 3.5).

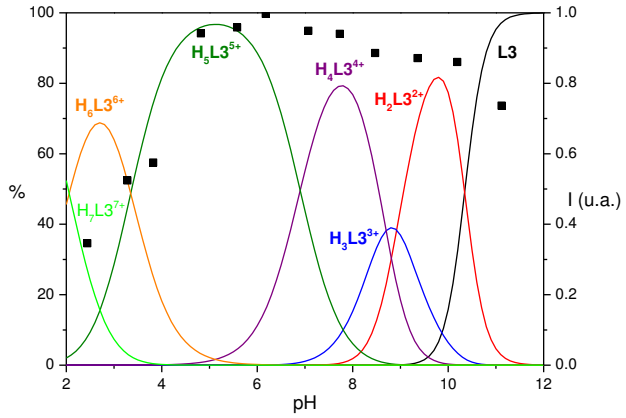

Figure 3.5. Emission intensity at 320 nm (■) of L3 as a function of pH, overlapped with the distribution diagram of the protonated species ([L3] = 8×10^{-5} M, NaCl = 0.1 M, T = 298K, λex = 290 nm).

In a wide range of pH, from pH 5 to a strongly alkaline pH values, we do not observe significant variation of the fluorescence intensity. We can also note that the emission intensity in all the spectra is very weak, i.e. the ligand is not particularly luminescent in the absence of coordinated metal cations. This is attributable to the PET effect that is caused by the nitrogen atoms of receptor, which inhibits the emission of photons by dipyridyl in its excited state.

3.4.4- Coordination of metal ions with L3

To analyze the coordination characteristics of tligand L3 toward metal cations, we first performed potentiometric and spectrophotometric measurements in aqueous solution in the presence of Zn^{2+}, Cd^{2+}, Cu^{2+} and Hg^{2+}.

The potentiometric measurements allowed to determine the complexes formed and their stability constants. As a next step, the

absorption spectra were recorded at different values of pH to determine whether the optical properties of the system change with the formation of different species in solution. Subsequently, we analyzed the coordination effect on the luminescence properties of the ligand by performing fluorescence emission measurements either at fixed pH or at different pH values to clarify the chemosensing ability of this ligand for the investigated metal cations.

3.4.5- Determination of the stability constants of complexes with L3

We first determined the stability constants of metal complexes by potentiometric measurements, which are reported in Table 3.2.

The ligand L3 consists of two receptor units. Thus it can form both mono- and dinuclear complexes, as clearly shown in Table 3.2.

Equilibrium	Zn^{2+}	Cd^{2+}	Cu^{2+}	Hg^{2+}
$L3 + M^{2+} = L3M^{2+}$	15.96	15.55	18.53	28.76
$L3M^{2+} + H^{+} = L3MH^{3+}$	8.98	-	9.16	-
$L3MH^{3+} + H^{+} = L3MH_2^{4+}$	8.44	-	8.97	-
$L3M^{2+} + 2H^{+} = L3MH_2^{4+}$	-	17.33	-	18.01
$L3MH_2^{4+} + H^{+} = L3MH_3^{5+}$	6.57	6.56	6.55	-
$L3M^{2+} + OH^{-} = L3MOH^{+}$	-	4.45	-	-
$L3M^{2+} + M = L3M_2^{4+}$	9.88	10.42	14.54	24.7
$L3M_2^{4+} + OH^{-} = L3M_2OH^{3+}$	4.68	6.62	5.35	-
$L3MOH^{3+} + OH^{-} = L3M_2(OH)_2^{2+}$	5.24	-	-	-

Table 3.2 Formation constants of the metal complexes formed by L3 with Zn^{2+}, Cd^{2+}, Cu^{2+} and Hg^{2+} (T=298 K, 0.1 M NaCl).

The Zn^{2+} and Cd^{2+} complexes feature similar stability, while Cu^{2+} and Hg^{2+} complexes are more strongly bound by the receptor. The greater stability of the Cu^{2+} complex is attributed to the crystal field stabilization energy (CFSE), which is absent in the other metal cations. The formation constant observed for the Hg^{2+} complexes is instead a typical characteristic of the coordination compounds of Hg^{2+} with polyamines, which are generally characterized by a high stability as a consequence of the high affinity of amine donors for this metal cation.

Table 3.2 also shows the formation of mononuclear complexes with various protonation degrees. In these complexes the metal ion is coordinated by a single cyclen unit. The second macrocyclic unit can therefore easily be protonated in solution. Clearly, the dinuclear complexes do not form protonated species, because both cyclen units are engaged in the coordination of a metal cation.

Hydroxylated species are also formed at alkaline pH values. Ther formation implies deprotonation at alkaline pH of coordinated water molecules and is often observed in metal complexes featuring a metal cation whose coordination environment is not saturated by the ligand donors, as often observed in cyclen based complexes.

By using the data in Table 3.2 we can obtain the distribution diagrams of the complexes. Clearly, the species present in solution strongly differs in the presence of 1 or 2 equivalents of metal cation. As exemplifying example, we are reported below the distribution diagrams calculated in the case of Zn^{2+} complexation.

Figure 3.6 shows the complexe formed by L3 in the presence of 1 equivalent of the metal. At pH < 4, no complex is formed in solution and only protonated species of the ligand are present in solution. As the pH increases, we can observe Zn^{2+} complexation. The solution chemistry is characterized by the formation of a series of protonated mononuclear species from pH 4 to 9. Only at strongly alkaline pH values a dinuclear hydroxilated species is observed in solution.

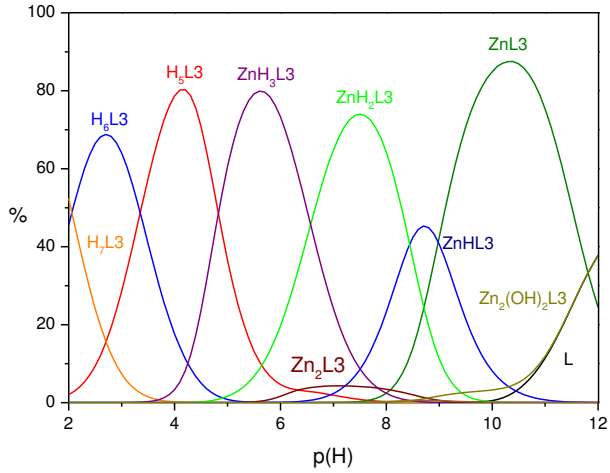

Figure 3.6 Distribution diagram of the complexed formed by L3 in the presence of 1 equivalent of Zn^{2+} ([L3]=8×10^{-5} M, NaCl 0.1 M, 298 K).

In the presence of two equivalents of Zn^{2+}. The ligand mainly forms dinuclear complexes, which are the prevalent species from pH 6 to strongly alkaline pH values, where the prevalent species are hydroxylated dinuclear complexes, as shown in Figure 3.7.

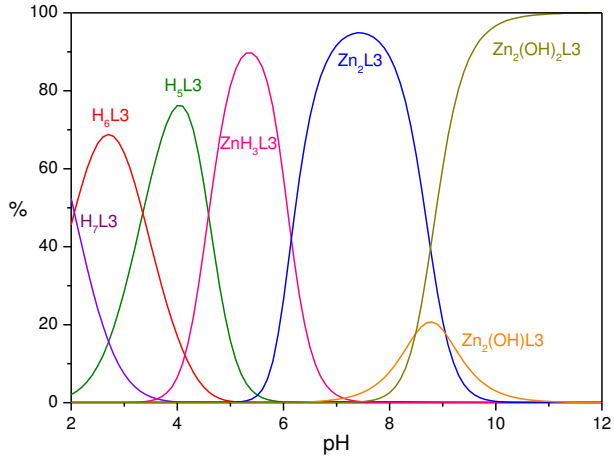

Figure 3.7 Distribution diagram of the complexed formed by L3 in the presence of 2 equivalents of Zn^{2+} ([L3]=8×10^{-5} M, NaCl 0.1 M, 298 K).

We studied the complexes of Zn^{2+} and Cd^{2+} through their absorption and emission spectra in detail as described below.

3.4.6- UV-visible spectroscopic measurements

To determine the coordination characteristics of the ligand L3 and to get information on complexes in aqueous solution, we performed Uv-vis spectra at different pH values in the presence of metal cations, in particular Zn^{2+} and Cd^{2+} which often enhance the emission of fluorogenic units. The absorption bands of the chromophore units are may be in fact sensible to the protonation and deprotonation equilibria that involve them.

Considering that the ligand can form both mono-and dinuclear complexes, we recorded spectra at different pH values of solutions containing the free ligand and one or two equivalents of each metal ion.

3.4.6.1- UV-vis spectra of the complexes with Zn^{2+}

UV-Vis spectra were recorded in the presence of 1 and 2 equivalents of Zn^{2+}, as shown in Figure 3.14 and Figure 3.15.

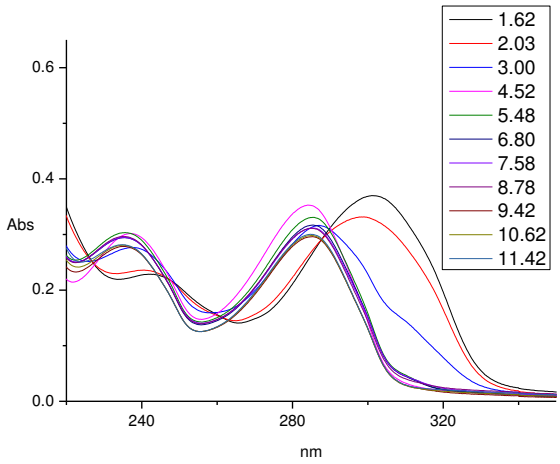

Figure 3.14 UV-Vis spectra of L3 in the presence of 1 equiv. of Zn^{2+} at different values of pH ([L3]=8×10^{-5} M, 298 K).

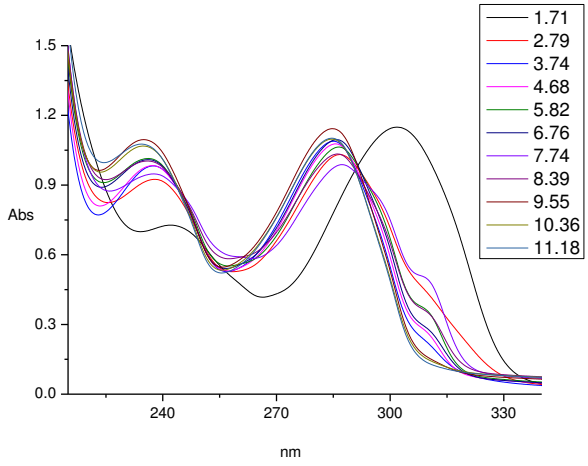

Figure 3.15 UV-Vis spectra of L3 in the presence of 2 equivalents. of Zn^{2+} at different values of pH ([L3]=8×10^{-5} M, 298 K).

We note that the absorption spectra of mono-nuclear and di-nuclear complexes for Zn^{2+} are similar with the spectra of the free ligand. From alkaline to weakly acidic values of pH, where the complexes are formed in aqueous solution, the absorption spectra are typical of the free ligand and with the nitrogen atoms of dipyridyl in trans position. This suggests that the metal ions are coordinated only by single cyclen unit in both mono- and dinuclear complexes, without any involvement of dipyridyl in metal binding.

At pH < 4 the two bands of dipyridyl are shifted to longer wavelengths to give an overall bathochromic effect. Superinposition of the distribution diagram of the species in solution with the absorption band at 300 and at 284 nm, shows that this effect is due to the formation of the highly protonated species of the free ligand, where the dypiridyl unit is protonated, as already observed above. This result is obtained in the presence of both 1 or two equivalents of the metal (see Figures 316 and 3.17).

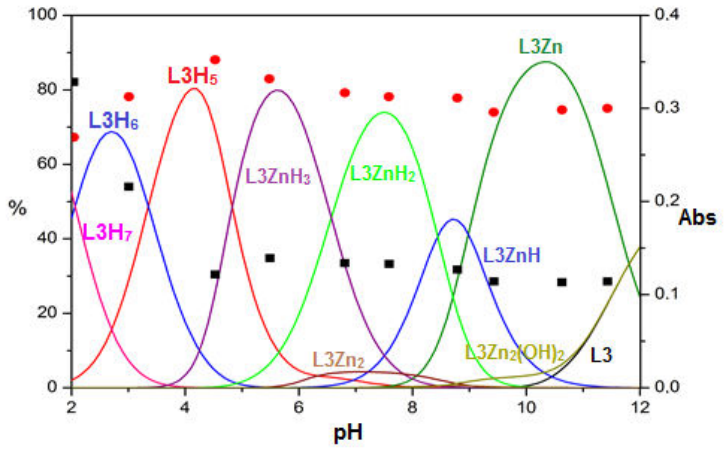

Figure 3.16 Absorbance at 300 nm (■) and at 284 nm (●) of L3 at different values of pH, overlapped to the distribution diagram of the species ($[L3]=[Zn^{2+}]=8\times10^{-5}$ M, NaCl= 0.1 M, T = 298K).

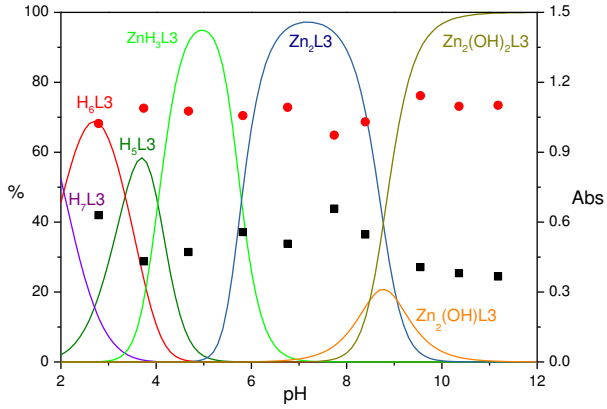

Figure 3.17 Absorbance at 300 nm (■) and at 284 nm (●) of L3 at different values of pH, overlapped to the distribution diagram of the species ([L3]=8×10^{-5} M, [Zn^{2+}]=1.6 x 10^{-4} M, NaCl= 0.1 M, T = 298K).

Uv-vis spectra were also recorded on the ligand in the presence of increasing amounts of Zn^{2+} to a solution of the ligand at pH 7.5, as shown in Figure 3.18.

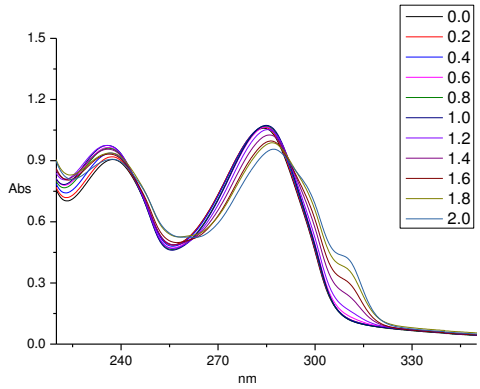

Figure 3.18 UV-Vis spectra of L3 in the presence of increasing amount of Zn^{2+} at pH=7.5 ([L3]=8×10^{-5} M , T = 298K).

We note that the changes in the absorption spectrum of the ligand with increasing amount of Zn^{2+} are small but not negligible. Metal addition induces the formation of a shoulder at 310 nm. This may indicate either a weak interaction of the metal center coordinated by a cyclen unit with a nitrogen atom of a bipyridyl unit or, more likely, a slight conformational change of the bipyridyl unit upon coordination of the metal by the macrocycle.

The same behavior was also observed in the presence of other metal cations, such Cd^{2+}.

3.4.7- Fluorescence emission spectroscopic measurements

Finally, the tested the chemosensing ability of the ligand as fluorescent chemosensor for the metal ions, focalizing our attention on Zn^{2+} and Cd^{2+}.

To this purpose we recorded the fluorescence emission spectra in aqueous solution at different values of pH in the presence of one or two equivalents of Zn^{2+} and Cd^{2+}. This study could make possible to define the emission characteristics of the various species formed in solution by the ligand with each metal ion. In addition, we also carried out measurements at fixed pH with increasing amounts of a metal ion.

3.4.7.1- Emission spectra of the complexes of Zn^{2+}

As in the case of the UV-vis spectra, we recorded the fluorescence emission spectra of the ligand in the presence of one and two equivalents of Zn^{2+} and the results are shown shown in Figure 3.19 and Figure 3.20.

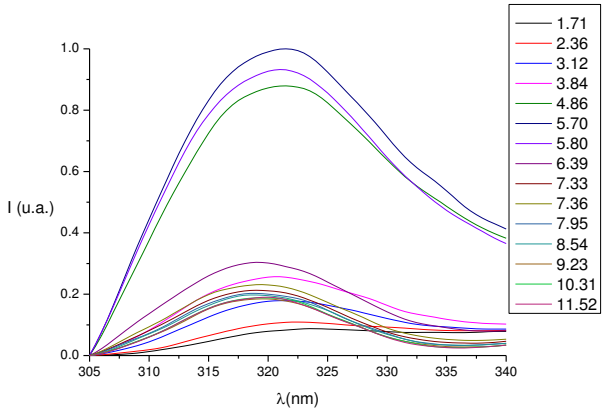

Figure 3.19 fluorescence emission spectra of L3 in the presence of 1 equiv. of Zn^{2+} at different values of pH ([L3]=8×10^{-5} M, T=298K, λ_{ex}=290 nm).

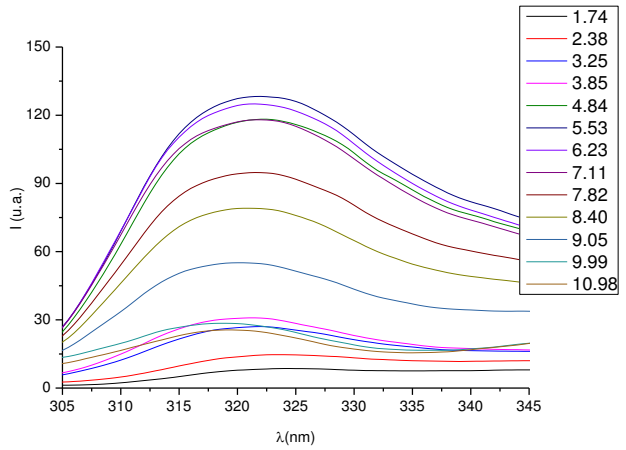

Figure 3.20 fluorescence emission spectra of L3 in the presence of 2 equivs of Zn^{2+} at different values of pH, ([L3]=8×10^{-5} M, T=298K, λ_{ex}=290 nm).

All spectra show the typical emission band of bipyridyl in trans conformation, characterized by a maximum about 320 nm. We superimposed the values of the emission at 320 nm (as in case of absorption), with distribution diagrams of the species obtained in the presence of 1 and 2 equivs of Zn^{2+}, in order to clarify the emission properties of the complexes formed in solution. Figure 3.21 reports the distribution diagram of the species formed in the presence of 1 equivalent of Zn^{2+}, compared with the emission intensity at 320 nm at different pH values.

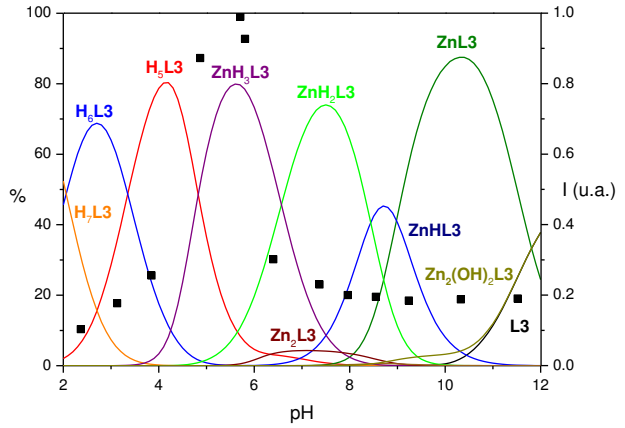

Figure 3.21 Emission intensity at 320 nm (■) of L3 as a function of pH, in the presence of 1 equivalent of Zn^{2+}, overlapped to the distribution diagram of the complexed species ([L3] = 8×10^{-5} M, NaCl = 0.1 M, T = 298K, λ_{ex} = 290 nm).

Figure 3.21 shows that the maximum values of the emission is obtained at slightly acidic pH, between pH 4 and 6, e.g., in the presence the species $L3ZnH_3^{5+}$. At strongly acidic values of pH, the species present in solution are only protonated species of the ligand with a high degree of protonation and the complex is not formed in this conditions, justifying the low fluorescence intensity. At alkaline values of pH, we can note that the emission is weak

compared to the values obtained for the species $L3ZnH_3^{5+}$, even though in this pH range mononuclear Zn^{2+} complexes are present in solution. These data are in accord with the previous hypotheses. In the mono-nuclear complexes, the metal ion is coordinated by a single cyclen unit and the other macrocyclic unit could undergo a successive series of protonation by varying pH. At neutral or alkaline values of pH, where the species $L3Zn^{2+}$, $L3ZnH^{3+}$ and $L3ZnH_2^{4+}$ are present in solution, the non-coordinated cyclen unit can turn off the fluorescence emission through the PET effect. The further increase of acidic protons localized on this macrocyclic unit probably inhibits the PET effect leading to an increase of the emission intensity.

Figure 3.22 reports the distribution diagram of the species formed in the presence of 2 equivalents of Zn^{2+}, compared with the emission intensity at 320 nm at different pH values.

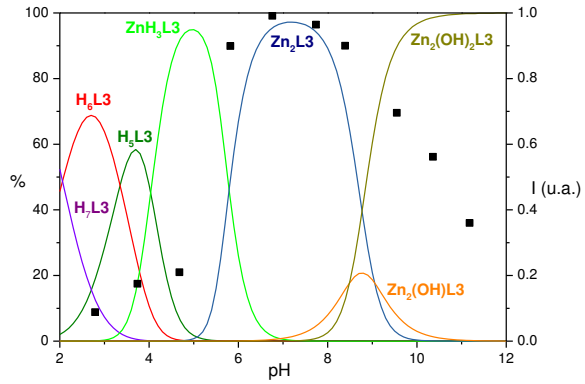

Figure 3.22 Emission intensity at 320 nm (■) of L3 in function of pH, in the presence of 2 eq of Zn^{2+}, overlapped to the distribution diagram of the protonated species ([L3] = 8×10^{-5} M, NaCl = 0.1 M, T = 298K, λ_{exc} = 290 nm).

Figure 3.23 shows a comparison between the emission of the ligand alone and in the presence of 1 and 2 equivalents of Zn^{2+},

which well outlines the CHEF effect observed in particular in the presence of two Zn^{2+} cations.

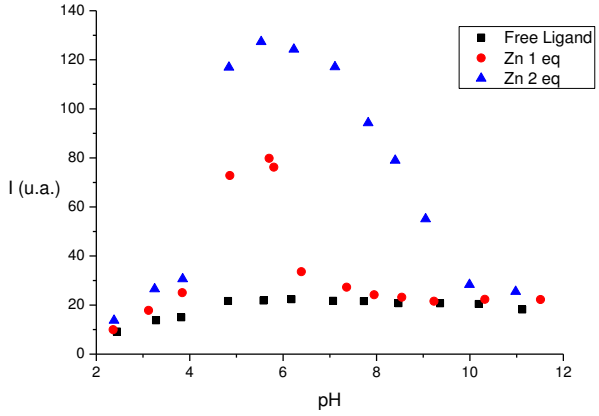

Figure 3.23 Emission intensity at 320 nm in function of pH, of the ligand-Free and in the presence of 1eq and 2 eq of Zn^{2+}([L3] = 8×10^{-5} M, T = 298K, λ_{ex} = 290 nm).

Finally, we also recorded emission spectra of the ligand in the presence of increasing amount of Zn^{2+} at pH=5.9. At this pH values, in fact, the receptor shows the most evident enhancement of the emission in the presence of Zn^{2+}. Figure 3.24 and 3.25 shows that emission of the ligand progressively increases upon the addition of increasing amount of Zn^{2+} and does not undergo significant changes after the addition of ca 3 equivalents of the metal.

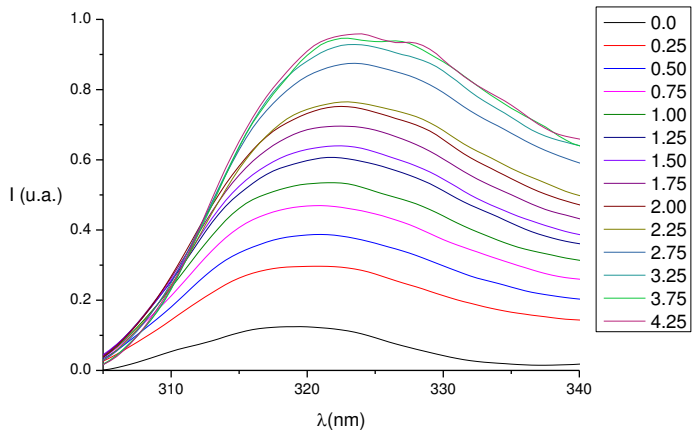

Figure 3.24 Fluorescence emission spectra of the ligand at pH=5.9 in the presence of increasing amount of Zn^{2+} ([L3] = 8×10^{-5} M, T = 298K, λ_{ex} = 290 nm).

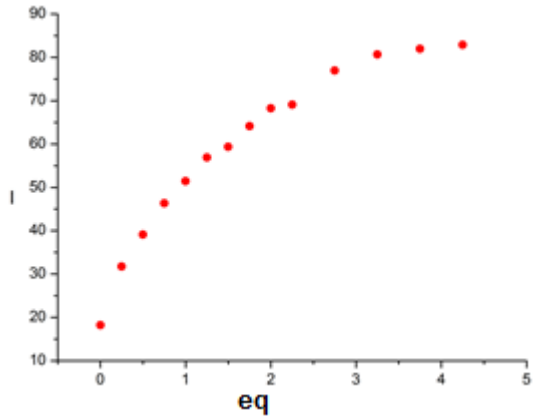

Figure 3.25 Emission intensity at 320 nm in the presence of increasing amount of Zn^{2+} at pH=5.9 ([L3] = 8×10^{-5} M, T = 298K, λ_{ex} = 290 nm).

Once again, the emission spectra show a band at 320 nm, whose intensity depends on pH and on the equivalent of Cd^{2+} present in solution. However, the emission of bipyridyl is almost not influenced by the presence of 1 equivalent of Cd^{2+}. In the presence of 2 equivalents of Cd^{2+} we can observe a slight increase of the

emission between pH 5 and 7 and a large enhancement at alkaline pH values. These results are summarized in Figure 3.29, which compare the emission of the ligand alone and in the presence of 1 and 2 equivalents of metal.

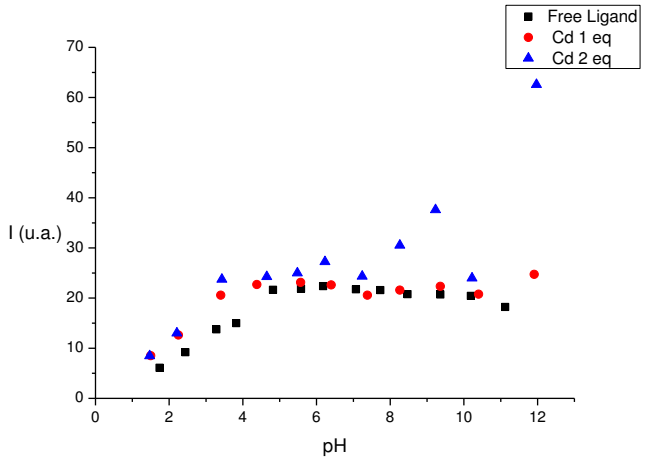

Figure 3.29 Emission intensity at 320 nm in function of pH, of the ligand-Free and in the presence of 1eq and 2 eq of Cd^{2+}([L3] = 8×10^{-5} M, T = 298K, λ_{ex} = 290 nm).

In order to verify the selectivity of the response of the chemosensor in metal coordination of metal ions, we analyzed the variation of the emission of the free ligand and the solution of the ligand in the presence of 2 equivalents of several metal ions: Zn^{2+}, Cd^{2+}, Co^{2+}, Cu^{2+}, Hg^{2+}, Mn^{2+}, Ni^{2+} and Pb^{2+} (Figure 3.30).

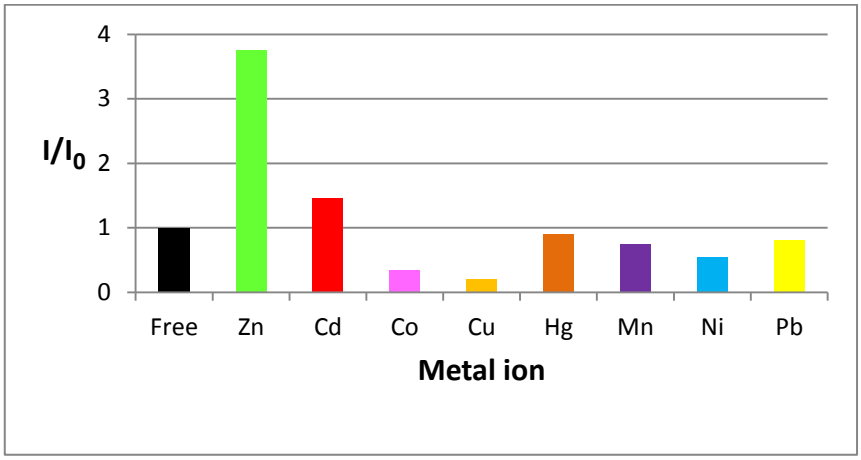

Figure 3.30 Value of I / I_0 of the ligand L3 in the presence of different metal ions. I is the intensity of emission at 320 nm in the presence of two equivalents of metal ion and I_0 is the intensity of emission of L3 in the absence of metals ([L3]=8×10^{-5} M, pH=7.5, buffer TRIS, λ_{ex}=290 nm).

The emission intensity fourfold increases in the presence of Zn^{2+} and, at a much lower extent, in the presence of Cd^{2+}. The intensity in the presence of metal ions such as Co^{2+}, Cu^{2+}, Mn^{2+} and Ni^{2+} decreases compared with the free ligand. This quenching effect is attributed to the paramagnetism effect of these metal ions. The quenching of the fluorescence in the case of metal Hg^{2+} and Pb^{2+} was substantially expected considering the heavy atom effect.

3.5- Ligand L4

3.5.1- Determination of the protonation constants of L4

The structure of the ligand presents two cyclic polyamine-based receptor moieties and two bipyridyl photoactive units, both possessing nitrogen atoms which can give rise to protonation equilibria in competition with the coordination of metal ions in aqueous solution.

L4 can bind up to a maximum of eight protons in aqueous solution. However, the potentiometric measurements allows the determination of six protonation constants in aqueous solution. In fact, in the case of the formation of the H_2L4^{2+} cation the constants relative to the addition of a single acidic proton to the species L4 and $[HL4]^+$ cannot be separately determined and only the constant relative to the equilibrium $L4 + 2H^+ = [H_2L4]^{2+}$ was determined. This is probably due to the fact that the equilibria $L4 + H^+ = HL4^+$ and $HL4^+ + H^+ = H_2L4^{2+}$ take place in a very similar range of pH and therefore the measurement system is not capable to separately detect the two protonation equilibria. Similar consideration apply to the $[H_2L4]^{2+} + 2H^+ = [H_4L4]^{4+}$ equilibrium.

As in the previous ligands, the protonation constants obtained for this receptor (4,4'-bis ((1,4,7,10-tetraazacyclododecane)methyl)-2,2'-bi-dipyridyl, named L4) were determined by potentiometric measurements in aqueous solution and their values are reported in Table 4.1.

Equilibrium	log K
$L4 + 2H^+ = [H_2L4]^{2+}$	19.60(8)
$[H_2L4]^{2+} + 2H^+ = [H_4L4]^{4+}$	19.06(4)
$[H_4L4]^{4+} + H^+ = [H_5L4]^{5+}$	7.28(5)
$[H_5L4]^{5+} + H^+ = [H_6L4]^{6+}$	4.78(6)
$[H_6L4]^{6+} + H^+ = [H_7L4]^{7+}$	3.44(6)
$[H_7L4]^{7+} + H^+ = [H_8L4]^{8+}$	2.95(6)

Table 4.1 Protonation constants of L4 (298 K, NaCl=0.1 M).

By using the protonation constant values, the distribution diagram of species at different pH values can be obtained and is reported in Figure 4.1.

We can note that the first two protonation constants are remarkably high. This suggests that the first and second equilibria of protonation take place on the nitrogen atoms of cyclen. As previously mentioned in the other ligands cyclen is particularly basic, its first two protonation constant being $\log K_{1Cyclen}$ = 11.27 and $\log K_{2Cyclen}$ = 9.96. However, the values of successive protonation constants are lower, as expected considering that they refer either to the protonation of the remaining amine groups of cyclen or the nitrogen atoms of bipyridyl ($\text{Log}K_{bipy}$= 5.3).

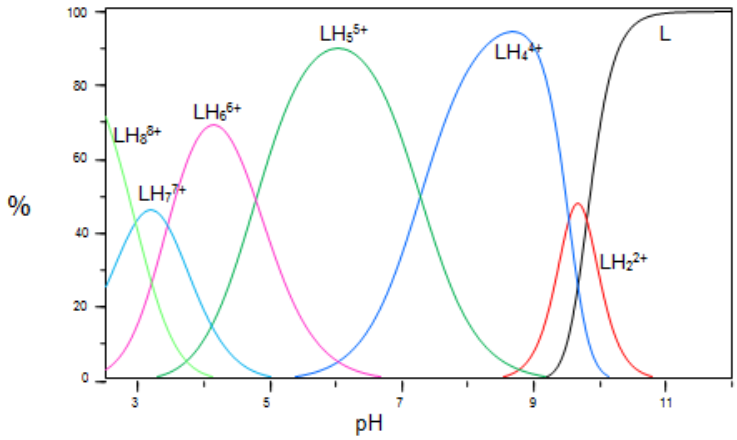

Figure 4.1 Distribution diagram of protonated species of L5 (T = 298K, NaCl = 0.1 M).

The ligand forms several species with different degrees of protonation as the pH changes in solution. The species $[H_8L4]^{8+}$ and $[H_7L4]^{7+}$ are present at pH < 3, while the polyprotonated species $[H_6L4]^{6+}$, $[H_5L4]^{5+}$, $[H_4L4]^{4+}$ and $[H_2L4]^{2+}$ prevail in solution between pH 4 and 9.5. Finally, the free ligand is present in solution only at strongly alkaline pH values.

UV-vis and fluorescence emission spectra were recorded at different values of pH to achieve more information on the protonation sites in the different protonation states of the ligand.

3.5.2- UV-Visible spectroscopic study of L4

The UV-Vis spectra of ligand L4 recorded at different values of pH in aqueous solution are shown in Figure 4.2.

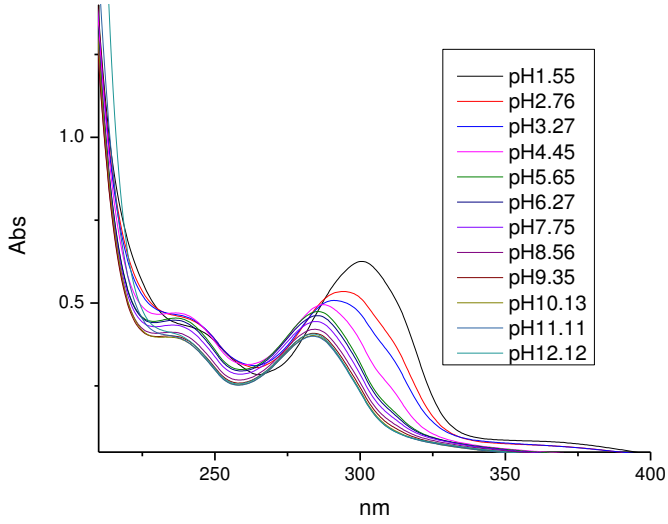

Figure 4.2 UV-Vis spectra of L4 at different values of pH ([L4]=1.56×10^{-5} M ,T = 298 K).

We can note that the ligand at alkaline and neutral pH values is characterized by two bands, at 237 and 284 nm, respectively. These bands are typical of not-protonated bipyridyl, as previously described in the case of ligand L3 (see paragraph 3.4.2).

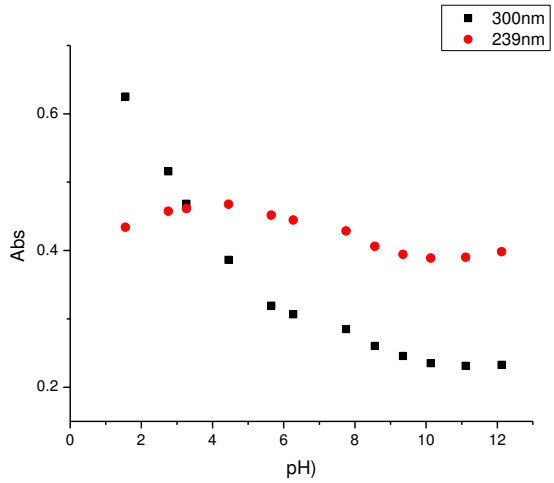

Figure 4.3 Absorption intensity at 239 nm (●) and 300 nm (■) of L4 at different pH values ([L4]=1.56×10^{-5} M ,T=298 nm).

However, the band at 284 nm undergoes a progressive red-shift at acidic pH values, originating a new absorption band at 300 nm, as also shown in Figure 4.3. The formation of this new band is likely to be due to protonation of the bipyridyl unit at acidic pH values.

3.5.3- Fluorescence emission spectroscopic measurements of L4

To elucidate the characteristics of fluorescence emission of L4, were recorded emission spectra in aqueous solution at different values of pH, as shown in Figure 4.4.

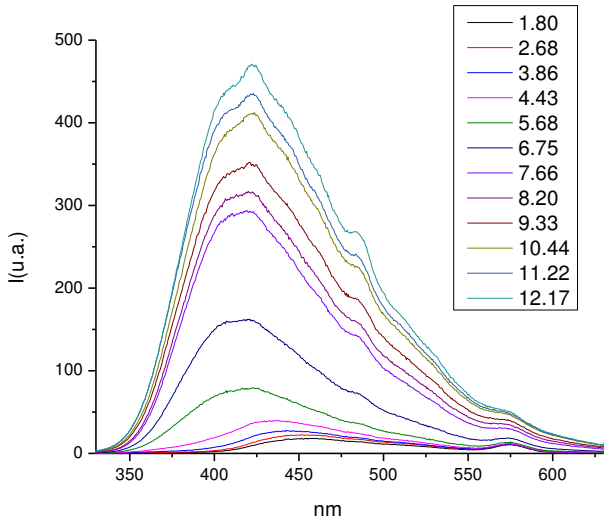

Figure 4.4 Fluorescence emission spectra of L4 at different values of pH ([L4]=4.14×10^{-5} M , T = 298K).

Surprisingly, the ligand feature a band at 420 nm, whose intensity increases from acidic to alkaline pH values. A slight blue shift is also observed by increasing pH. This emission band cannot attributed to the excited bipyridil unit, which normally shows a weak emission at 320 nm. Most likely, this band emission at 420 can be attributed to the formation of an excimer, e. g. a complex in the excited state, between the two bipyridyl units kept at a short distance by the ligand architecture. The observed emission intensity decrease at acidic pH values could be related to the fact that ligand protonation can enelarge the overall cyclic structure of

the ligand, thus increasing the distance between the bypiridyl units and disrupting the exciplex.

3.5.4- Determination of stability constants of complexes with L4

As a preliminary study, we determined the stability constants of Cu^{2+} complexes by potentiometric measurements, which are reported in Table 4.2.

The ligand L4 consists of two receptor units. Thus it can form both mono- and dinuclear complexes, as clearly shown in Table 4.2.

Equilbrium	Log K
$L4 + Cu^{2+} = [CuL4]^{2+}$	15.02(9)
$[CuL4]^{2+} + 2H^{+} = [H_2CuL4]^{4+}$	20.48(8)
$[Cu\ H_2L4]^{4+} + H^{+} = [CuH_3L4]^{5+}$	7.46(7)
$[H_3CuL4]^{5+} + H^{+} = [H_4CuL4]^{6+}$	5.14 (9)
$[CuH_4L4]^{6+} + H^{+} = [CuH_5L4]^{7+}$	4.23(8)
$[CuL4]^{2+} + Cu^{2+} = [Cu_2L4]^{4+}$	6.75 (8)
$[Cu_2L4]^{4+} + 2H^{+} = [Cu_2H_2L4]^{6+}$	9.28 (7)
$[Cu_2L4]^{4+} + 2OH^{-} = [Cu_2(OH)_2L4]^{2+}$	6.10 (1)

Table 4.2 Formation constants of Cu^{2+} complexes formed by L4 (T=298 K, 0.1 M NaCl).

Figure 4.5 shows the complexes formed by L4 in the presence of 1 equivalent of the metal. At pH < 4, no complex is formed in solution and only protonated species of the ligand are present in solution. As the pH increases, we can observe Cu^{2+} complexation. The

solution chemistry is characterized by the formation of a series of protonated mononuclear species from pH 4 to 11.

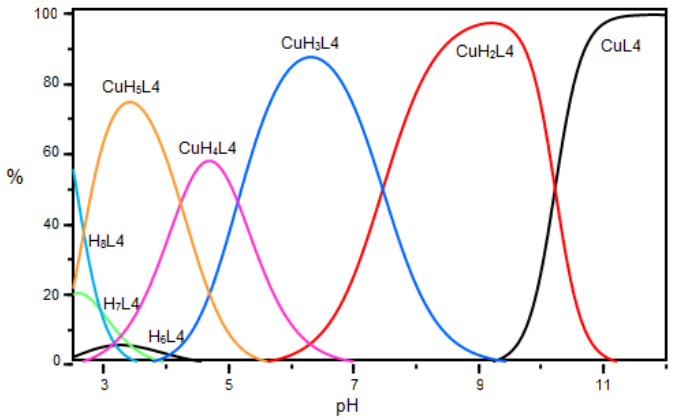

Figure 4.5 Distribution diagram of the complexed formed by L4 in the presence of 1 equivalent of Cu^{2+} ([L4]=4.14×10^{-5} M, NaCl 0.1 M, T=298 K).

In the presence of two equivalents of Cu^{2+}. The ligand mainly forms dinuclear complexes, which are the prevalent species from pH 7 to strongly alkaline pH values, as shown in Figure 4.6.

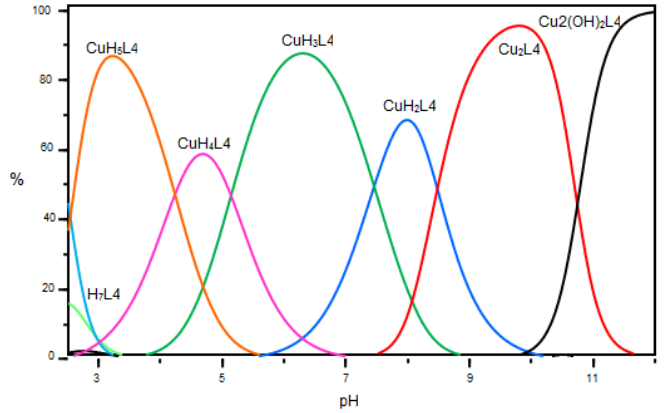

Figure 4.6 Distribution diagram of the complexed formed by L4 in the presence of 2 equivalents of Cu^{2+} (([L4]=4.14×10^{-5} M, NaCl 0.1 M, T=298 K).

3.5.5- Fluorescence emission spectroscopic study of the metal complexes with L4

To determine the possible ability of the ligand in metal cation signalling in aqueous solution, we preliminary recorded fluorescence emission spectra on solutions at different values of pH in the presence of the Zn^{2+}, Cd^{2+} and Cu^{2+} metal ions. In fact, Zn^{2+} and Cd^{2+} often increases the emission of polyamine ligands, while Cu^{2+} represents an example of metal cations that normally quenches the emission because of its paramagnetic nature.

To elucidate the effect of metal coordination on the emission properties of the complexes we carried out by recording fluorescence emission spectra of an aqueous solution of the ligand L4 in the presence of Zn^{2+} and Cu^{2+} at a fixed pH. In particular, we recorded the emission spectra of the ligand in the presence of increasing amounts of Zn^{2+} at pH 6, using TRIS as buffer (Figure 4.7). We note that Zn^{2+} leads to the formation of the typical emission band of monomer bipyridyl at 328 nm, whose intensity increases with Zn^{2+} concentration This band results much more intense with respect to the exciplex band. Its formation is likely due to the inhibition of the PET effect from the amine groups of cyclen to dypiridyl. Addition of Zn^{2+} does not significantly change the exciplex band, which is still present even in the presence of two equivalents of Zn^{2+}. This fact cannot be explained on the basis of the present results a requires a more accurate investigation in the future.

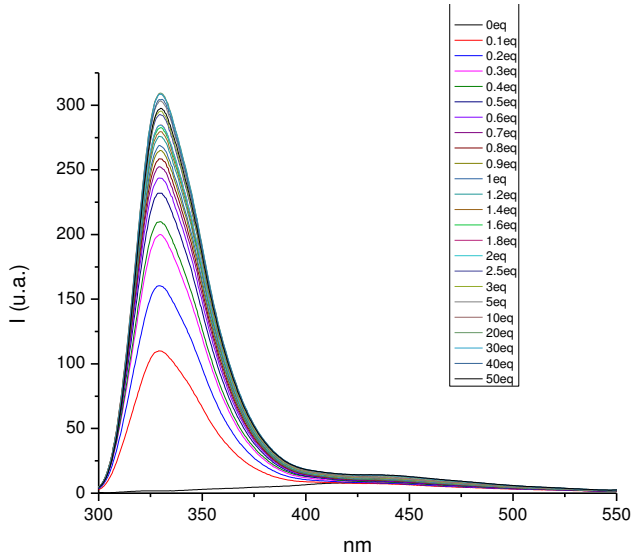

Figure 4.7 fluorescence emission spectra of L4 in the presence of increasing amount of Zn^{2+} at pH=6 ([L4]=4.14×10^{-5} M , T=298 K).

Figure 4.8 reports the emission intensity of the ligand at 328 nm as a function of the added equivalents of Zn^{2+}. The coordination of the metal ion leads to a linear increase in the intensity of emission up to the addition of ca 1.2 equivalents of Zn^{2+}. The addition of amounts of metal cation greater than 2.5 equivalents does not lead to further increase of the emission intensity, indicating the formation of stable complexes with 1:2 stoichiometry in solution.

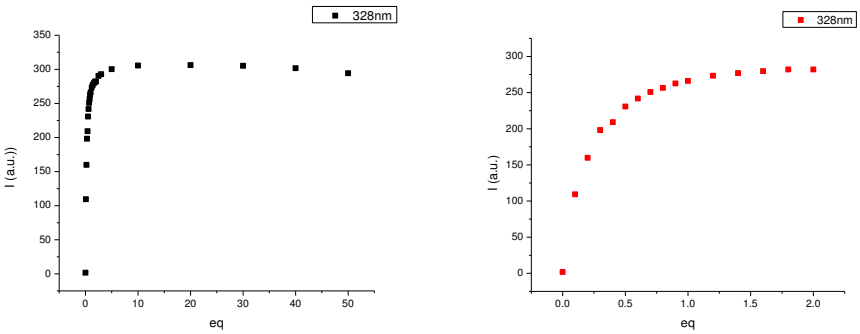

Figure 4.8 Emission intensity of L4 at 328 nm in the presence of increasing amount of Zn^{2+} at pH=6 ([L4]=4.14×10^{-5} M , T=298 K).

We also recorded spectra of L4 in the presence of increasing amounts Cd^{2+} at fixed pH = 6 using TRIS buffer (Figure 4.9). Similarly to Zn^{2+}, the spectra feature the typical band of bypiridyl at 328 nm, whose intensity increase with Cd^{2+} concentration. The enhancement of the emission is likely to be due to inhibition of the PET effect, as already observed in the case of Zn^{2+}.

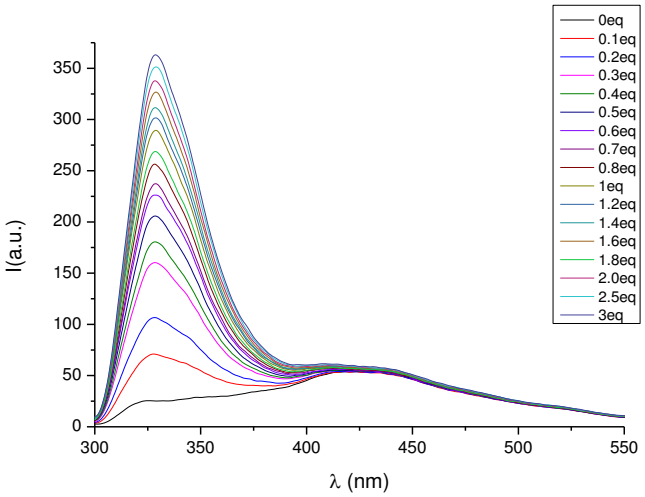

Figure 4.9 fluorescence emission spectra of L4 in the presence of increasing amount of Cd^{2+} at pH=6 ([L4]=4.14×10^{-5} M , T=298 K).

Figure 4.10 reports the emission intensity of the ligand at 328 nm as a function of the added equivalents of Cd^{2+}. The coordination of the metal ion leads to a linear increase in the intensity of emission up to the addition of ca 1 equivalent of Cd^{2+}. The addition amounts of metal cation greater than 1 equivalent does not lead to further increase of the emission intensity.

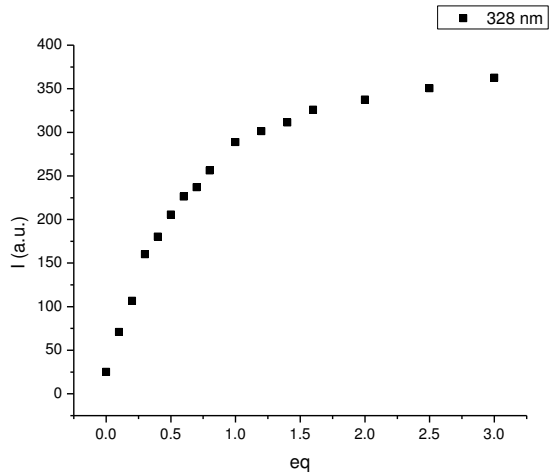

Figure 4.10 Emission intensity of L4 at 328 nm in the presence of increasing amount of Cd^{2+} at pH=6 ([L4]=4.14×10^{-5} M , T=298 K).

Finally we recorded spectra of L4 in the presence of increasing amounts Cu^{2+} at fixed pH = 6 using TRIS buffer (Figure 4.11). Differently from Zn^{2+} and Cd^{2+}, metal addition also quenches the exciplex addition. Once again, this different behavior cannot be explained and needs further studies In the future.

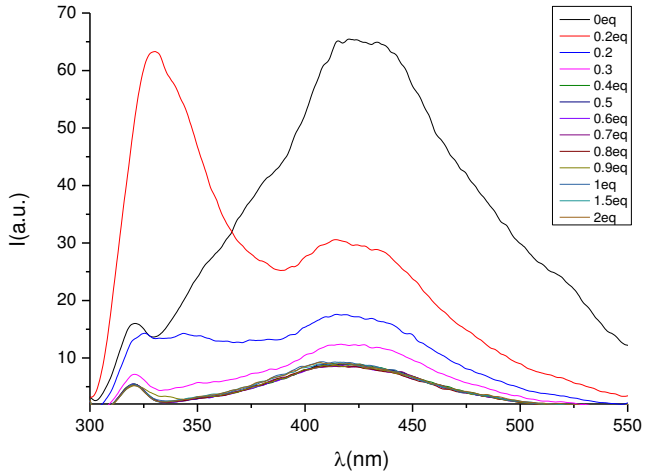

Figure 4.11 fluorescence emission spectra of L4 in the presence of increasing amount of Cu^{2+} at pH=6 ([L4]=4.14×10^{-5} M , T=298 K).

We finally compared the emission intensities at 328 nm (see Figure 4.12) in the spectra of the solution of the ligand in the presence of increasing amount of Zn^{2+}, Cd^{2+} and Cu^{2+} at pH=6. The emission intensity at 328 nm increases progressively upon addition of increasing amount of Zn^{2+} and Cd^{2+}, while decreases with the addition of increasing amount of Cu^{2+}.

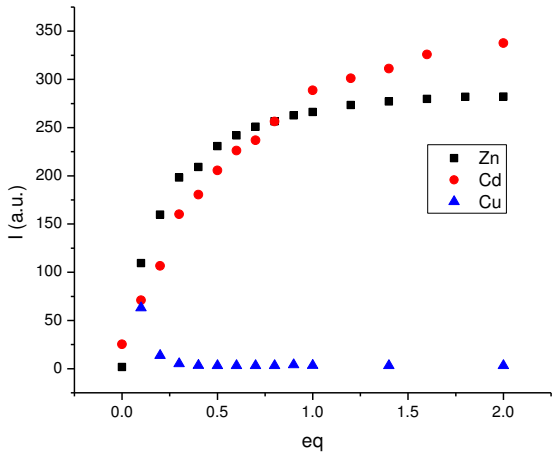

Figure 4.12 Emission intensity at 328 nm of the ligand L4 in the presence of increasing amount of $Zn^{2+,}$ Cd^{2+} and Cu^{2+} ([L4]=4.14×10^{-5} M , T = 298K).

These preliminary studies on L4 shows that the ligand alone forms and excimer type complex, with emission at 420 nm. Conversely, Zn^{2+} and Cd^{2+} coordination strongly enhance the emission intensity of bipyridyl at 320 nm.

3.6- Ligand L5

3.6.1- Acid-base properties of ligand L5

The coordination properties of ligand Acry-bis[9]ane-NS3 = L5 were studied by means of potentiometric, UV-Vis absorption fluorescence emission measurements in water - acetonitrile solution (V:V=50:50). The latter were carried out both at fixed pH and at different pH values.

The ligand L5 presents three potential sites of protonation, the nitrogen atom of the acridine unit and the two amine groups of the macrocyclic units. The protonation constants of the ligand and their values are reported in Table 5.1.

Equilibrium	log K
$L5 + H^+ = L5H^+$	6.87
$L5H^+ + H^+ = L5H_2^{2+}$	5.54
$L5H_2^{2+} + H^+ = L5H_3^{3+}$	2.97

Table 5.1 Protonation constants of L5 in water- acetonitrile solution (50:50) (errors on the log K values lower than the 0.02 logarithmic units (T=298 K, H_2O/CH_3CN 1:1 V:V, NMe_4Cl=0.1M).

The ligand can bind with a maximum of three acidic protons in solution. Considering that the nitrogen atom of the acridine unit is less basic than the amine nitrogen atoms, we can assume that the first two equilibria of protonation occur on the [12]aneNS_3 macrocyclic systems, while the protonation of the heteroaromatic nitrogen atom occurs only at strongly acidic pH (pH < 4, see Figure 5.1.). The distribution diagrams of the protonated species are reported in figure 5.1. In the pH range 3 - 7, the monoprotonated and diprotonated species are predominant in the solution, the uncharged ligand being prevalent in solution at pH> 7.

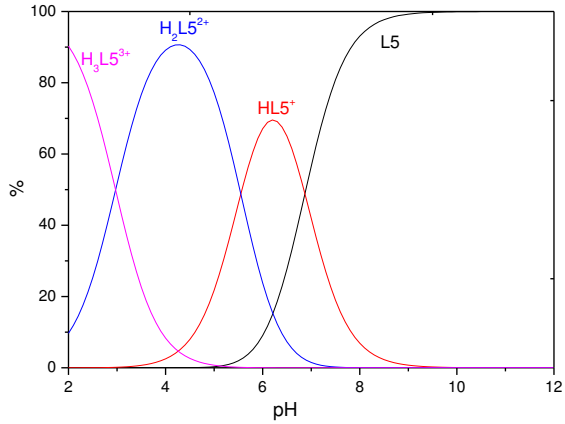

Figure 5.1 Distribution diagram of protonated species of L5 ([L5]=5×10^{-4} M, T = 298K, H_2O/CH_3CN 1:1 V:V, NMe_4Cl=0.1M).

3.6.2- UV-Visible spectroscopic study of L5

Subsequently, we recorded UV-vis and fluorescence emission spectra at different values of pH (see Figure 5.2). The spectra are characterized by the typical band of the emission of the acridine unit with a maximum at 358 nm and they do not significantly differ in the pH range 11.45 - 4.20. Only below pH 4 we can note a significant increase in the absorption at 358 nm and the formation of two shoulders at about 340 nm and 375 nm, which can be attributed to the protonation of the nitrogen atom of the acridine and the consequent change in the charge distribution on the heterocyclic system.

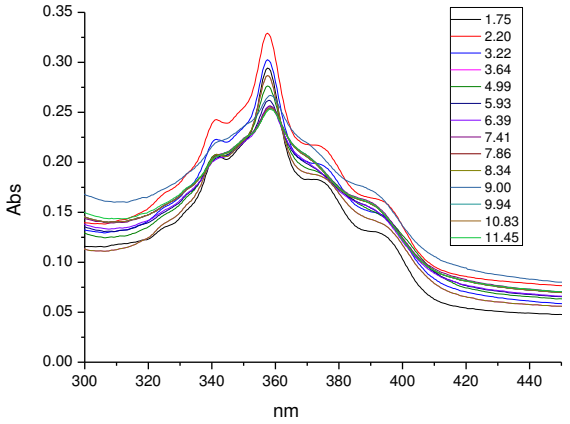

Figure 5.2 UV-Vis spectra of L5 at different values of pH, ([L5]=8·7×10^{-6} M, T = 298 K, H_2O/CH_3CN 1:1 V:V, NMe_4Cl=0.1M).

3.6.3- Fluorescence emission spectroscopic measurements of L5

We also recorded fluorescence emission spectra at different pH values. The spectra are strongly influenced by pH, as shown in Figure 5.3. In the alkaline pH range, the ligand is characterized by a weak emission. At pH < 6.8, we note a considerable increase in the emission with the formation of a structured band with a maximum at 412 nm. Finally, below pH 3 we can note a red-shift of the emission band, the spectra at pH=2.93 and pH=1.87 featuring a band with a maximum at 435 nm.

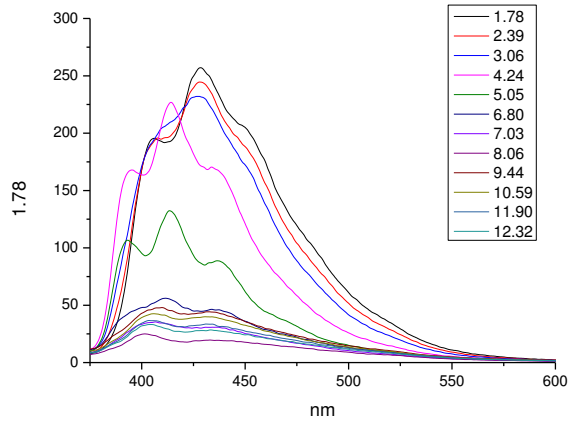

Figure 5.3 Fluorescence emission spectra of L5 at various values of pH, ([L5]=9.92×10^{-6} M, T = 298 K, H_2O/CH_3CN 1:1 V:V, NMe_4Cl=0.1M).

The superimposition of the emission intensity measured at 412 nm and 428 nm with the distribution diagram of the protonated species in solution at different values of pH is shown in Figure 5.4.

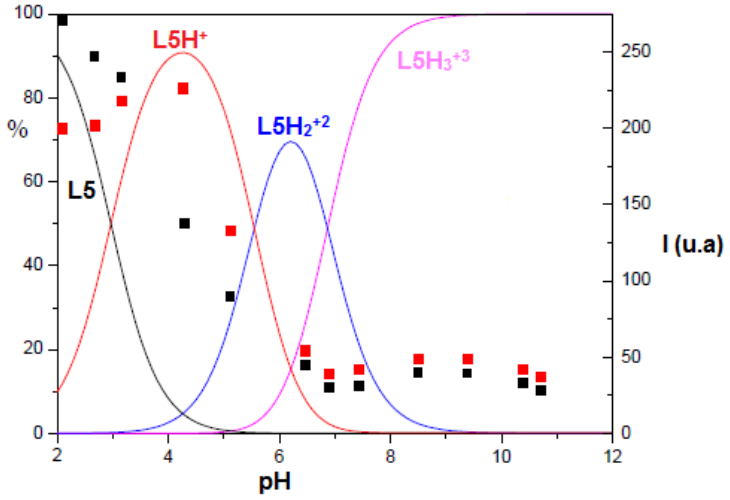

Figure 5.4 Emission intensity at 412 nm (■) and 428 nm (■) of L5 as a function of pH, overlapped to the distribution diagram of the protonated species ([L5]=5×10^{-6} M, T = 298 K).

We note that the ligand in its not protonated and mono-protonated species $L5H^+$ are not much emissive. This is probably related to the presence of a not protonated amine group of one of two macrocyclic units [12]aneNS3. The free lone pair of the nitrogen atom can turn off the emission of the fluorophore by PET effect, e. g., a process of photoinduced electron transfer occurs from the nitrogen atom to the fluorophore in its excited state. The formation of the $L5H_2^{2+}$species, where both the aliphatic amine nitrogen atoms are protonated, leads to an increase of the emission with the formation of the typical band of acridine at 412 nm, because of the complete inhibition of the PET effect. Finally, the formation of the specie $L5H_3^{3+}$, where the nitrogen atom of acridine is also protonated, induces a red-shift of the emission band, as normally found in the spectra of the acridinium species.

3.6.4- Determination of the stability constants of the complexes with L5

We determined the stability constants of metal complexes by means of potentiometric measurements in water-acetonitrile solution V:V 50:50. The potentiometric studied was performed in the presence of the Zn^{2+}, Cd^{2+}, Pb^{2+} and Cu^{2+} ion. The formation constant of the complexes are reported in Table 5.2.

Equilibrium	Log K			
	Zn^{2+}	Cd^{2+}	Cu^{2+}	Pb^{2+}
$L5 + M^{2+} = L5M^{2+}$	9.2(2	7.1(2)	10.3(1)	3.8(3)
$L5H^{+} + M^{2+} = L5HM^{3+}$	6.3(4)	3.3(1)	6.2(2)	-
$L5M^{2+} + M^{2+} = L5M_2^{4+}$	6.9(5)	4.0(2)	6.8(2)	-

Table 5.2 Formation constants of the metal complexes for the ligand L5 with Zn^{2+}, Cd^{2+}, Cu^{2+} and Pb^{2+} (T=298 K, NMe_4Cl=0.1 M, V:V 50:50).

We note that Zn^{2+}, Cd^{2+} and Cu^{2+} form both mono- and dinuclear complexes with the ligand. Beside the simple $L5M^{2+}$, Zn^{2+}, Cd^{2+} and Cu^{2+} form also a protonated species $L5HM^{3+}$. In the case of Pb^{2+}, precipitation of the complexes is observed in the presence of more than 1 equivalent of the metal in solution. This prevents the study of the system under these conditions.

Considering the complexes with a stoichiometric ratio L:M 1:1, the stability of the complexes decreases in the order: $Cu^{2+} < Zn^{2+} < Cd^{2+} < Pb^{2+}$. The greater stability of the complex of Cu^{2+} is attributed to the crystal field stabilization energy (CFSE), absent in the case of the other metal ions. The stability of the complex of Zn^{2+} is greater than the stability of the complex of Cd^{2+}. This result is somewhat unexpected considering the presence of donor atoms of sulfur, which have notoriously soft characteristics which would lead to stabilize the complexes with soft metal as in the case of Cd^{2+}.

We can give an explanation to this result considering that the metal ion in the mononuclear complexes is coordinated by a single [12]aneNS_3 unit. Therefore, the smallest Zn^{2+} could have more suitable dimensions to fit the macrocyclic cavity compared to Cd^{2+}, leading to a stabilization of the complex. The largest Pb^{2+} forms a complex characterized by a stability much lower than the others, and this can confirm this hypothesis.

On the basis of the data in Table 5.2, we can calculate the distribution diagram of the complexed species at different pH values in solution. As an example, Figures 5.5 and 5.6 show similar distribution diagrams calculated for the Zn^{2+} complexes with a ligad to metal 1:1 and 1:2 molar ratio, respectively.

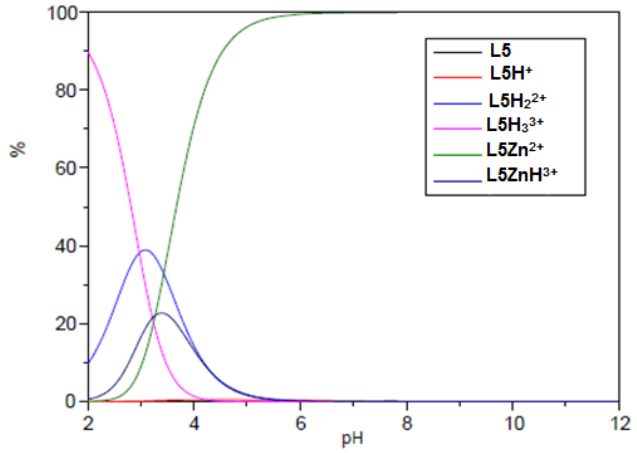

Figure 5.5 Distribution diagram of Zn^{2+} complexes with L5 calculated with a L5:Zn^{2+} 1:1 a stoichiometric ratio (298 K, H_2O/CH_3CN 1:1 V:V, NMe_4Cl= 0.1 M, [L5] = 5×10^{-6} M).

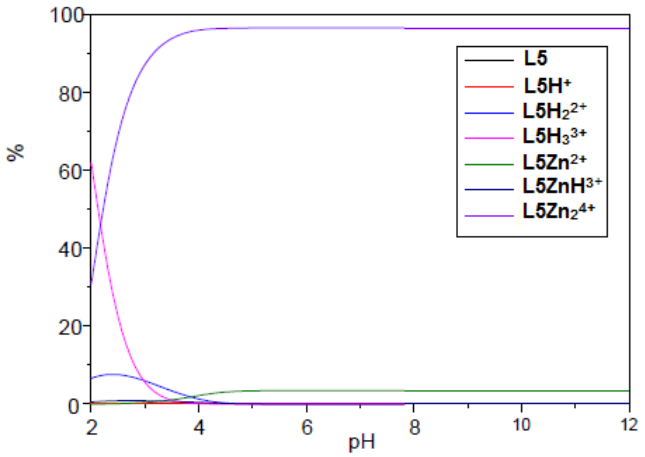

Figure 5.6 Distribution diagram of Zn^{2+} complexes with L5 calculated with a L5:Zn^{2+} 2:1 a stoichiometric ratio (298 K, H_2O/CH_3CN 1:1 V:V, NMe_4Cl= 0.1 M, [L5] = 5×10^{-6} M).

In figure 5.5 (metal to ligand molar ratio 1:1) from alkaline to a weak acidic values of pH, we can note the presence of only one species ($L5Zn^{2+}$), formed in solution in a wide range of pH, while at pH=4, we can observe the formation of the protonated species $L5ZnH^{3+}$. Considering the molecular architecture of the ligand, in the $L5Zn^{2+}$species the metal ion is probably coordinated by a single macrocyclic unit, while the other macrocyclic unit is not involved in the coordination. In the species $L5MH^{3+}$ a metal ion is likely to be coordinated by a single unit of [12]aneNS_3 and the acidic proton is probably localized on the nitrogen atom of the other macrocyclic unit, which is more basic than the nitrogen atom of the acridine unit.

The addition of a second metal ion leads to the formation of stable dinuclear complexes and the solutions containing L5 and the metal ion in L:Zn^{2+} 1:2 stoichiometric ratio, predominantly contain the species $L5M_2^{4+}$, as shown in Figure 5.6. The percentages of mono nuclear complexes are very low (about 5%) in these conditions.

The nitrogen atom of the acridine unit in both mono- and dinuclear complexes could theoretically be involved in the coordination of at least a metal ion. Indeed, the complex formation does not alter the characteristics of the absorption spectra of the heteroaromatic unit.

3.6.5- UV-visible spectroscopic measurements

In fact, we recorded the UV-Vis spectra of the ligand L5 at pH 7 in the presence of increasing amount of Zn^{2+} and Cd^{2+}. The spectra are shown in Figure 5.7 and 5.8. The absorption characteristics of acridine that do not alter in the presence of the metal ions, indicating that the nitrogen atom of the acridine is not involved in

the coordination of the metal ion in both mono- and dinuclear complexes.

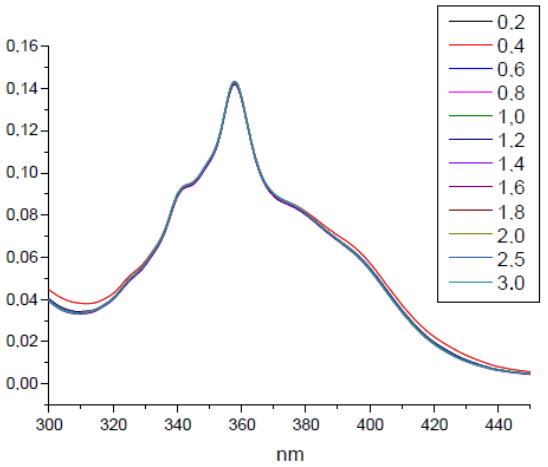

Figure 5.7 UV-Vis spectra of the ligand L5 in the presence of increasing amount of Zn^{2+} at pH 7 (T=298 K, H_2O / CH_3CN 1: 1 V:V, TRIS buffer, [L5] = 3.1×10^{-6} M).

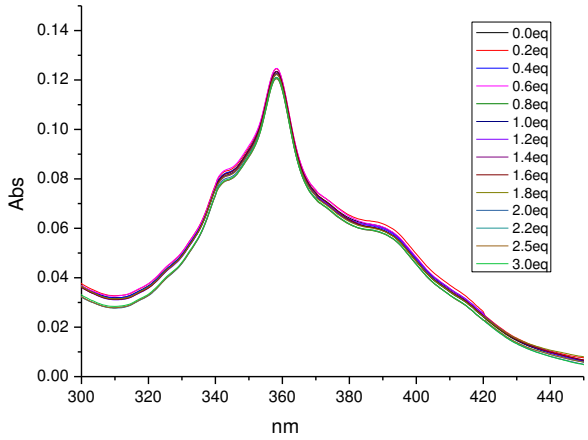

Figure 5.8 UV-Vis spectra of the ligand L5 in the presence of increasing amount of Cd^{2+} at pH 7 (T=298 K, H_2O / CH_3CN 1: 1 V:V, TRIS buffer, [L5] = 2.5×10^{-6} M).

3.6.6- Fluorescence emission spectroscopic measurements

Considering the fluorescence emission characteristrics of the ligand, the emission spectra are profoundly altered by the presence of the metal ions, in particular Zn^{2+} and Cd^{2+}. The emission spectra of the ligand in the presence of increasing amount of Zn^{2+} are reported in Figure 5.9. The addition of Zn^{2+} leads to an increase of the emission at 460 nm, which appears to be increased more than four times in the presence of two equivalents of the metal ion.

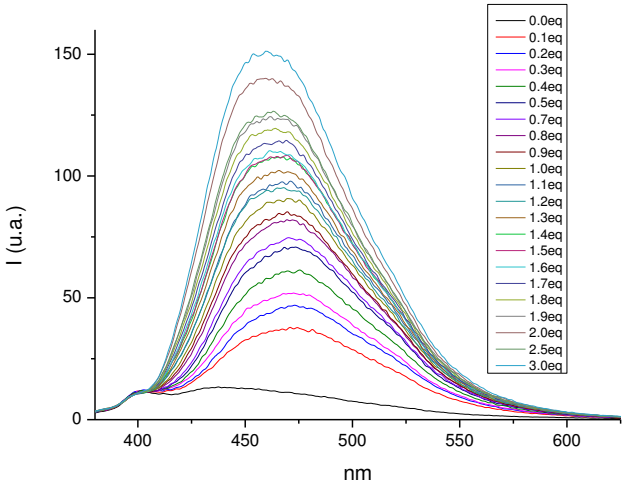

Figure 5.9 Fluorescence emission spectra of the ligand in the presence of increasing amount of Zn^{2+} at pH 7 ([L5] = 2.5 x 10^{-6} M, buffer TRIS, T=298 K, H_2O / CH_3CN 1: 1 V:V).

Figure 5.10 shows the emission intensity of the ligand at 460 nm in the presence of increasing amount of Zn^{2+} at pH=7.

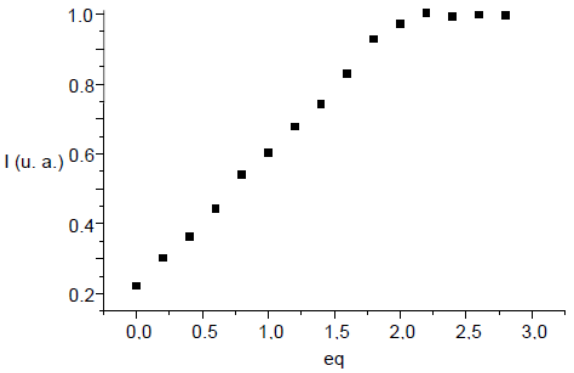

Figure 5.10 Emission intensity of the ligand L5 at 460 nm, in the presence of increasing amount of Zn^{2+} at pH=7 ([L5] = 2.5×10^{-6} M, T=298 K, buffer TRIS, H_2O/CH_3CN 1:1 V:V).

The increase of the emission intensity at 460 nm is almost linear up to a L:M 1:1.8 molar ratio, as shown in Figure 5.10. The emission intensity does not change for a metal to ligand ratio greater than 2.2 and this leads us to suppose that the formation of a stable dinuclear complex, where the two metal ion of Zn^{2+} are coordinated independently from each other. The observed emission enhancement at 460 nm is attributed to the progressive inhibition of the PET effect exerted by the coordination of the metal cations to the amine groups, as often observed in the complexes of Zn^{2+} with ligands containing amine group as donor atoms. We can also note that this band undergoes a shift toward the red compared with the emission of the acridine in the absence of the metal ion. This effect could be due to a charge transfer within the acridine moiety upon the coordination of Zn^{2+} as sometimes found in the complexes with chemosensosr constituted by a fluorescent system linked to a chelating unit.

We also recorded fluorescence emission spectra of ligand L5 in the presence of increasing amount of Cd^{2+}, as shown in Figure 5.11. We can observe that also the coordination of Cd^{2+} leads to increase the emission intensity at 460 nm. The emission appears to be increased more than 15 times in the presence of two equivalents of Cd^{2+}.

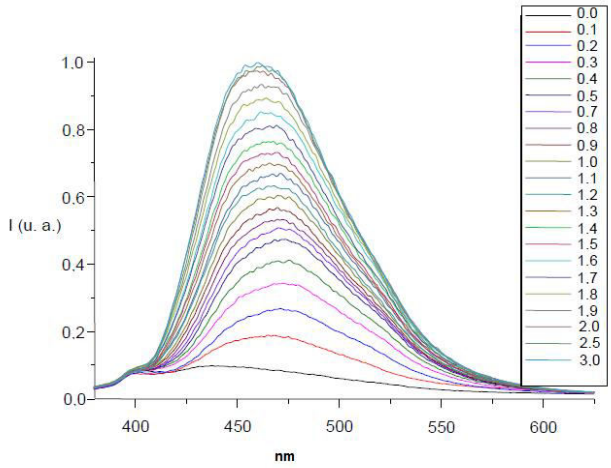

Figure 5.11 Fluorescence emission spectra of the ligand in the presence of increasing amount of Cd^{2+} at pH 7 ([L5] = 1.5×10^{-6} M, buffer TRIS, T=298 K, H_2O / CH_3CN 1: 1 V:V).

The increase of the emission intensity at 460 nm with increasing amount of Cd^{2+} is linear up to a metal to ligand 1:0.7 molar ratio, then the slope changes and the increase starts again to be linear as the metal to ligand molar ratio increases from 1.2 to 1.8.(see Figure 5.12). Finally, we can note that the intensity does not undergoes further changes upon the addition of two equivalents of Cd^{2+}. These results indicates the formation of a 1:1 complex with metal to ligand molar ratios lower than 1, followed by the formation of a dinuclear complex in the presence of more than 1 equivalent of Cd^{2+}.

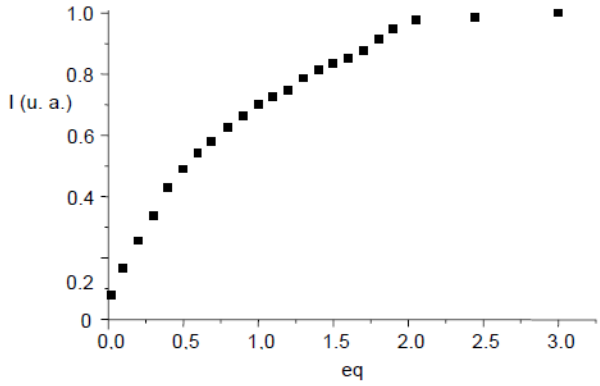

Figure 5.12 Emission intensity of the ligand L5 at 460 nm, in the presence of increasing amount of Cd^{2+} at pH=7 ([L5] = 1.5×10^{-6} M, T=298 K, buffer TRIS, H_2O/CH_3CN 1:1 V:V).

We also made a comparison between the emission intensities at 460 nm of the solution at different pH values of the ligand in the absence and in the presence of Zn^{2+}, Cd^{2+}, Pb^{2+} and Cu^{2+} with a L: M 1:2 molar ratio, as shown in Figure 5.13. The CHEF effect is high in the presence of Cd^{2+} compared with the other metal ions, in particular between pH 6 and 9. In other word, the ligand presents a good specificity for the Cd^{2+}. The coordination of Cu^{2+} leads to a slight decrease of the emission intensity, while the coordination of Pb^{2+} does not alter the fluorescence emission.

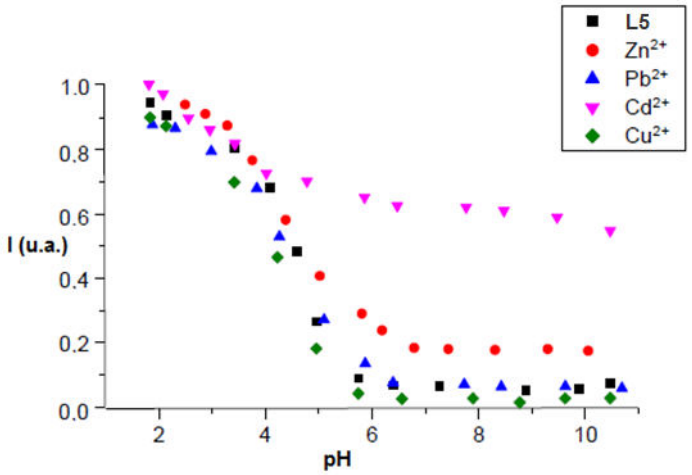

Figure 5.13 Emission intensity at 460 nm in function of pH, of the ligand-Free and in the presence of 2 eq of Zn^{2+}, Cd^{2+}, Cu^{2+} and Pb^{2+} at different values of pH, ([L5] = 1.5×10^{-6} M, T=298 K, H_2O/CH_3CN 1:1 V:V).

At acidic values of pH < 5, the presence of the metal cations does not significantly change the emission intensities as expected considering decomplexation upon the formation of protonated species of the ligand at acidic pH values.

Finally, we analyzed the emission intensity of the ligand at pH 7 at 460 nm in the absence and in the presence of two equivalents of different metal ions (transition metal ions, alkali and alkaline earth metal ions), as shown in Figure 5.14. We can observed that the ligand shows a good selectivity for Cd^{2+}. With the only exception of Zn^{2+}, which gives a slight increase of the fluorescence emission, other transition metals reduce the emission of the ligand, while alkali and alkaline earth metal ions do not change the emission intensity.

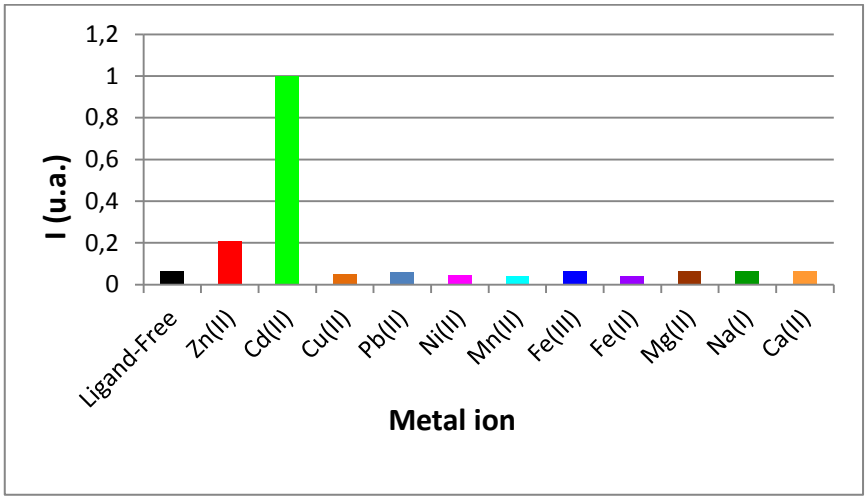

Figure 5.14 Emission intensity of the ligand L5 at 460 nm in the presence of 2 eq of various metal ions at pH 7 ([L5] = 1.5×10^{-6} M, TRIS buffer, T=298 K, H_2O / CH_3CN 1: 1 V:V).

4- CONCLUSION

The purpose of this thesis has been the development of new molecular devices able to selectively bind and signal in aqueous solution metal cations, in particular transition metal cations of biological and/or environmental interest. With this in mind, we have synthesized new fluorescent receptors featuring one or more macrocyclic units linked to different fluorescent moieties. While the macrocyclic units act as metal binding sites, the luminescent moieties can signal the binding event through changes of their emission characteristics.

In our approach, we have exploited the bis-aminal synthetic procedure to produce fluorescent macrocyclic or macropolycyclic structures. This synthetic methodology, in fact, allows for the introduction of one or more functional units, including fluorescent moieties, in specific position of linear or cyclic polyamines. In our case, we have chosen as metal binding site the 1,4,7,10-tetraazacyclododecane (cyclen) macrocyclic polyamine, a well known chelating agent in coordination chemistry, capable to form stable complexes with transition metals. By using the bis-aminal procedure we have linked two fluorescent moieties to the amine groups in 1 and 7 position of cyclen (quinoline and 8-hydroxyquinoline). The remaining amine groups have subsequently been functionalized with acetate groups, achieving the final receptors H_2L1 and H_4L2. These receptors can bind metal cations not only by using the four amine groups of cyclen, but also exploiting the carboxylate units and the heteroaromatic nitrogen of quinoline. In the case of H_4L2 the hydroxyl groups could also be involved for metal binding.

The same synthetic procedure can be used to obtain macropolycyclic structures composed by two polyamine units linked by one or two fluorogenic units. In the course of this work, we have synthesized ligands L3 and L4, composed respectively by two cyclen macrocycles linked by one and two 2,2'-bipyridyl moieties. Finally, ligand L5, constituted by two 1-aza-4,7,10-trithio-

cyclododecane macrocycles linked by an acridine fluorescent unit, has been synthesized at the Department of Chemistry and Geology of the University of Cagliari, by using a standard procedure.

The synthetic work has been followed by the analysis of the acid-base properties of the ligands and of their binding and sensing ability in solution. This study has been performed by coupling different techniques, including potentiometry, UV-vis absorption spectroscopy and, overall, fluorescence emission spectroscopy.

The determination of the acid-base properties of the receptors is a necessary preliminary study in the analysis of their metal binding and sensing ability, since protonation strongly competes with metal coordination in aqueous solutions. This study showed that the emission properties of the receptors are strongly influenced by pH. The receptors are often not luminescent at alkaline pH values, where the polyamine units are not protonated or scarcely protonated and an efficient photoinduced electron transfer process from the amine groups to the excited fluorophores may occur. However, also protonation/deprotonation equilibria occurring on the heteroaromatic moieties can determine the pH dependence of the emission.

Considering metal binding and sensing, both H_2L1 and forms remarkably stable complexes with 1:1 metal to ligand stoichiometry. The sensing ability, however, is quite different. H_2L1 show an enhancement of the emission in the presence of the sole Zn^{2+} and Cd^{2+} ions, while other first-row transition metals and heavy post-transition metal cations do not change or quench the emission of quinoline. Conversely, the emission of H_4L2 is not enhanced by the presence of none of the metal ion studied. This fact demonstrates that small structural changes in the receptor structure, such as replacement of quinoline with 8-hydroxyquinoline, can have a deep impact on the emission properties of these receptors.

Receptors L3, L4 and L5 con form both mono and dinuclear complexes with first-row transition and post-transition metal cations in aqueous solution. The most interesting finding is the different sensing ability displayed by ligand L3 and L5. In fact, L3 is able to selectively sense the Zn^{2+} ion thanks to a marked enhancement of the emission of 2,2'-bipyridyl in the presence of this metal, while L5 results an optimal fluorescence chemosensor for Cd^{2+}, its emission being strongly increased only in the presence of this metal. In both cases, however, the emission properties are modulated by the number of metal cations bound to the receptors and by the pH of the medium.

Acknowledgment

Thanks go out to everyone along the way who made this work possible, especially to my supervisor Prof. Andrea Bencini. Thanks to Prof. Claudia Giorgi, to Prof. Barbara Valtancoli and to the Phd coordinator Prof. Andrea Goti. I offer them my heartfelt thanks for their tireless support and encouragement of my work and solving my difficult situations abroad . Those people have inspired me along the way and have made my trek a little easier.

I would like to send a big thank to my lovely group and Lab partners, to Francesco Bartoli, to Tiziano Marzo, to Luca Conti, to Riccardo Rapini, to Stefano Puccioni and to my real friend Azzurra Crocini. Thank you all for being with me and for supporting me the whole period I stayed in the university of Florence. The brotherhood that I felt with you overcame my homesickness and shortly I started to feel that I am home. I wish you all the best and success in your career.

I would like to stop for seconds and remember my homeland, Syria, and ask Allah to save the Syrian people, to stop this destructive war and to bestow mercy and peace upon our wounded country so that we again have the chance to go back and live peacefully with family and friends.

I dedicate this thesis to my parents, Khaled and Fareda, who always dreamed of the moment that I get my Phd degree, they never complain, they willingly took all the sorrow and troubles of being far away. They never despair but kept armed with patience and prayers. It's been four years since the last time i've seen them and we still dream of the day that we meet again. As much as I feel happy and accomplished as much as I feel sad and wounded going through this important period in my life without them. The moment I started writing to them, I felt blank and empty because no matter what I say or what I do, I don't believe that I can ever pay them back for every single thing they have done to me. I have nothing to offer them but my love and this thesis recording the

results of every single moment I've been through for four years. Every single line I wrote was for me as a step on my long road back to them. I hope I was able to put a tiny smile on your faces and happiness in your virtuous hearts.

I also dedicate this thesis to my sisters and brothers, to Ranim, to Nesrin, to Muhammad, to Safy, and to Khaldoun. I miss you all, and I wish I can pay you back for your endless love and support. Hearing you and talking to you were the only motives to overcome sadness and to push me forward. I miss our times together and the places we've been together.

To my brother in law, Ismaeal Kara Hassan, who has his own creative way of reshaping sadness in a happy way. He always astonishes me with his incredible capacity to overcome difficult situations. To my beautiful grandchildren Jana, Asia and Ali.

To the only person who planted the seeds of love in my heart and took me out of my fears and sadness to see the world in a brighter way, to my love Bashar Hanawi. I pray to Allah to keep us together and bestow happiness and tranquility upon us.

To my darling uncle Nizam Ramadan and his family, to my dear aunts Abeer and Fadya Ramadan, to my aunts Hayat Zartit and all my relatives: uncles and cousins (Saaid, Abd al-Halim, Abd al-Basset, Salim, Mohammed, Hosam, Alaa, Manal, Yousef, Rabii, Tamer, Lina, Rama, Rawan and Asmaa).

To my italian family, to the loving person who always treated me with all the kindness and tenderness like a real mother in my alienation Roberta Bertocci, to her husband Marco Folini and their sons Stefano and Francesco. To the sincere friend and the compassionate sister Barbara Monne. To Source of kindness Censa Cucco.

Last but not least, I would like to offer my heartfelt thanks to my friends and relatives. To the real brother Wasseem Morshed, to my

best friend Khaled Awada, to the sincere friend Omar Abo Fakher, to my honest sister Zahya al-Hallak and her family Mohammad Othman and Zahraa. To my lovely sisters: Nagla Fallaha and Kinana al-Sabah, I love you both. To Dr. Abd al-Sattar al-Najm and Dr. Iyad Hafez.

To the great man who helped me for getting PhD degree, my dear uncle Samir Khashouf.

To Mohamed Rabii Kadib al-Ban and his fiancee Adila Fakch, to Uncle Abd al-Wahab Fakch. To Yehia Abd al-Rahman, to Leila el-Khaffaji and Fiorentina Mecaj, to Maram Othman, to Rita Falcone, to Ilaria Ruffo, my lovely neighbours. To Khaled Reda and Sobhy Kekati, to Sanaa Seddati and Soumia Maach and their families, to Ouijdane Moussaid.

To my dear sister with sincere love Lama Assad.

To Rawda Raii, Huda Akrama, Lamaan Salhb, Nadima Abdou, Marah Saleh, Zainaa Laila and their family, Arwa Hassan, Samya Majzoub, Khadeja Kara Hassan, Weam al-Abd, Abeer Hammado Samr Break and her husband Alaa Morshed and many many others.

Thanks go out to every single person I've met along my way and helped me by any mean. Thank You All